Commission of the European Community

JOINT
RESEARCH
CENTRE

NEANDC (E) 272 "U" Vol. III Euratom
INDC (EUR) 020/G

ANNUAL PROGRESS REPORT ON NUCLEAR DATA

1985

CENTRAL BUREAU FOR NUCLEAR MEASUREMENTS

GEEL (BELGIUM)

September 1986

Commission of the European Community

JOINT
RESEARCH
CENTRE

NEANDC (E) 272 "U" Vol. III Euratom
INDC (EUR) 020/G

ANNUAL PROGRESS REPORT ON NUCLEAR DATA

1985

CENTRAL BUREAU FOR NUCLEAR MEASUREMENTS

GEEL (BELGIUM)

September 1986

TABLE OF CONTENTS

1 NUCLEAR DATA

1.1 NUCLEAR DATA FOR STANDARDS

1.1.1 Neutron Data for Standards

Background Evaluation in ^{10}B (n,α) / ^{6}Li (n,α) Measurements

C. Bastian, H. Riemenschneider

The measurement of this cross section ratio contributes to the improvement of these cross section standards, which are widely used in neutron fluence measurements.

An experiment was performed of the $^{10}B(n,\alpha_0\alpha_1)^{7}Li,^{7}Li^{*}$ and $^{6}Li(n,\alpha)T$ cross-section ratio at the linear accelerator at neutron energies between some eV and 400 keV using a xenon gas scintillation detector. For γ-ray attenuation a 10 mm thick ^{238}U filter was put in the beam. Time of flight and pulse height were recorded when a ^{10}B-coated, a ^{6}LiF-coated and a dummy quartz cylinder were positioned successively in the neutron beam within the xenon gas scintillation detector. Three time-of-flight spectra according to the three samples were obtained. Figure 1 shows a part of these spectra in the few-eV region.

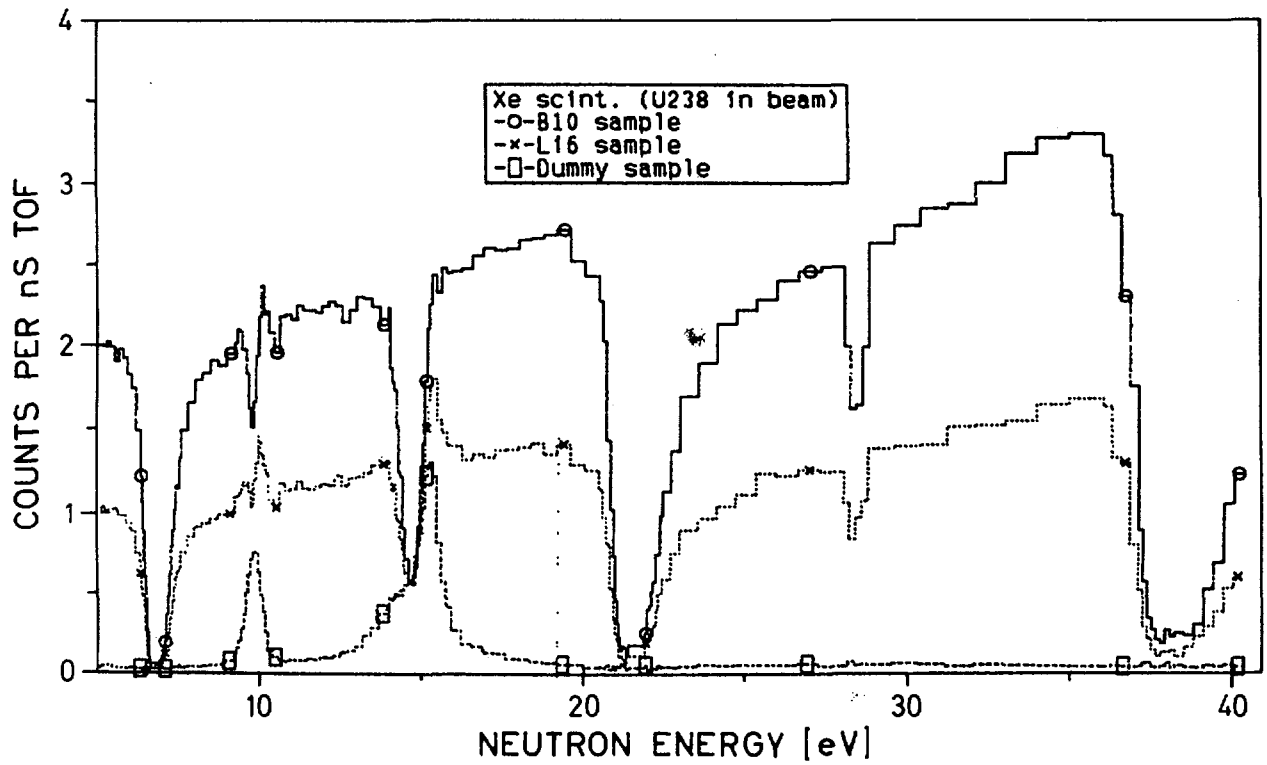

Fig. 1. Uncompensated time-of-flight spectra with dummy sample recording

The background component measured with the empty quartz cylinder in the beam shows to be non-neglible, especially in the xenon resonances at 9.44 and 14.4 eV. Figure 2a and b show pulse height spectra, in Fig. 2a all events in the whole neutron energy range are summed up and in Fig. 2b events of the same energy range but without the region of the xenon resonances are shown. Most of the events with low pulse height in the ^{10}B and ^{6}Li spectra are from neutron interactions with the material of the scintillation detector, especially with the Xe. Time-of-flight spectra from $^{10}B(n,\alpha)$ and $^{6}Li(n,\alpha)$ are shown in Fig. 3, where the background measured with the dummy sample was subtracted. The background subtracted pulse height spectra are shown in Fig. 4. They still show a small number, 1 ‰, of low pulse height events compared to the whole spectrum. This systematic error has to be incorporated into the full analysis of the experiment.

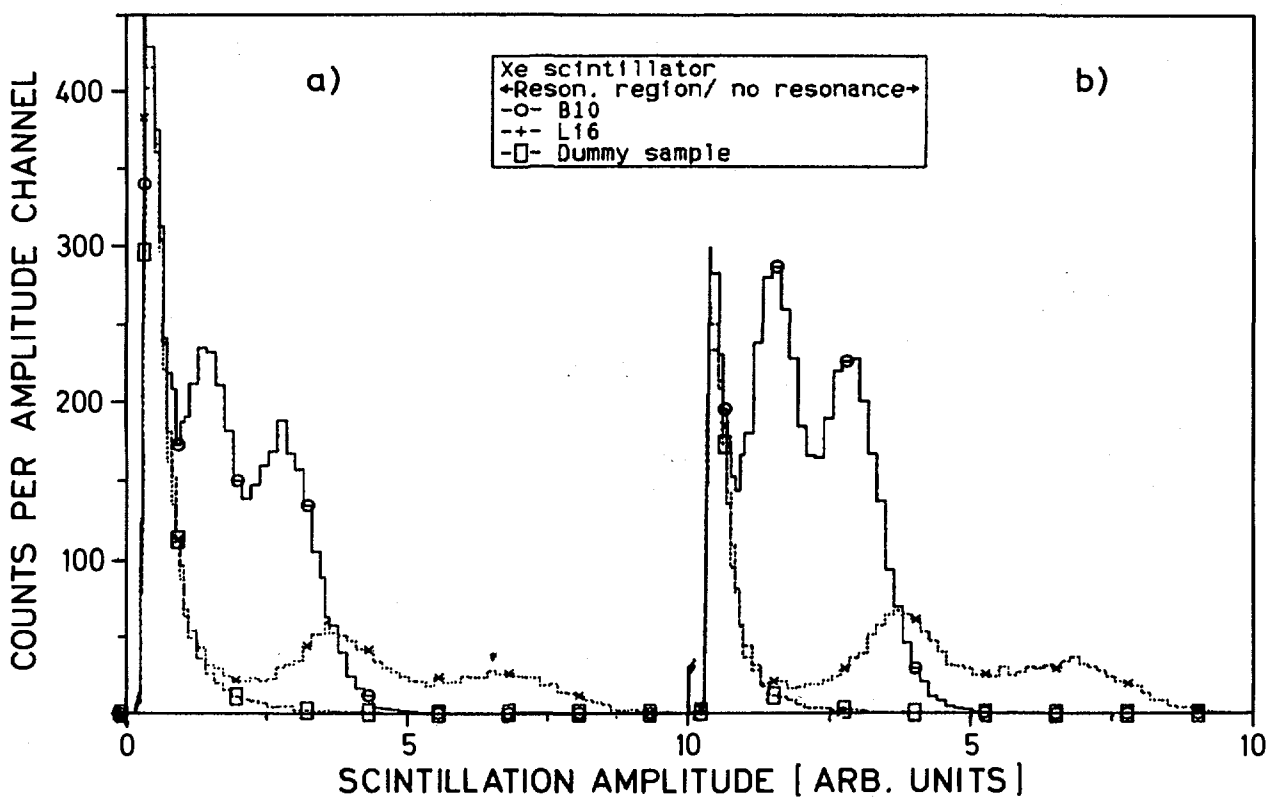

Fig. 2. Uncompensated amplitude spectra with dummy sample recording

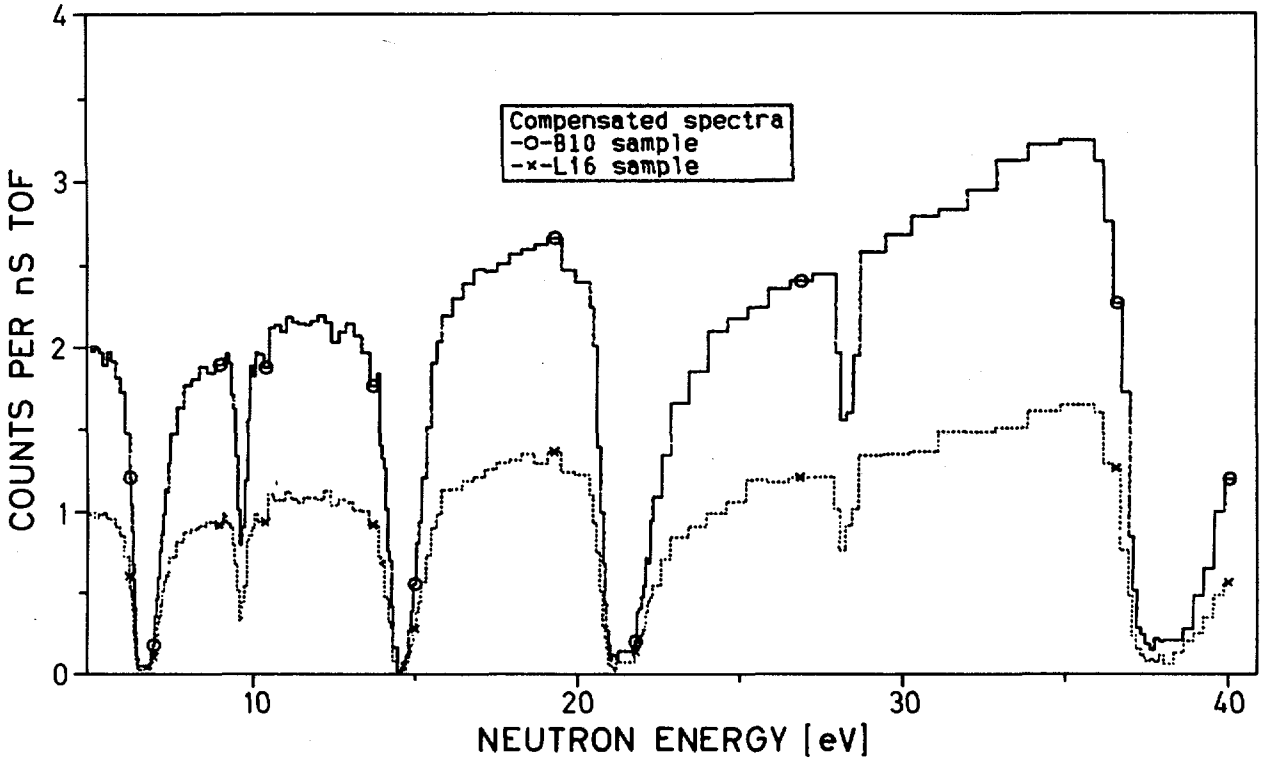

Fig. 3. Compensated time-of-flight spectra

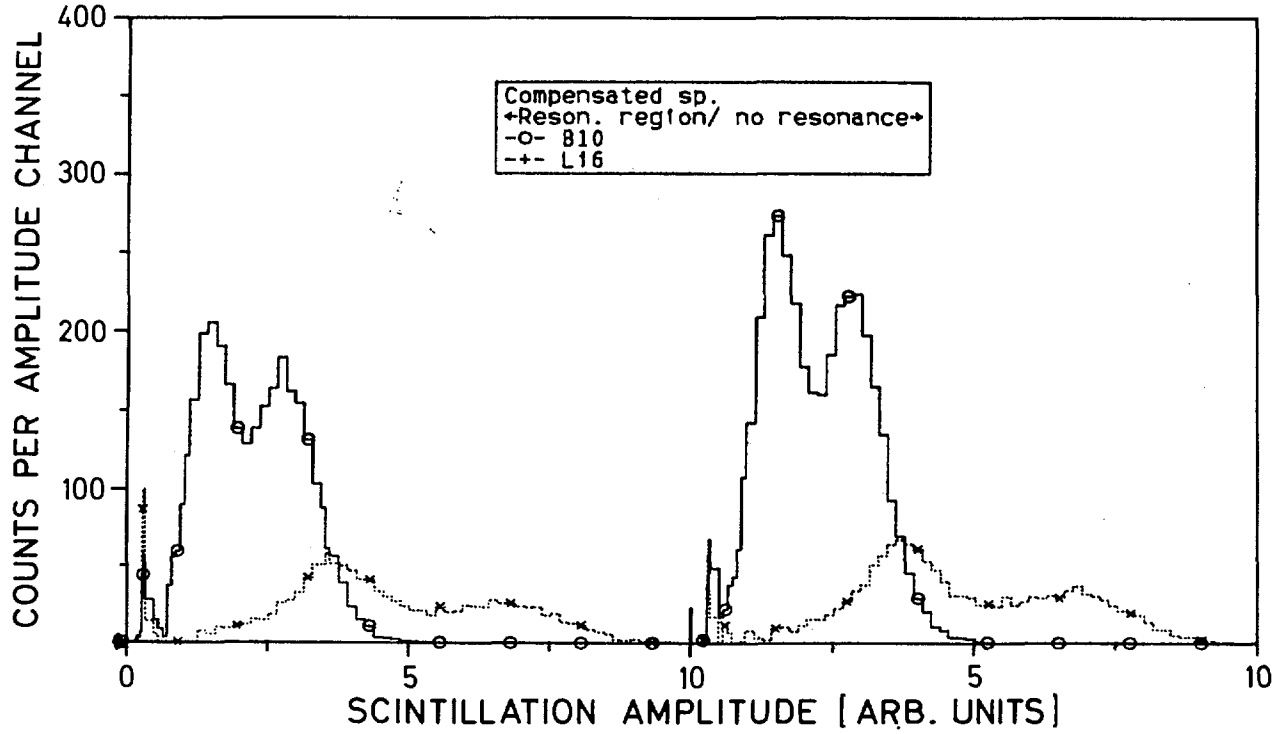

Fig. 4. Compensated amplitude spectra

^{235}U(n,f) Fragment Mass, Angle, and Kinetic Energy Distributions for Thermal ≤ E_n < 1 MeV

F.J. Hambsch*, H.-H. Knitter, C. Budtz-Jørgensen, R. Vogt, H. Bax
(WRENDA request N° 781192R)

Important for the use as a standard of the ^{235}U fission cross section are experimental data on the details of the mass, energy and angular distributions of the fission fragments, and the mass versus energy and mass versus angular distribution correlations as function of excitation energy.
In a previous experiment it was observed that the fragment average total kinetic energy at an incident neutron energy of only 500 keV is considerably higher than the thermal value. Also the fragment angular distributions which are of importance in the application of the ^{235}U fission cross section as a standard, showed a rather strong dependence on the incident neutron energy.

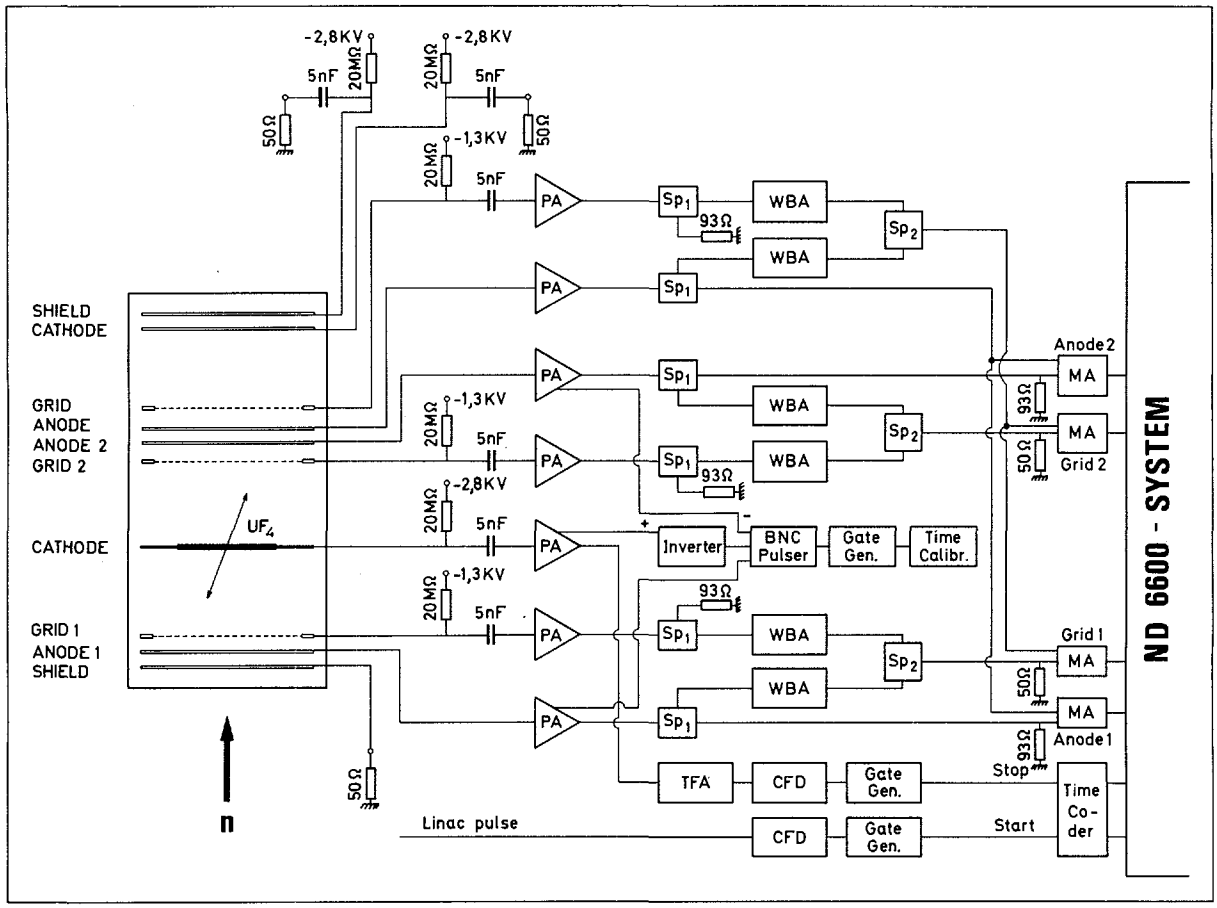

Fig. 5. Schematic view of the experimental setup

---

* EC Fellow.

To study the above-mentioned fission properties as function of neutron energy and in the resonance region as function of the resonances and their quantum numbers, an experiment at a 10 m flight path station at GELINA was set up. Figure 5. shows a schematic drawing of the experiment. The fission fragment parameters are measured with a twin ionization chamber. A compensation technique is applied by the use of an unloaded ionization chamber to compensate for the signals induced by the GELINA γ flash in the detector. These signals would otherwise disturb the measurement in the high energy part of the presently desired neutron energy range which must ensure the overlap with the previous measurements.
The data acquisition was started and both high (800 Hz) and low (40 Hz) repetition frequencies at GELINA were used. The advantage of the low frequency was that the neutron energy range could be extended to thermal. All events were stored on-line on magnetic tapes. Approximately $8 \cdot 10^6$ fission events for neutron energies between 1 eV and 2 MeV were recorded. Data analysis has been started.

Evaluation of the Thermal Constants of ^{233}U, ^{235}U, ^{239}Pu, and ^{241}Pu, and the Fission Neutron Yield of ^{252}Cf

E.J. Axton*

For inclusion in the ENDFB VI file now being prepared it is necessary that the output data from the recent evaluation[1] of these constants should be written in ENDFB format. However, it appears that the present ENDFB file system is inadequate to accept all of the correlation matrix of the output data. From discussions with experts at Saclay, (OECD, NEA Data Bank) it appears that the correlations between the various cross sections for the four nuclides can be put into ENDFB, but not the correlations between the cross sections and nubar and the g-factors, or between nubar and the g-factors.
Consequently, if the proposed ENDFB VI file is used to compute functions of the fitted variables which are required for reactor calculations, (e.g. 20°C Maxwellian values for eta, alpha, and K1), the calculated uncertainties of these derived parameters will be wrong.

---

* Visiting Scientist from NPL, Teddington, UK.

(1) E.J. Axton, IAEA Tecdoc 335, 214, (1985).

The solution to this problem would be to establish a new ENDFB file which could accommodate all the parameters and their correlations. It is worth pointing out at this stage that both the construction and the use of ENDFB files would become simpler if they were put into APL instead of Fortran.

Another obstacle is the reluctance on the part of some reactor physicists to accept the current output data because it is said to conflict with the results of certain criticality experiments. Some tests have been carried out to investigate possible sources of these supposed discrepancies.

The first criticism was that the fission cross section of ^{235}U (582.8 b) was too low, a value nearer to 585 b being preferred. Since this is close to the value obtained with only monoenergetic data (table 6 [1]), it was suggested that table 6 should be considered as a candidate for ENDFB in view of possible errors in Maxwellian data due to uncertainties in the important low energy (below 20 meV) parts of reactor spectra.

However the real problem lies not with the fission cross section but with the K1 value for ^{235}U. The current updated evaluation value (718.5 ± 2.2) compares with a preferred value of 722.7 ± 3.9 which is based on a reassessment of the Oak Ridge criticality experiments (J. Hardy, private communication to A. Carlson, NBS). The latter is now part of the input data. The difference of 4.2 ± 3.9 cannot be regarded as a serious discrepancy.

The next criticism relates to the scattering cross sections, which appear in the input file not as measurements, but as an evaluation. The scatter entries are required to derive the absorption cross section from total minus scattering cross sections. If scatter entries are deleted, there is no longer any need to include the total measurements because they no longer contribute to the fitted values of the required constants. Without the total and scatter entries, K1 for ^{235}U becomes 719.4 and the difference between this and 722.7 ± 3.9 (see above) becomes 3.3 ± 3.9. In fact this set of output data seems to be quite acceptable, and can be regarded as a serious candidate for inclusion in ENDFB as an alternative to the set derived from monoenergetic data only.

Eta for ^{239}Pu has also been quoted as discrepant for several years. The fitted value (2.115 ± 0.005) is said to conflict with the value of 2.090 required to satisfy criticality experiments (M.J. Halsall, private communication from J.L. Rowlands). No uncertainty is given for the 2.090, but once again, it seems that the problem lies not with eta but with K1

(M.J. Halsall, private communication from J.L. Rowlands). A preferred value for K1 is not yet available.

In conclusion, none of the criticisms so far raised represent discrepancies. The contents of the proposed ENDFB file have yet to be determined. Many of the tests described above are diagnostic, and they provide some insight into what goes on in the least squares fit, but it is important to guard against making changes to the input file for no other reason that they produce a preconceived set of output data. Such a result can be achieved with much less effort, and without a least squares fit. For the time being the output data based on the complete set of input data is recommended.

^{252}Cf Spontaneous Fission Neutron Spectrum

C. Budtz-Jørgensen, H.-H. Knitter, R. Vogt, H. Bax
(WRENDA request N$^{os.}$ 792189R, 821026R)

The neutron energy spectrum of the spontaneous fission of ^{252}Cf is regarded as a neutron spectrum shape standard. This standard is widely used for neutron detector calibration purposes. It is however not clear with which mathematical parametrization the spectrum can be best described, especially at higher neutron energies. Therefore more detailed experimental effort is needed to obtain a realistic, theory-based spectrum shape description.

In December 1984 a ^{252}Cf source on a thin backing has been received. A multi-parameter experiment for a detailed study of the prompt fission neutron spectrum was set up as shown in Fig. 6. Fission fragment detection is made using the gridded twin ion chamber developed at CBNM with which the fission fragment angle and the kinetic energies of the two fission fragments are measured in an advantageous geometry where all fragments of the source are detected. The time information of the fission events is obtained from the common cathode giving a resolution of less than 0.7 ns. The neutron detector is located on the axis of the ionization chamber, at a distance of 0.52 m from the ^{252}Cf source.

Neutron energies are determined using the time-of-flight technique. Both, the pulse height as well as the pulse shape for n/γ discrimination are recorded in order to distinguish between γ-ray and neutron emission in the fission process. For each fission event where a neutron is detected, the 7 parameters are measured simultaneously. They are digitized and stored sequentially on magnetic tape for off-line analysis.

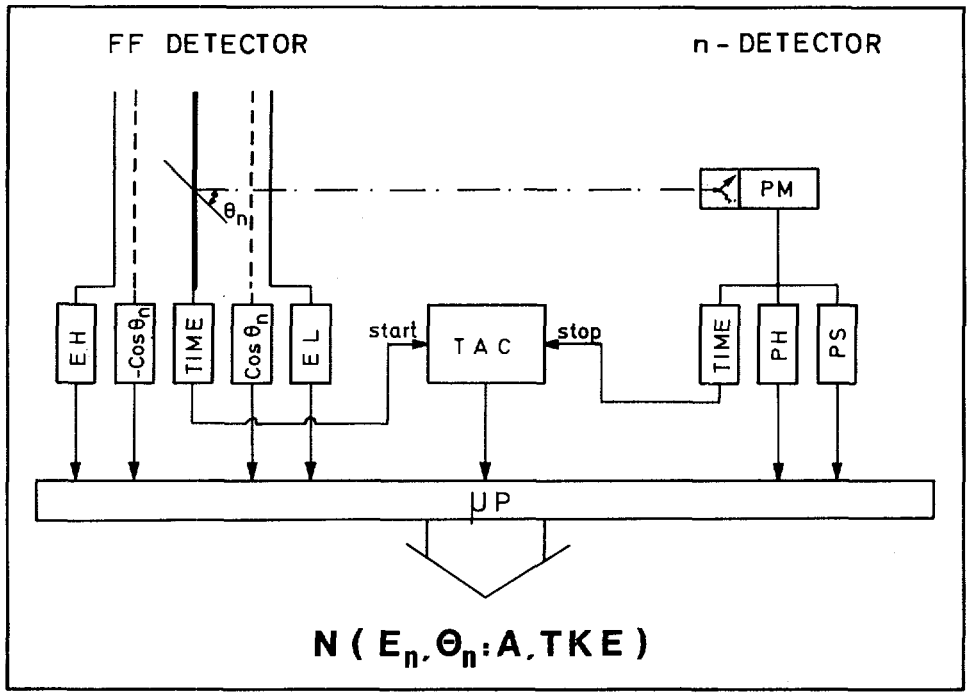

Fig. 6. Experimental set-up for the study of the ^{252}Cf neutron emission

The double energy information is used to derive the fission fragment masses. The excellent energy and mass resolution of this detector is illustrated in Fig. 7. which shows a part of the measured ^{252}Cf light fragment mass distribution. Here the fragment kinetic energies are selected so high (cold fragmentation) that neutron emission is improbable and accordingly no corrections for the mass determination have to be made. A mass resolution of 0.5 atomic mass units or a corresponding kinetic energy resolution of less than 0.5 MeV is observed.

The fragment angle information is obtained as the cosine of the angle between the fragment emission direction and the chamber symmetry axis. The cos θ resolution is typically 0.05. Figure 8 displays measured fragment-neutron angular distributions integrated over all fragments for neutron energies between 1 and 14 MeV.

These results are based on $1.5 \cdot 10^6$ fission events recorded in a measuring time of about 450 hours. A second, 10 times stronger ^{252}Cf source was delivered in October 85, and data taking was continued.

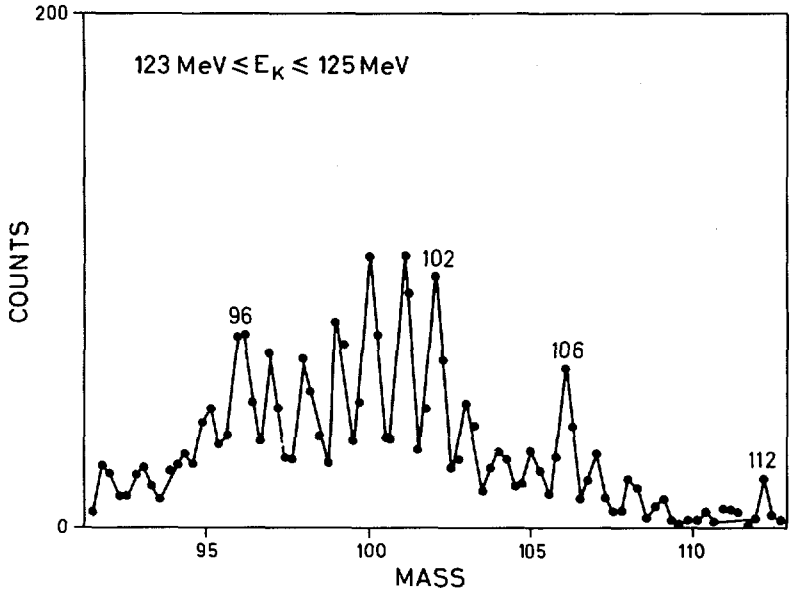

Fig. 7. Mass distribution of cold fragments

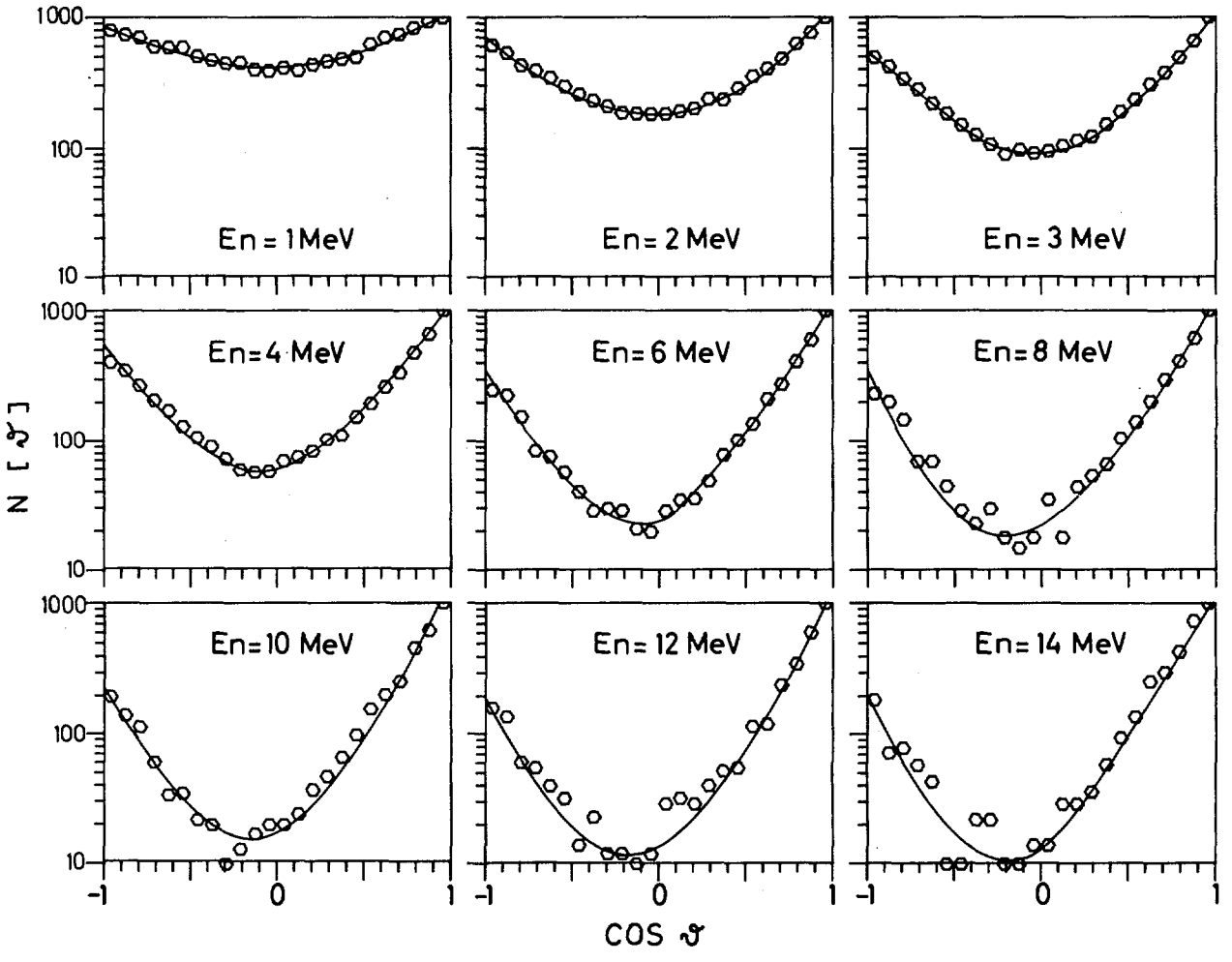

Fig. 8. Neutron angular distributions for energies between 1 and 14 MeV

From the angular distributions averaged over all fragment masses the intensity ratio N(90°)/N(0°) was evaluated as function of the neutron energy and is plotted in Fig.9. The present data agree fairly well with the early results of BOWMAN et al.[1] below 4 MeV. However, at higher neutron energies our data are much more anisotropic with intensity ratios N(90°)/N(0°) more than one order of magnitude smaller than those of Bowman above 8 MeV. The comparison between the present angular anisotropy measurements as function of fission neutron energy and those of Bowman is shown in Fig. 9. The full line in Fig. 9.represents calculations of the angular anisotropy as function of the neutron energy with the assumption that all neutrons are emitted from the fully accelerated fragments.

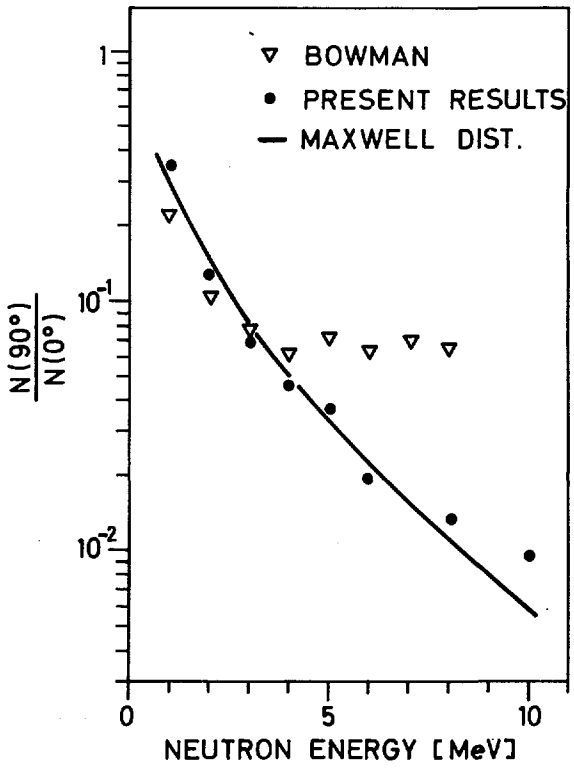

Fig. 9. The neutron-fragment intensity ratio N(90°)/N(0°) versus the neutron energy

The energy dependence of the present N(90°)/N(0°) intensity ratio agrees with the assumption that all neutrons are emitted from the fully accelerated fragments and the existence of a hard (T = 2.0-2.5 MeV) scission neutron component which Märten[2] concluded from the Bowman angular distributions must be refuted. A more thorough analysis of our angular distributions is needed in order to decide whether perhaps a soft component is present.

A preliminary evaluation of the mass integrated prompt fission neutron spectrum of $^{252}Cf(S,F)$ was made from a part of the available data. For this evaluation the neutron detection efficiency, which is needed to obtain the spectrum shape, was calculated using the Monte-Carlo code from the thorough

---

(1) H.R. Bowman, S.G. Thompson, J.C.D. Milton, W.J. Swiatecki, Phys. Rev. 126,2120 (1962).

(2) H. Märten, Proc. IAEA Consultants' Meeting, Smolenice, INDC(NDS)-146, 195 (1983).

detector efficiency investigation of Dietze and Klein[1]. This code calculates the absolute neutron detection efficiency for a given pulse height threshold. These calculations will in future also be backed up by detector efficiency measurements. The spontaneous fission process is not only accompanied by neutrons but also by γ rays which might be detected by the neutron detector. Most of the γ-emission occurs at the instant of scission and up to a few ns later. In this time interval also the highly energetic neutrons are emitted with a very low intensity. In the present evaluation special attention was given to avoid interference of the γ-rays with the neutron spectrum.

This spectrum divided by $E^{\frac{1}{2}}$ is plotted in Fig. 10 versus the incident neutron energy. The full line in Fig. 10 represents the result of a least squares fit through the experimental data using a Maxwellian energy distribution. This preliminary neutron energy spectrum shows no major deviations from the Maxwell distribution in the neutron energy range from 0.8 MeV to 20 MeV. The deviations from the Maxwell distribution are in general less than 5% in the above-mentioned range. The dashed line corresponds to the experimental spectrum measurements of Märten et al.[2], who found a large excess of neutrons above 20 MeV. With the presently evaluated data we cannot confirm nor contradict the measured excess of neutrons.

From a total of about $2 \cdot 10^6$ events the statistics obtained in the high energy region above 20 MeV is not sufficient. The two data points with values $>10^{-2}$ at the highest neutron energy contain only one event each. Points plotted at the 10^{-2}-line contain zero events.

The grid signals of the twin ionization chamber are energy-, angle-, mass- but also nuclear charge dependent. Using both the anode and the grid signals a procedure was developed to extract the information on the nuclear charge of the fission fragments. This was done for fission events where the total kinetic energy for a specific mass split was ~ 30 MeV higher than the average total kinetic energy. With this condition neutron emission from fragments is rather improbable and therefore the fragment masses are unequivocally defined by the light and heavy fragment kinetic energies.

---

(1) G. Dietze and H. Klein, Bericht ND-22, PTB (1982).

(2) H. Märten, D. Seeliger, B. Strobinski, Proc. Int. Conf. Nucl. Data for Sci. Techn., Antwerp 1982, p.488.

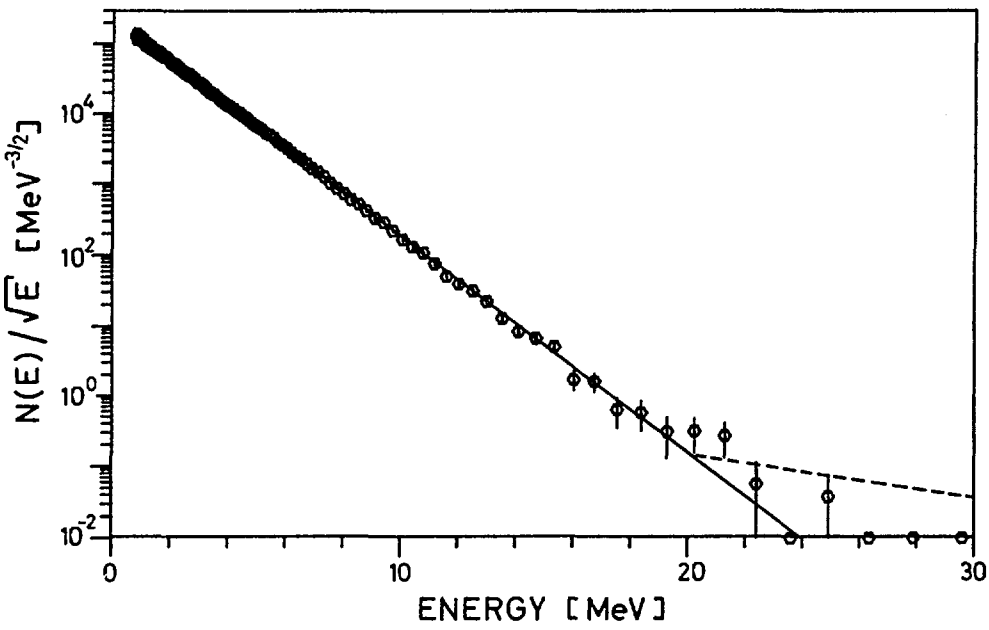

Fig. 10. Preliminary neutron energy spectrum divided by $E^{\frac{1}{2}}$ versus the neutron energy.

The result for the Z-distribution for all fragments with TKE $\geq \overline{\text{TKE}}$ + 30 MeV is shown in Fig. 11.

One can see that the even charges from Z = 40 to 48 are very pronounced and well resolved. For further illustration of the Z-resolution the Z-distributions for the specific light fragment masses 104 and 106 are selected in Fig. 12, also for TKE $\geq \overline{\text{TKE}}$ + 30 MeV.

The Z-distribution for mass 106 is almost entirely composed of Z = 42, with only very small contributions of nuclear charges 41 and 43, as indicated in Fig. 12.

In contrast to mass 106, the Z-distribution of mass 104 is composed of the nuclear charges 40, 41, 42 and 43 with almost equally large contributions for Z = 41 and 42 and with clear satellites of Z = 40 and 43 ($\Delta Z/Z \simeq 1/40$). This is the first time that a useful resolution for nuclear charges of fission fragments could be obtained with an ionization chamber and this independently of the fragment emission angle with respect to the chamber axis.

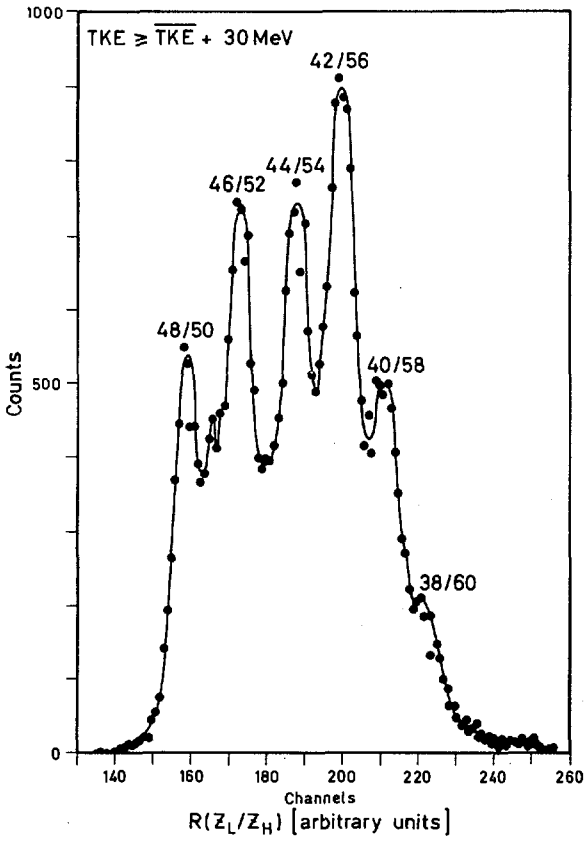

Fig. 11. R(Z_L/Z_H)-distribution for ^{252}Cf(S,F)

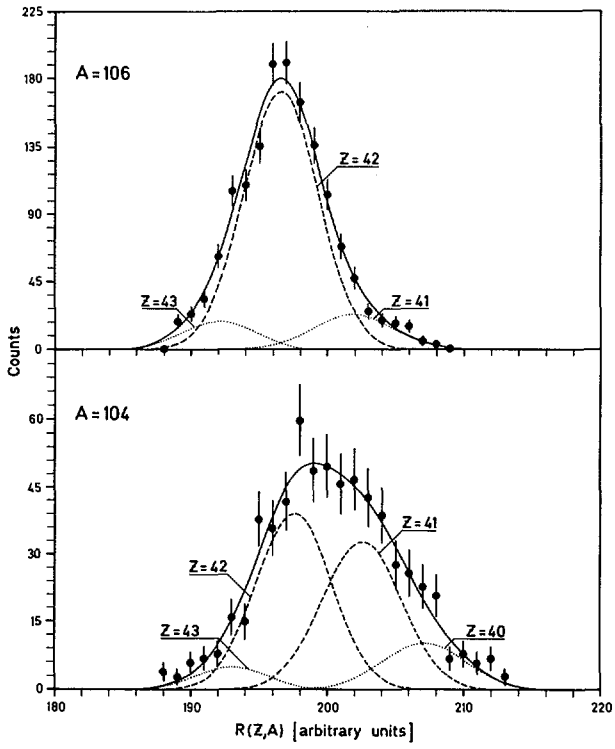

Fig. 12. Isobaric R-distributions

Proportional Counter for Absolute Neutron Flux and Standard Neutron Cross-Section Measurements

K.H. Böckhoff, A. Brusegan, H. Riemenschneider, T. van der Veen

A proportional counter for absolute neutron flux and standard neutron cross-section measurements has been constructed with following basic design considerations.

- Flexibility: The counter can be easily disassembled into its elements by using metal joints and metal-ceramic connections as they are used in ultrahigh-vacuum applications. Therefore counting wires and anodes can be exchanged without destructing the counter.
- Cleanliness: The counter can be baked at 400°C to avoid contamination by ions as far as they could stem from molecular layers on the inner surfaces of the construction elements.
- No wall effects: The difference between the neutron collimation and the cathode diameters is such that neither from the $^{1}H(n,p)$ nor from the $^{10}B(n,\alpha)$ reaction the respective charged particles can reach the cathode (for the highest neutron energy considered).
- Counting volume independent of the neutron energy and reaction type (equivalent to the condition that the end effects are small and can be measured with appropriate accuracy): This can be fulfilled by the addition of "field counter tubes" on either side of the counter which have the same diameter and the same potential as the main tube.
- Reasonable rise time of the pulses: This implies a comparatively thick counting wire and a high tension (corresponding to the chosen multiplication factor), together with a reduced gas pressure.

The counter is schematically represented in Fig. 13.

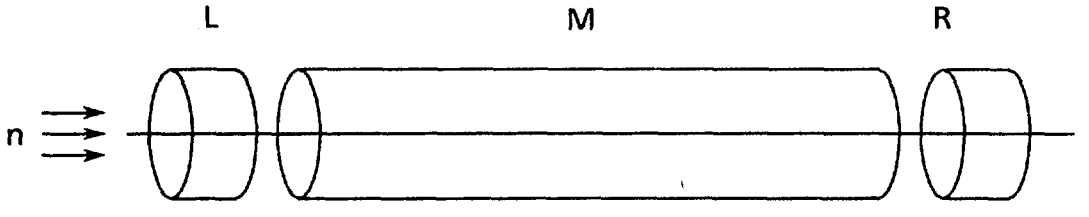

Fig. 13. Schematic view of the counter

The first choice of design and operation parameters (see Fig. 13) is listed below:

lengths	M	:	30 cm
	L and R	:	10 cm
wire diameter		:	0.08 cm
cathode diameters		:	13 cm
gas filling		:	CH_4 at 30 kPa
voltage		:	6 kV

Consideration of the end effects: At the ends of the counter tube the electrical field is disturbed, leading there to locally decreasing multiplication factors. The consequence is a worsening of the amplitude resolution and an unsufficiently defined counter volume. The field distortion is effective over a length of about one cathode diameter, measured from the counter faces inward.

The classical approach to avoid or reduce such end effects is to add on either side of the counter one or more "field tubes" of different diameters. They are kept on different potentials calculated to achieve an optimum field homogenization. In addition the counter wire outside the counter is made so thick that there no multiplication can occur. By this means the counter volume can be more precisely defined.

The deficiencies of this method are:

Although there is no multiplication outside the counter, it still counts reactions which happen outside: Charged particles generated from reactions close to the end faces of the counter may reach the counting volume and hence are measured. These parasitic events which have a smaller amplitude than corresponding "good" pulses have to be considered in precision neutron flux measurements.

Reactions which are generated inside the counter M but close to the end faces do not spend all their charged particle energy inside M and are registered with too small amplitudes.

In the approach chosen here the field tubes have the same diameter and potential as the counter tube. The gap between the tubes L and M as well as that between M and R are very small as compared to the cathode diameter. The lengths of L and R are equal to one cathode diameter. In this way the field distortion at the ends of counter M is minimized.

The main difference to other solutions is that the field tubes also have the function of proportional counters. By demanding coincidence between respectively the L/M and M/R counters and summing the amplitudes of the coincident pulses, one can reconstruct the pulse shape of all those events which happen in the "correction zones" on either side of each end face of the counter M. By means of this information one can determine directly the required correction for the end effects of the counter. A detailed treatment of the method yields in good approximation:

$$R_o = R_m - R_{1m1}$$

with R_o: number of reactions originated exclusively in M

R_m: number of all reactions which have charged particle traces ending in M (also from those originated in L and R)

R_{1m1}: number of reactions which have charged particle traces both in L or R and M ("coincident events")

Achievements: The counter has been assembled, baked out, filled and put into operation. First test runs have been made on the last two working days of the year. They will be continued and supplemented by a series of other tests after the cold neutron campaign in the beginning of 1986.

1.1.2 Non-Neutron Data for Standards

Decay Data of ^{47}Sc

D. Reher, H.H. Hansen, R. Vaninbroukx

The nuclide ^{47}Sc is mainly used in nuclear medicine for tumor imaging. In addition it can be used for efficiency calibration of solid-state detectors at 160 keV. This calibration is specially needed in activity measurements of the short-lived ^{123}I nuclide which emits γ rays of 159 keV and is also applied in nuclear medicine.

Subsequent to an international comparison to measure the radioactivity concentration of a ^{47}Sc solution several important decay-scheme data were remeasured in a joint effort by NPL, LMRI and CBNM. A common publication together with these laboratories is in press [1].

---

[1] D. Reher, H.H. Hansen, R. Vaninbroukx, M.J. Woods, C.E. Grant, S.E.M. Lucas, J. Bouchard, J. Morel, R. Vatin, Int. J. Appl. Radiat. Isot. in press.

The recommended values deduced from the results of the three laboratories are:

Half life	: $T_{1/2}$ = (3.3492 ± 0.0006)d
γ-ray emission probablity	: P_γ = 0.683 ± 0.004
β-ray emission probabilities	: P_{β_1} = 0.316 ± 0.006
	: P_{β_2} = 0.684 ± 0.006
β-ray endpoint energies	: E_{β_1} = (600.5 ± 1.9) keV
	: E_{β_2} = (439.0 ± 1.6) keV
K-shell conversion coefficient	: α_K = (4.06 ± 0.21)·10^{-3}
L+M+ ...-shell conversion coefficient	: α_{L+} = (4.1 ± 1.0)·10^{-4}
Total conversion coefficient	: α_T = (4.5 ± 0.3)·10^{-3}

Decay of ^{133}Ba

H.H. Hansen, D. Mouchel, R. Vaninbroukx, W. Zehner

The nuclide ^{133}Ba is widely used as a radioactivity standard for detector calibration. The exact knowledge of the half life is most important. JRC-Geel is following the decay of this nuclide for several years. New sets of γ-ray spectra for the determination of the half life of ^{133}Ba have been recorded with the HPGe detector and with the NaI(Tl) spectrometer. The measurements will be continued.

Half Life of ^{241}Pu

R. Vaninbroukx

The half-life value of ^{241}Pu is requested to an accuracy of 0.5 % for mass determination and non-destructive assay. One experiment of CBNM performed by mass-spectrometric means yielded a value of (14.33 ± 0.02)a[(1)]. A result with such narrow uncertainty limits has to be confirmed by at least a second measurement employing other experimental methods in order to be able to detect possibly hidden experimental errors in the previous experiment.

---

(1) P. De Bièvre, M. Gallet, R. Werz, Int. J. Mass Spectr. Ion Phys., 51, 111 (1983).

Direct decay measurements were started 2.6 years ago using a high-purity Ge detector and four ^{241}Pu sources. The decrease of the count rates in the peaks of the uranium $K_{\alpha 2}$ X rays and the gamma rays at 148.6, 164.6 and 208.0 keV, respectively, was followed. The increasing amount of ^{241}Am grown into the sample makes the evaluation of the uranium $K_{\alpha 2}$ X ray less accurate due to interferences from the neptunium K X rays. The results obtained for the gamma rays are more reproducible and reliable than the uranium $K_{\alpha 2}$ X ray results. During the 2.6 years of observation only 12 % of the ^{241}Pu decayed. Consequently, the accuracy is not better than 1.5 %. The preliminary result is $T_{1/2}(^{241}Pu) = (14.3 \pm 0.2)a$. There is a good agreement with the mass-spectrometric experiment, but the uncertainty is still a factor of 10 larger. The measurements will be continued.

Decay of ^{242}Pu

R. Vaninbroukx, G. Bortels, B. Denecke

For accurate assay of Pu samples containing ^{242}Pu, for Pu-mass determination and for environmental studies, α-particle and γ-ray emission probabilities of ^{242}Pu are required both with accuracies of 5 %. In literature there were only very few experimental data available with uncertainties between 5 and 40 %.
The α-particle emission probabilities in the decay of ^{242}Pu were measured using a surface-barrier detector in connection with a small magnet which eliminated most of the conversion electrons. The γ-ray emission probabilities were deduced from the γ-ray emission rates, measured with calibrated high-purity Ge detectors, and the ^{242}Pu disintegration rates, determined by α-particle counting in well-defined solid angles. For some of the sources they were also calculated from the ^{242}Pu content measured by mass-spectrometric isotope dilution. The results are shown in Table 1. The measurements reduced the inaccuracies by a factor 5 to 20.
A paper describing this study has been submitted for publication to Int. J. Appl. Radiat. Isot.[1].

---

[1] R. Vaninbroukx, G. Bortels, B. Denecke, submitted for publication to Int. J. Appl. Radiat. Isot.

Table 1. Measured α-particle (P_α) and γ-ray (P_γ) emission probabilities

Levels in ^{238}U (keV)	Emission energies		P_α	P_γ
	E_α (keV)	E_γ (keV)		
307	4598	158.8		$(2.6 \pm 0.7)\ 10^{-6}$
148	4755	103.5	$(2.90 \pm 0.14)10^{-4}$	$(2.63 \pm 0.09)10^{-5}$
45	4856	44.92	0.2352 ± 0.0017	$(2.72 \pm 0.07)10^{-4}$
0	4901	0	0.7645 ± 0.0017	

Decay of ^{241}Am

B. Denecke

The radionuclide ^{241}Am is widely used as γ-ray source in the energy region below 100 keV. It supplies calibration points for detector efficiency calibration in the energy region between 10 and 60 keV through two relatively intense γ rays at 26.35 and 59.54 keV and the L X-ray series of Np. In particular, the emission probability of the 59.54 keV γ rays is requested with the highest obtainable accuracy.

To meet these requirements the 4π-CsI(Tl)-sandwich spectrometer has been improved resulting from the experience gained from measurements in the ^{109}Cd standardization project.

Eight new ^{241}Am sources were prepared by evaporation of ^{241}Am under vacuum onto 450 $\mu g/cm^2$ thick mylar foils. The backing foils of the sources used until now suffered from radiation damage. The activities of the new sources were determined by α-particle counting in defined solid angles. The final measurements of will start in 1986.

Evaluation of X- and Gamma-Ray Emission Probabilities

W.. Bambynek, R. Vaninbroukx

This project originates from a consultants' meeting on Gamma-Ray Standards for Detector Calibration, which was held at the CEN Grenoble, 30 and 31 May 1985, on recommendation of the INDC to assess the current status of X-

and γ-ray emission data for detector calibration [1]. The JRC Geel accepted responsibility for all X-ray emission probabilities of the provisional list of nuclides drawn up during the meeting and for the γ-ray emission probabilities of ^{228}Th, ^{241}Am and ^{243}Am-^{239}Np. A thorough assessment has been made on the basis of two evaluations which were prepared for an IAEA Advisory Group Meeting on Nuclear Standard Reference Data in 1984 [2][3] and the final report of the IAEA Coordinated Research Project on the Measurement and Evaluation of Transactinium Isotope Nuclear Data [4].
A programme of data measurements and evaluations will be established under the auspices of an IAEA Coordinated Research Programme in which CBNM will participate. The aim of this effort is to establish a single internationally-accepted set of X- and γ-ray detector calibration data of improved quality to meet the needs in the various fields of applications.

Compilation of Experimental Values of Internal Conversion Coefficients and Ratios for Nuclei with Z > 60

H.H. Hansen

The compilation[5] contains about 12.500 data of experimental values of internal conversion coefficients and ratios from about 1100 references.
Results quoted with an error and published prior to October 1982 have been retained. Separate tables have been prepared for results from studies on radioactive nuclides, from nuclear reaction experiments, from measurements on E0 transitions ($0^+ \rightarrow 0^+$), and from studies in different chemical environments. The tables include information on the origin of the isotope, transition energies, spin and parity of initial and final levels, experimental technique used, and literature references.

---

(1) A. Lorenz, INDC(NDS)-171/GE, October 1985.

(2) R. Vaninbroukx, Nuclear Standard Reference Data, IAEA-TECDOC-335 (International Atomic Energy Agency, Vienna, 1985) p. 403.

(3) W. Bambynek, Nuclear Standard Reference Data, IAEA-TECDOC-335 (International Atomic Energy Agency, Vienna, 1985) p. 412.

(4) R. Vaninbroukx, W. Bambynek, Decay Data of the Transactinium Nuclides, Technical Report Series No. (International Atomic Energy Agency, Vienna, 1985) in press.

(5) H.H. Hansen, Physik Daten-Physic Data 17-2 (1985) (Fachinformationszentrum Energie, Physik, Mathematik, Karlsruhe).

Evaluation of K-Shell and Total Internal Conversion Coefficients for some Selected Nuclear Transitions

H.H. Hansen

Recommended values of K-shell and total internal conversion coefficients for a series of selected nuclear transitions suitable for detector calibration have been deduced by evaluating published experimental data[1]. Relevant information on the individual evaluation of the considered transitions is given. Theoretical internal conversion coefficients have been interpolated from appropriate tabulations for reasons of comparison. A list of the recommended values is given in Table 2.

Table 2. Recommended values for some internal conversion coefficients

Energy E_γ (keV)	Origin	Recommended values	
		α_K	α
14.413	^{57}Co	7.35 ± 0.19	8.18 ± 0.11
88.034	^{109}Cd	11.1 ± 0.2	26.0 ± 0.3
122.061	^{57}Co	(2.14 ± 0.12)·10^{-2}	(2.40 ± 0.14)·10^{-2}
136.474	^{57}Co	0.122 ± 0.013	0.137 ± 0.015
145.444	^{141}Ce	0.372 ± 0.006	0.435 ± 0.009
165.853	^{139}Ce	0.2146 ± 0.0010	0.2516 ± 0.0007
279.197	^{203}Hg	0.1640 ± 0.0010	0.2271 ± 0.0012
320.078	^{51}Cr	(1.54 ± 0.03)·10^{-3}	(1.69 ± 0.05)·10^{-3}
336.23	^{115}In^m	0.843 ± 0.011	1.072 ± 0.014
391.688	^{113}In^m	0.437 ± 0.004	0.540 ± 0.004
411.804	^{198}Au	(3.01 ± 0.02)·10^{-2}	(4.4 ± 0.2) ·10^{-2}
834.843	^{54}Mn	(2.24 ± 0.10)·10^{-4}	(2.51 ± 0.11)·10^{-4}
1115.546	^{65}Zn	(1.66 ± 0.06)·10^{-4}	(1.85 ± 0.07)·10^{-4}
1173.238	^{60}Co	(1.51 ± 0.07)·10^{-4}	(1.68 ± 0.04)·10^{-4}
1274.545	^{22}Na	(6.3 ± 0.6) ·10^{-6}	(6.8 ± 0.4) ·10^{-6}
1332.513	^{60}Co	(1.15 ± 0.05)·10^{-4}	(1.28 ± 0.05)·10^{-4}

(1) H.H. Hansen, European Appl. Res. Rept. - Nucl. Sci. Technol., 6, 777 (1985).

1.2 NUCLEAR DATA FOR FISSION TECHNOLOGY

1.2.1 Neutron Data of Actinides

Neutron data of actinides are still on the IAEA and NEA high priority lists. Although most of these relate to fast fission reactors, there are still unresolved important neutron data issues also for thermal reactors. The investigations are concentrated on data of the major fission reactor core constituants.

A discrepancy is known to exist between the calculated temperature coefficient of reactivity for light water reactors and measured values obtained in integral experiments. It has therefore been proposed by Santamarina et al.[1] that the energy dependence of certain differential nuclear data in the sub-thermal neutron energy region be modified with respect to ENDF/B-V within their experimental uncertainties, in order to remove this discrepancy.

On the other hand it has been suggested by French and British reactor physicists to remeasure those quantities at the CBNM Linac (GELINA). To this end a liquid methane (- 170°C) moderator has been installed at GELINA and several campaigns of simultaneous measurements with cold neutrons have been performed.

Fission cross section of ^{235}U

C. Wagemans*, A. Deruytter, R. Barthélémy, J. Van Gils*
(European High Priority List NEACRP-A-568, NEANDC-A-180)

The cross section was measured relative to the standard ^{6}Li by means of large area surface barrier detectors at a distance of 8.2 m from the target. Figure 14 shows the results of the first series of measurements. Above 10 meV the data agree well with the ENDF-B/V evaluation. Below that energy the σ_f-values tend to be 1-2 % lower than those of ENDF-B/V and approximate more closely a $1/\sqrt{E}$ shape.

---

(1) A. Santamarina, C. Golinelli, L. Erradi, ANS Topical Meeting on Reactor Physics, Chicago 1984.

* SCK/CEN, Mol, Belgium.

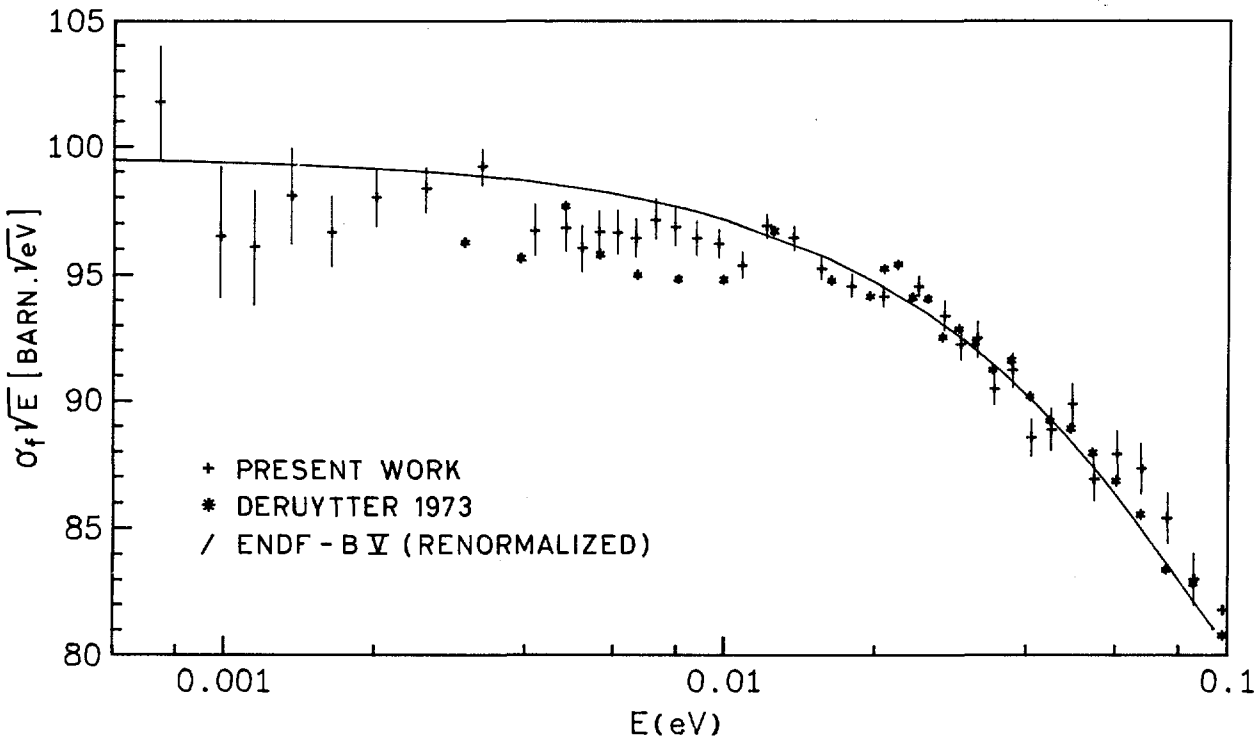

Fig. 14. The $\sigma_f(E)\sqrt{E}$-data obtained from the present experiments (+) compared with the data of Deruytter et al (*) and with ENDF/B-V (full line) renormalized to σ_f° = 587.6 barn

A second measurement campaign has been performed under identical conditions and with the same statistical accuracy as the first one. These data have been analysed. Also here the σ_f-values below 10 meV tend to be slightly lower than those of ENDF/B-V. To make sure that the σ_f-values obtained are independent of the neutron flux monitor used, an additional measurement using a $^{10}B(n,\alpha)^7Li$ flux monitor will be performed.

Eta(η) of ^{235}U

H. Weigmann, J.A. Wartena, C. Bürkholz
(WRENDA 83/84 request N° 465 and European High Priority List NEACRP-A-568, NEANDC-A-180)

An experiment has been set up to measure the energy dependence of eta of ^{235}U, the number of fission neutrons produced per neutron absorbed. A "black" ^{235}U sample which is sufficiently thick to absorb all neutrons with energies of interest is exposed to a neutron beam from the liquid methane

moderator. The relative number of fission neutrons emerging from this sample is measured with a NE213 liquid scintillator with pulse shape discrimination.

The neutron flux is monitored with two parallel plate proportional counters loaded with thin layers of ^{6}Li and $^{235}UF_4$. The definite measurement of the neutron flux shape at the position of the black uranium sample is done in separate runs by recording the yield of 480 keV γ rays from a thick ^{10}B slab replacing the black uranium sample.

The main problem in the present experiment is due to background events in the measurement of fission neutrons with the liquid scintillator: The number of neutrons per time-of-flight interval in the neutron beam at times corresponding to energies above ~ 20 meV is 2 orders of magnitude larger than at 2 meV. Essentially each of these neutrons hitting the black uranium sample produces 2.4 fission neutrons which may be slowed down in the surroundings of the sample and eventually initiate a background fission event in the sample at a later time when the foreground due to a much smaller incoming flux is to be measured. In order to keep this background as small as possible, the black uranium sample was placed into a cylindrical ^{6}Li sleave to protect it against backscattered neutrons, and a 2 cm thick Be filter was placed in the neutron beam which reduces the neutron flux above 6.8 meV energy by a factor of 4 while leaving the flux at low energies almost unchanged.

Another problem is presented by the dead-time of the Pulse Shape Discrimination (PSD) circuit. Every signal which is analysed by the PSD produces a dead-time of this circuit of about 2 μs, also if the event is rejected as being due to a γ ray. The rate of γ-ray events is rather high, especially at short flight times. Corrections necessary due to the PSD dead-time are smaller than 1 % for neutron energies below 0.3 eV, but become considerably larger above that energy.

Apart from dead-times and backgrounds, the data have to be corrected for incomplete absorption and scattering in the "black" uranium sample and in the ^{10}B slab. These corrections have been calculated by an approximate analytical expression as well as by a Monte-Carlo routine, using total and scattering cross sections as given in the literature. The error introduced in this calculation due to uncertainties in the cross sections used is smaller than 0.5 % below 0.3 eV. For higher energies it increases rapidly, to about 2.5 % at 0.5 eV. This fact, together with the PSD dead-time correction, limits the energy range for which reliable data are obtained in the present experiment to below about 0.4 eV.

Two independent measurement campaigns have been performed up to now. The results obtained for the energy dependence of eta of ^{235}U is shown in Fig. 15. They are compared to the "reference shape" as well as to the modification proposed by Santamarina et al.[1] The experimental data have been normalized to an average value of 2.082 between 20 and 40 meV neutron energy. The errors are mainly due to the uncertainty in the backgrounds (at low energies) and in the calculation of the correction factors (at high energies) and are thus highly correlated.

The preliminary results from the present experiment agree with the essentially flat energy dependence of eta as given in ENDF/B-V, rather than with the modification proposed by Santamarina et al. In order to reduce the systematic uncertainty of the present experiment, the background due to out-of-time neutrons, especially in the measurement with the black uranium sample, has to be reduced. The best way to reach this goal would be the use of a pulsed mono-energetic neutron beam.

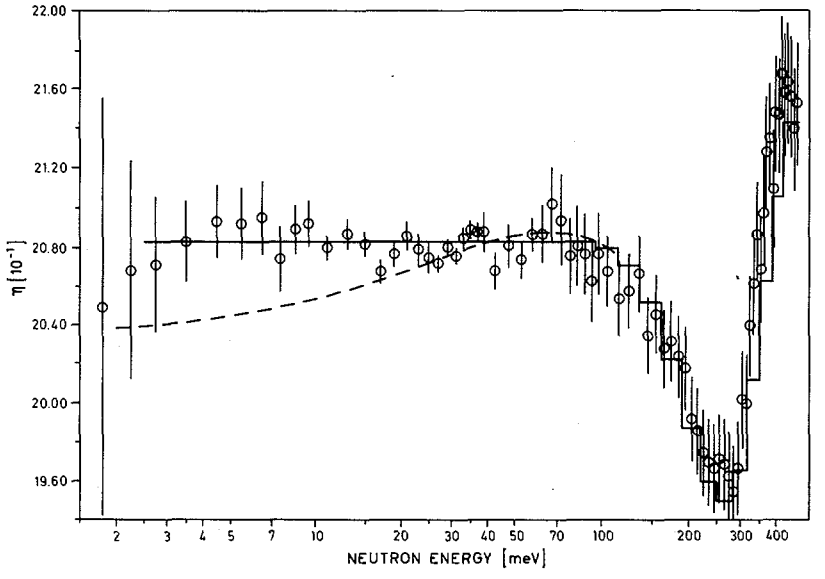

Fig. 15. The measured energy dependence of eta of ^{235}U compared to the reference shape (—) and the modification (-----) proposed by Santamarina et al.[1]

---

(1) A. Santamarina, C Golinelli, L. Erradi, ANS Topical Meeting on Reactor Physics, Chicago 1984.

Capture Cross Section of ^{238}U

F. Corvi, A. Prevignano*, H. Riemenschneider, T. van der Veen
(WRENDA 83/84 request N° 1028 and European High Priority List)

A first measurement campaign was carried out with a metallic foil of highly enriched (99.999 %) uranium metal of 13.78 g. The sample, surrounded by a 6 mm thick ^{6}Li sleeve was viewed by four C_6D_6 liquid scintillators housed in a large shielding facility on loan from SCK/CEN, with walls made of 14 cm thick lead and 25 cm thick borated wax. Best signal-to-background conditions were obtained by counting coincidences between pulses from any two detectors. It is believed that in this particular case the coincidence rate is proportional to the total capture rate since the shape and multiplicity of the capture γ-ray spectrum are not expected to vary appreciably in this small energy range for a nucleus such as ^{238}U with fixed spin and parity (at thermal energy) and high level density.

Time dependent background was measured by replacing the sample with an equivalent graphite scatterer. On the other hand, neutron flux was measured by replacing ^{238}U with a ^{10}B slab 0.6 mm thick and looking at the 480 keV γ rays with the same detectors: the constancy of the flux during the various runs was checked by a double gridded ionization chamber placed in the beam before the shielding and loaded with back-to-back deposits of ^{10}B of 5 $\mu g/cm^2$ thickness.

In a second measurement campaign the metallic sample was replaced by a 60 g sample of U_3O_8 enriched to 99.999 % ^{238}U. This material was measured immediately after a chemical purification carried out by the Sample Preparation group so that the amounts of radioactive decay products, and in particular of thorium, were strongly reduced with respect to the secular equilibrium case. As a consequence, the constant background due to sample activity decreased accordingly as compared to the first run, however this was partly compensated by an increase of the energy dependent background due to multiple scattering from the sample and to neutron-capture in the aluminium container.

---

* EC Fellow.

The results of both runs were found in reasonable agreement: in Fig. 16 is plotted the cross-section curve proposed by Santamarina et al.[1] together with the present results for the U-oxide case. These last data, which have been normalized to the previous curve in the region around 0.100 eV, are clearly in disagreement with the suggestion of ref. [1].

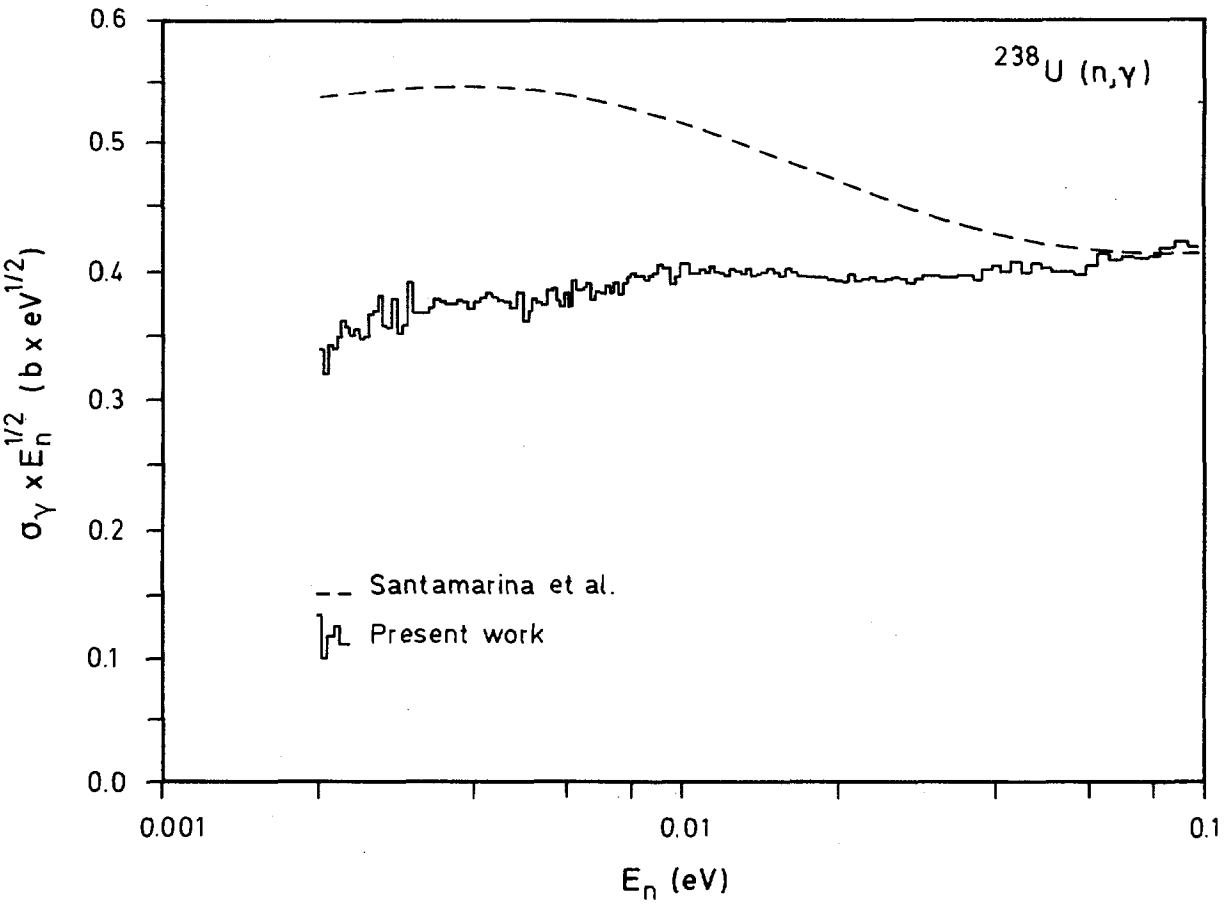

Fig. 16. Present results compared to the cross section curve suggested by Santamarina et al.[1]

(1) A. Santamarina, C. Golinelli, L. Erradi, ANS Topical Meeting on Reactor Physics, Chicago 1984.

Fission Fragment Mass and Energy Distributions for the Spontaneous Fission of the Pu Isotopes.

C. Wagemans*, P. Schillebeeckx*, A. Deruytter, R. Barthélémy

The study of the energy and mass characteristics of spontaneously fissioning $^{238,240,242}Pu$ isotopes has been finalised. All three fissioning systems were calibrated with the $^{239}Pu(n_{th},f)$ reaction. The corresponding fission fragment mass-distributions are shown in Fig. 17. This figure shows strongly varying structures due to neutron shell effects, which can be interpreted in terms of the static scission point model of Wilkins et al.[1] and Moreau and Heyde[2]. The dominant peak for heavy masses (~135) in the spontaneous fission of ^{242}Pu is due to the combined influence of the neutron shells N = 82 in the heavy and N = 64 in the light fragment. For ^{238}Pu on the other hand, only the neutron shell N = 82 plays a role, which explains the smaller peak yield. Another example is the higher peak yield observed in ^{238}Pu(s.f.) around mass 142, which can be explained by the combined influence of the neutron shells N ≈ 86 in the heavy and N ≈ 58 in the light fragment. For ^{242}Pu(s.f.) both shells do not coincide, which explains the reduced yield at mass ≈ 142.

Fission cross section of ^{243}Am

H.-H. Knitter, C. Budtz-Jørgensen, R. Vogt, H. Bax
(WRENDA request Nos. 712111R, 792236R)

The cross sections of this isotope are of interest for nuclear waste management. The fission cross section was measured at the 7 MeV Van de Graaff between 0.3 MeV and 9.95 MeV and at GELINA between 1 eV and 1.4 MeV.

The measurements which were performed relative to the fission cross section of ^{235}U and to the $^{6}Li(n,\alpha)$ cross section used a fast ionization chamber which was previously also applied in similar measurements on ^{238}Pu and ^{240}Pu. The results covering more than 6 orders of magnitude in neutron energy are shown in Figs. 18, 19 and 20.

---

* SCK/CEN, Mol, Belgium.

(1) B.D. Wilkins, E.P. Steinberg, R.R. Chasman, Phys. Rev. C14, 1832 (1976).

(2) J. Moreau, K. Heyde, Phys. Mag. 5, 91(1983).

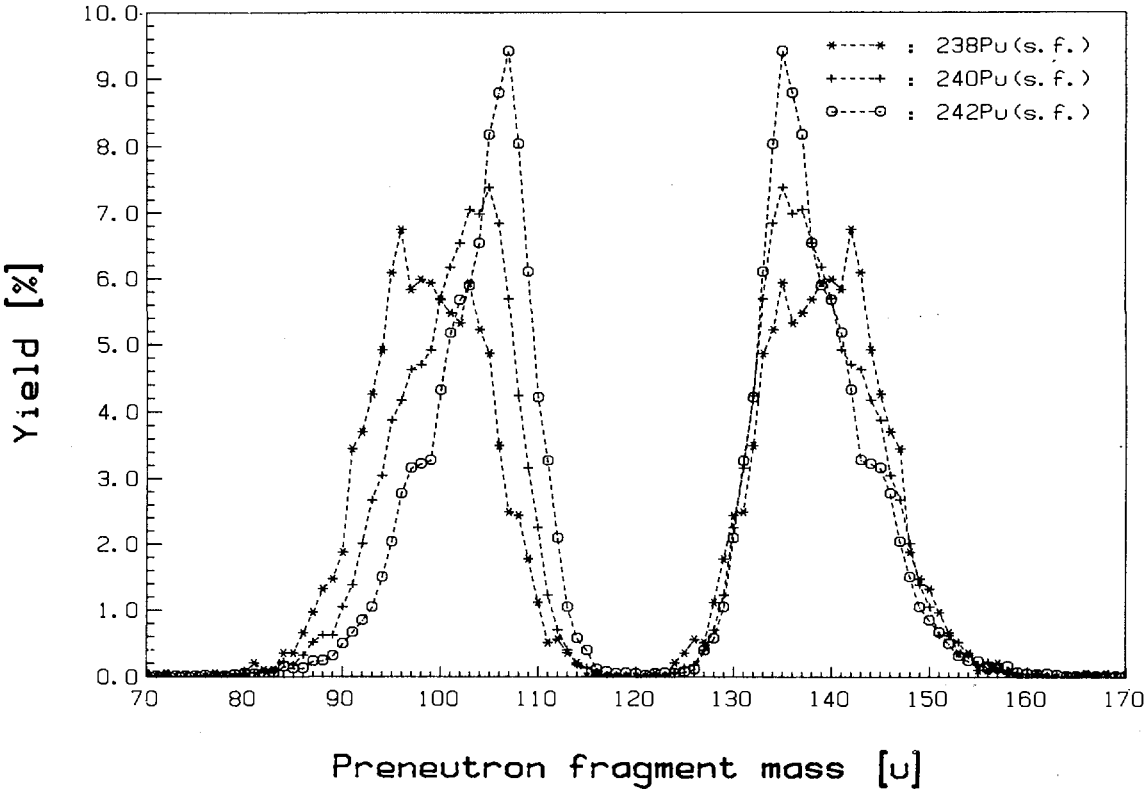

Fig. 17. Comparison of the mass yield distributions for ^{238}Pu, ^{240}Pu and ^{242}Pu

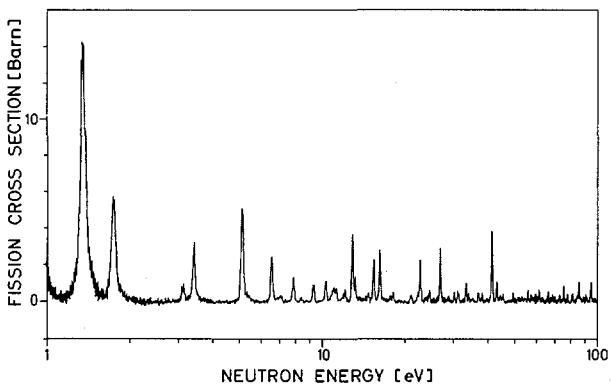

Fig. 18. ^{243}Am fission cross section

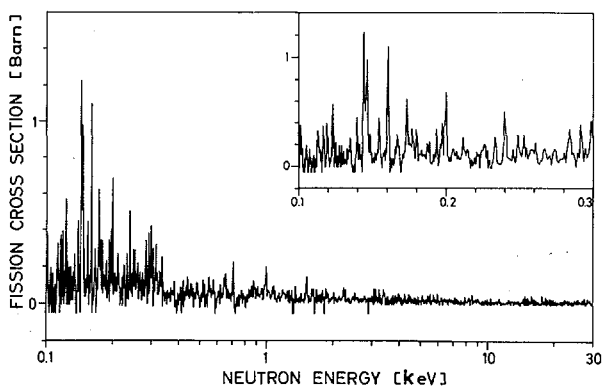

Fig. 19. ^{243}Am fission cross section

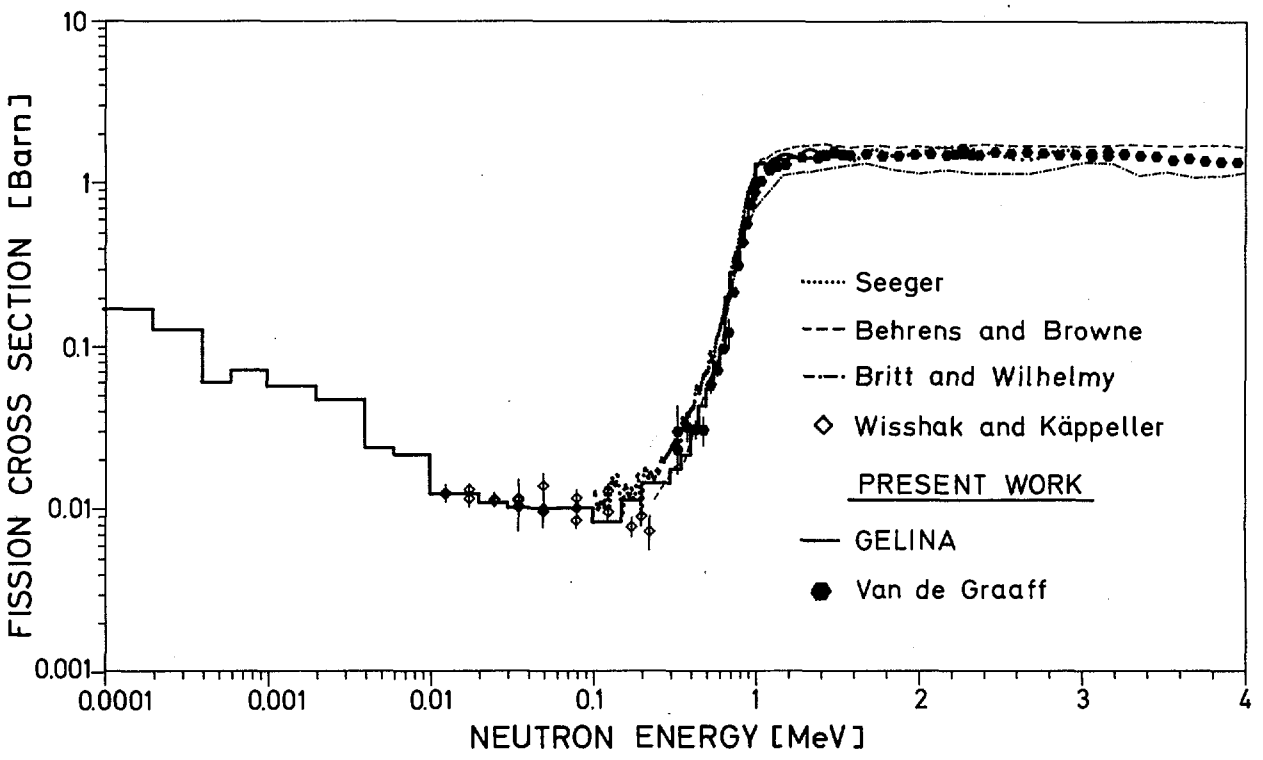

Fig. 20. ^{243}Am fission cross section

1.2.2 Neutron Data of Structural Materials

A fast nuclear power reactor core contains about 25 % of stainless steel. The most stringent neutron data requirements result from neutron balance conditions which are mainly affected by the radiative capture of neutrons in those materials below 0.5 MeV neutron energy. The commonly accepted goals for the design accuracy in k_{eff} and breeding gain of 0.5 to 1 % and 2 % respectively, lead to a request of the capture cross-section uncertainty of 5 to 10 % for Fe and 10 to 20 % for Cr and Ni. The capture measurements on the isotopes of these elements are exceedingly difficult, due to the scattering process dominating the capture process by 3 to 4 orders of magnitude. The γ-ray multiplicity is low with a large share of high energy γ-rays and complicates the measurements.Despite the large effort which was spent at various laboratories (Oak Ridge, Lucas Heights, Harwell, Karlsruhe, Geel), some results are still discrepant in particular for the 1.15 keV resonance of ^{56}Fe which dominates the neutron capture in the structural material present in a fast reactor.

Determination of the Response Function of C_6D_6 Detectors to Monochromatic γ Rays

F. Corvi, A. Prevignano*, T. van der Veen, H. Riemenschneider
(relevant to 1.15 keV task force of NEANDC)

In order to assess the efficiency and response function of C_6D_6 liquid scintillators to high energy γ rays, measurements of (p,γ) reactions have started at the 7 MV Van de Graaff. This exercise is important in order to shed light into the longstanding problem of the 1.15 keV resonance in ^{56}Fe, where an unexplained discrepancy of about 20 % between capture and transmission data still persists. The experimental set-up is shown in Fig. 21. Proton-capture γ rays emitted from the target are detected by a C_6D_6 scintillator and an intrinsic Ge detector. Both single and coincident events are recorded. When capture is dominated by a few strong two-step cascades, as it is often the case in resonances of some light nuclei, the C_6D_6 efficiency for one γ ray can be derived via the coincidence method i.e. by calculating the ratio between the peak areas of the complementary γ ray in the coincident and single Ge spectra, respectively. Similarly, the response function of a given γ ray is obtained from those C_6D_6 pulses which are in coincidence with the full peak of the complementary transition. Targets of ^{26}Mg, ^{30}Si and ^{34}S have been used at proton energies of 2220, 1398 and 1211 keV, respectively. Also, two step cascades in radioactive sources of ^{22}Na and ^{88}Y have been measured in the same geometry. After some preliminary tests in August, extensive measurements were carried out in September and October. Data sorting and analysis is in progress. The preliminary results are satisfactory, showing the feasibility and reproducibility of the method. The only problem encountered so far was a strong interference of fluorine γ rays in the ^{26}Mg run.

The experiment is performed in collaboration with Prof. P.B. Smith of Groningen University: the possibility is envisaged of repeating the measurements there with better conditions, on a machine which is specialised for (p,γ) work.

---

* EC Fellow.

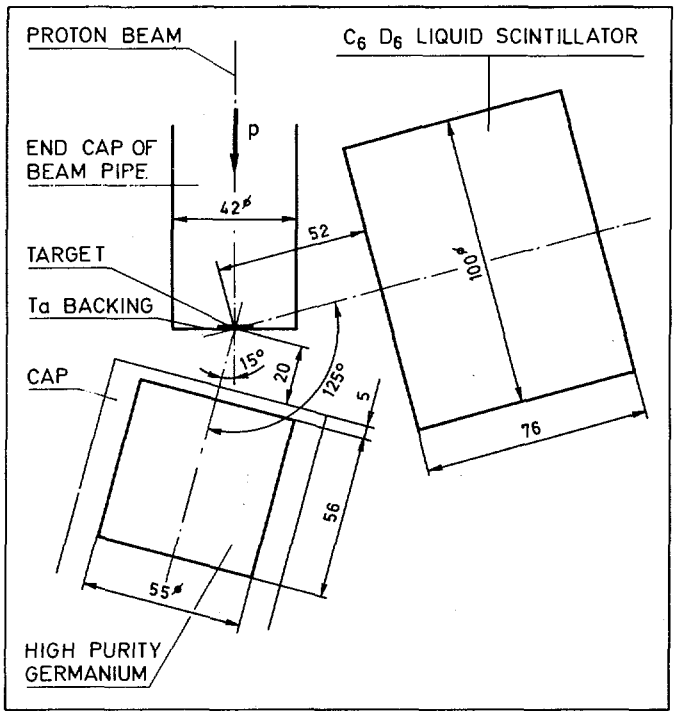

Fig. 21. Experimental set-up for the determination of the γ-ray response function of a C_6D_6 detector using (p, γ) reactions.

Resonance Parameters of Iron Isotopes

^{54}Fe

E. Cornelis*, L. Mewissen**, F. Poortmans**, I. Van Marcke***
(WRENDA 83/84 request N^{os} 356, 357, 361, 362)

The analysis of the transmission data is completed. Neutron resonance widths have been determined between 50 keV and 800 keV using the multi-level shape fitting code MULTI. For an important fraction of the resonances, the spin and parity were deduced from the peak total cross section, resonance-potential or resonance-resonance interference.

---

* RUC Antwerp, Belgium.

** SCK/CEN, Mol, Belgium.

*** Visiting Scientist from VU, Brussels, Belgium.

^{56}Fe

A. Brusegan, C. Van der Vorst
(relevant to the ^{56}Fe task force of NEANDC)

The data obtained recently at a 50 m and at a 100 m long flightpath of GELINA with a 1 mm and a 6 mm thick natural Fe sample (the latter one being cooled down to liquid nitrogen temperature) have been analysed using the SIOB program. Preliminary results are given in Table 3. Satisfactory agreement between the resonance parameters obtained with the different samples on one hand and between our parameters and those reported from ORNL on the other hand can only be achieved if the calculated resolution function width[1] is enlarged at least by 30 %. It is envisaged to study the resolution function experimentally.

Table 3. Preliminary results on ^{56}Fe resonance widths measurements

1 mm Fe sample 50 m flight distance		6 mm Fe sample (at -186°C) 100 m flight distance	
Γ_n(meV)	Γ_γ(meV)	Γ_n(meV)	Γ_γ(meV)
63.1 ± 1.0*	750. ± 61.*	57.7 ± 0.5*	612. ± 21.*
Resolution x 1.3			
62.6 ± 1.0*	560. ± 61.*	59.2 ± 0.5*	560. ± 21.*

* statistical errors only

(1) A. Bignami, C. Coceva, R. Simonini, EUR. 5157e, (1974).

Resonance Parameters of the Chromium Isotopes: ^{50}Cr, ^{52}Cr, and ^{53}Cr

A. Brusegan, R. Buyl, F. Corvi, L. Mewissen*, F. Poortmans*, G. Rohr, R. Shelley, T. van der Veen, I. Van Marcke**, C. Van der Vorst
(WRENDA 83/84 request N$^{os.}$ 286, 287, 288, 318, 319, 320)

The large campaign of data taking and data analysis for these isotopes, which covered several years of work with substantial manpower of the Linac-group, approaches an end. In total more than 400 resonances have been analysed from high resolution data obtained by neutron capture and two different kinds of transmission measurements. Results for ^{50}Cr, ^{52}Cr and ^{53}Cr up to 300 keV, 500 keV and 200 keV respectively were presented at the Santa Fé Conference 1985.
The analysis of the transmission measurements for the even isotopes has been extended up to 1 MeV. These measurements of the Cr-isotopes result in more complete and more precise sets of data for all three isotopes than those reported previously.

1.2.3 Matters Related to Fission Technology

Iron filter transmission measurements

A. Brusegan, C. Van der Vorst
(Request from GKSS Geesthacht)

Several resonances in Fe isotopes show deep minima in the total cross sections due to destructive interference of potential and resonance scattering. The resulting high transmission in narrow energy windows can be used to produce a number of quasi-monoenergetic reactor neutron beams, for which various applications exist.
High resolution transmission measurements through a thick composite filter consisting of Fe, Al, S and Ti have been performed and a complete analysis of the data has been made. The very satisfactory results have been transmitted to the requestor.
In Fig. 22 the "24.3 keV window" is shown for the two cases: a) no Ti in the beam; b) Ti in the beam. The plotted spectra have no background subtraction and are normalized simply to equal "monitor counts".

---

* SCK/CEN, Mol, Belgium.

** Visiting Scientist from VU, Brussels, Belgium.

In Fig. 23 the "windows" in the energy range from 225 keV to 375 keV are plotted. Above 30 keV, spectra measured with the Ti sample in the beam show "little differences" with those spectra obtained without Ti in the beam.

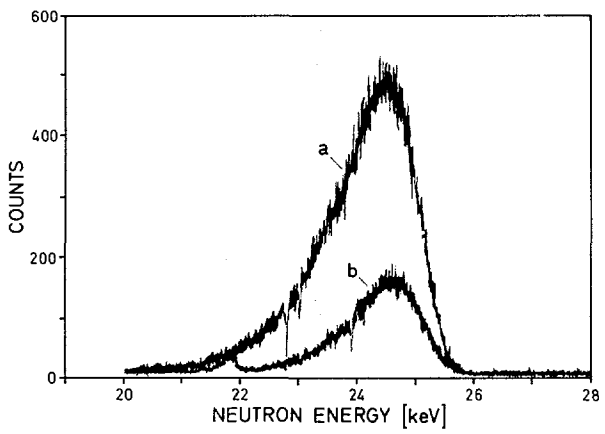

Fig. 22. "The 24.3 keV Fe window": a) Al + Fe + S composite filter; b) Al + Fe + S + Ti composite filter

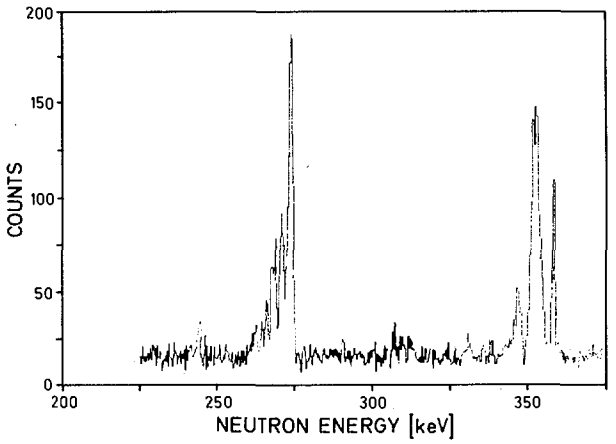

Fig. 23. Neutron spectrum transmitted through the composite filter "Al + Fe + S + Ti" vs neutron energy

1.3 NUCLEAR DATA FOR FUSION TECHNOLOGY

The present measurements aim at the improvement of the neutron data base for the tritium breeder material ^{7}Li, for the potential neutron multipliers Be and Pb and for the neutron induced helium production of structural materials.

Angular Distribution for $^{7}Li(n,n')^{7}Li^{*}(478)$ by Analyzing Doppler-broadened γ Lines

H. Liskien, S. Bao*

Blankets of future fusion reactors have to contain lithium as tritium breeding material and natural lithium consists of 92.5 atom % ^{7}Li. Therefore neutron transport calculations need double-differential ^{7}Li cross sections as input data. However, scattering experiments at higher neutron energy cannot separate the transition to the first excited state from the ground state transition by time-of-flight (TOF).

Our knowledge on the angle-integrated inelastic (Q = -478 keV) cross section stems from experiments observing the C.M.-isotropic 478 keV γ line. In the present work it is demonstrated that the missing neutron angular distributions can be deduced from the Doppler-broadened shape of this γ line.

The Doppler shift of γ rays emitted from excited nuclear recoils is determined by the recoil velocity component in the direction of observation at the moment of γ emission. For a given reaction and observation angle the γ-line shape depends on the distribution of these velocity components which in turn is determined by the angular distribution of the nuclear reaction, the half life of the excited state, and the stopping power of the sample material. If the half life is sufficiently short, the combined effect of half life and stopping power leads to only small corrections, while the main effect stems from the angular distribution of the nuclear reaction which can be deduced from the observed γ-line shapes.

---

* Visiting Scientist from University of Beijing, Beijing, PR of China.

Quasi-monoenergetic neutrons were produced via the $D(d,n)^3He$ source reaction. A pulsed deuteron beam (2 ns pulse width, 400 ns pulse distance, 2.5 μA, 5.1 MeV) bombarded a 36 mm long gas cell filled with 0.15 MPa D_2 gas. The sample consisted of a metallic lithium cylinder (36.8 mm ø x 29.9 mm) housed in an aluminium container with 0.2 mm wall thickness. An empty container for background determination was available. A 70 cm^3 (about 15 % relative efficiency) pure germanium detector at a distance of 1.2 m was used for γ-ray detection. To shield it against neutrons from the gas target and γ radiation not originating from the sample, this detector was mounted in a collimator made out of paraffin, lithium carbonate and lead.

Background problems have been studied in depth. Evidently a flat γ background under the Doppler broadened line is not influencing the line shape but should be kept small to reduce statistical uncertainties. It stems mostly from Compton-scattered γ rays which are produced in the Ge-detector itself by $Ge(n,n'\gamma)$ processes of neutrons which were before (elastically) scattered in the Li-sample. As may be seen from Fig. 24. the TOF-spectrum allows partly a distinction between γ rays produced in the sample and in the detector. By setting an appropriate window the flat background below the 478 keV line has been reduced. The contribution of the sample canning to this flat background remains small.

More important is the background from non-monoenergetic source neutrons which influences the line shape. The effect of X(d,n) neutrons produced by the structural material of the gas target (foil, beam stop etc.) has been found to be negligible below about 5.5 MeV deuteron energy (9 MeV neutron energy) by performing background runs with 0.15 and 0.075 MPa He gas in the target.

However, these tests revealed the effect of $^4He(d,n)$ neutrons for higher deuteron energies.

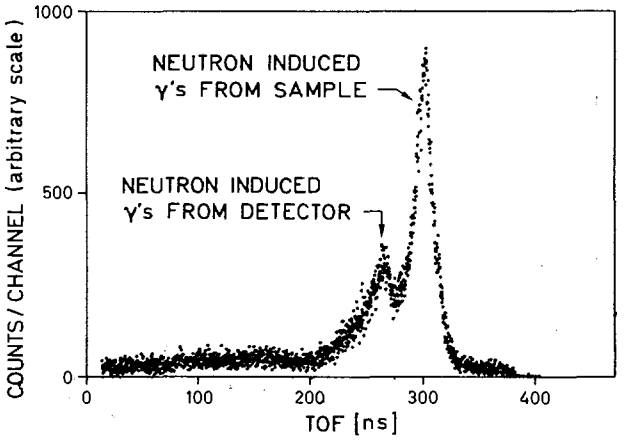

Fig. 24. TOF spectrum which allows partly distinction between γ rays from the sample and γ rays produced in the detector by scattered neutrons

Break-up neutrons from D(d,np)D reactions have been taken into account in the analysis based on published data[1] but play a role only above 8 MeV neutron energy.

Gamma spectra were acquired at five different observation angles. At forward angles smaller than about 40° the rate of fast neutrons reaching the γ-ray detector after being elastically scattered in the sample becomes very high. The deuteron-beam line prohibited measurements at greater backward angles. Data were collected with a channel width of 0.125 keV for about three hours at each observation angle. This time was distributed among a run with the ^{7}Li sample in position and the gas cell filled with D_2, a background run with the ^{7}Li in position but the deuterium gas replaced by He, and occasionally a background run with the empty aluminium container in position and D_2 in the gas cell.

At each observation angle at least one short calibration run with a ^{7}Be source was performed. $^{7}Be(T_{1/2} = 53\ d)$ emits the same γ line and is easily produced via the reaction $^{7}Li(p,n)^{7}Be$.

These calibration runs were performed under normal neutron production and served to check regularly the amplification gain and the detector resolution under neutron bombardment.

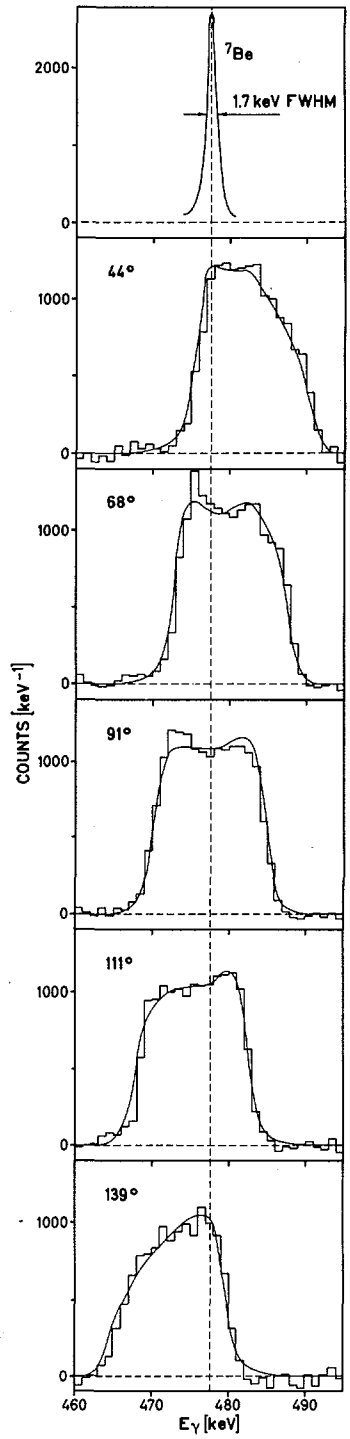

Fig. 25. The Doppler broadened γ lines at 8 MeV primary neutron energy. Position and shape change with observation angle. The line is the fit described in the text

(1) D.L. Smith, J.W. Meadows, Report ANL/NDM-9 (1974).

In this way a total of about 15000 events at each observation angle were collected as given for example in Fig. 25. Due to the limited statistics the spectra were condensed to a channel width of 1 keV. One sees clearly that the Doppler-effect has broadened the lines by nearly one order of magnitude compared to the 1.7 keV from the ^{7}Be source; that the line position changes with the observation angle in agreement with the fact that ^{7}Li recoils are emitted only in a certain forward cone; and that also the line shape depends on the observation angle. The symmetry at 90° is a direct consequence of the azimuthal symmetry of the reaction.

In the analysis of the data, a few minor corrections have to be incorporated which take into account the energy- and angle-distribution of the primary neutrons, the neutron scattering in the sample, the combined effect of half life and stopping power, and the γ-detector resolution.

With these corrections included, the measured spectra have been fitted starting from a Legendre polynomial expansion of the angular distribution up to the P_4 term.

The resulting fit is given as curves in Fig. 25. It is pointed out that this fitting procedure does not use any free parameters other than the four Legendre coefficients for P_1 to P_4, the coefficient for P_0 being fixed by normalizing to the total number of counts available. The fit has to describe at the same time, position, width and shape of the γ line, and this simultaneously for all observation angles. The technique has been applied at neutron energies between 4 and 10 MeV in steps of 0.5 MeV.

Preliminary results of this work below 8.5 MeV are given in Fig. 26. They are compared to theoretical calculations based on DWBA (P.G. Young, private communication (1981)) and on R-matrix calculations where the level scheme of ^{8}Li is based on a cluster model[1] or on shell model calculations[2]. Neither our experiment nor the calculations can say anything essential concerning the higher relative Legendre coefficients A_3 and A_4. Concerning the A_1 and A_2 coefficients one observes in the 4-5 MeV range excellent agreement with the results of Hopkins et al.[3] obtained by neutron TOF measurements. Although both R-matrix calculations originate from the same group they are inconsistent with each other.

---

(1) H.D. Knox, R.O. Lane, Nucl. Phys. A359 131 (1981).

(2) H.D. Knox, Proc. Int. Conf. Nucl. Data for Basic and Applied Sciences, Santa Fé, N.M., USA (1985) to be published.

(3) J.C. Hopkins et al., Report LA-3765 (1967).

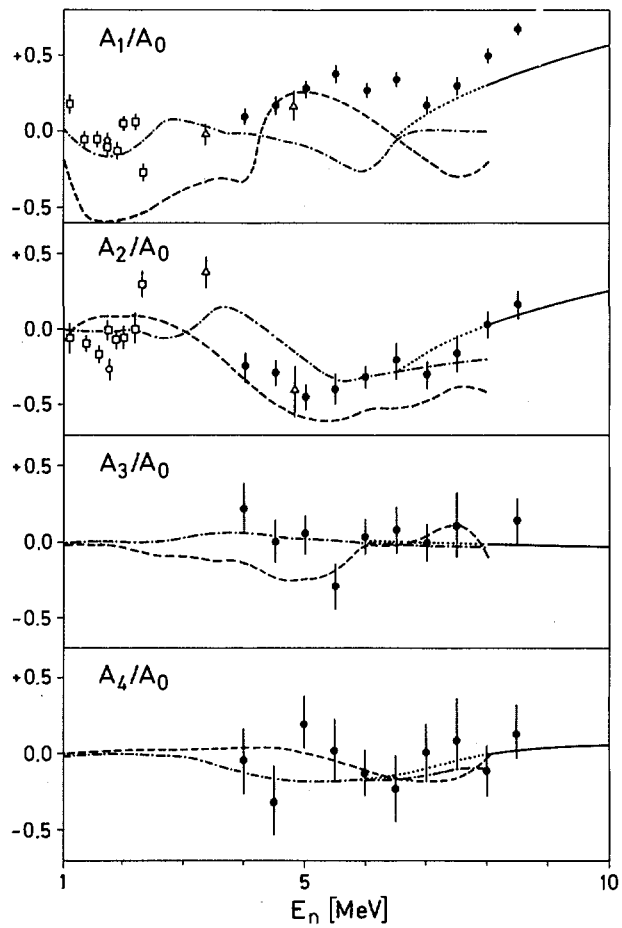

Fig. 26. Present knowledge of the neutron angular distribution of $^{7}Li(n,n'\gamma)$ Q = -478 keV
(● this experiment)
(Δ [J.C. Hopkins et al., LA-3765 (1967)])
(□ [H.-H. Knitter and M. Coppola, Report EUR-3903e (1968)])
(° [R. Batchelor and J.H. Towle, Nucl. Phys. 47 (1963) 385]).
Curves refer to theoretical calculations.(– Young) (--- Knox and Lane) (--- Knox).

Double Differential Neutron-Emission Cross Section for the $^{7}Li(n,xn)$ Reaction

E. Dekempeneer*, H. Liskien, L. Mewissen**, F. Poortmans**
(WRENDA 83/84 request N$^{os.}$ 53, 58, 65)

A neutron spectrometer for the measurement of double-differential neutron-emission cross sections has been set up at the linear accelerator. A simplified block diagram is shown in Fig. 27.

* Visiting Scientist from the University of Brussels, Brussels, Belgium.
** SCK/CEN, Mol, Belgium.

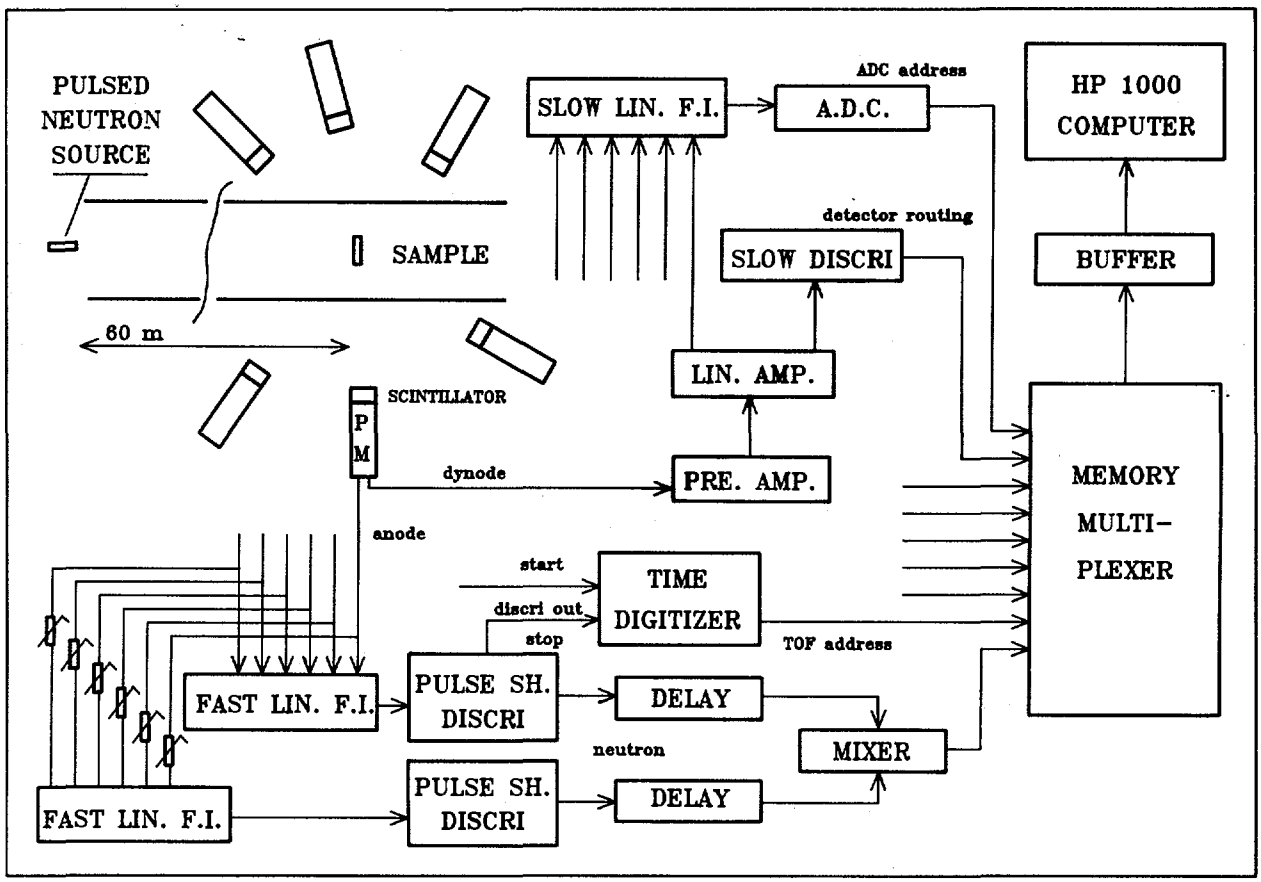

Fig. 27. Block diagram of the neutron spectrometer

The sample is mounted in a 2.4 m long evacuated Al tube at a distance of 60 m from the neutron source. The primary-neutron energy is determined by time-of-flight; the energy range from 1.6 MeV to 16 MeV is subdivided into 32 time-of-flight channels. The neutrons emitted from the sample are detected by six NE 213 liquid scintillator detectors (ø = 5 cm, h = 5 cm) which may be placed 20 cm from the sample at emission angles between 10 and 160 degrees. With this set-up it is possible to measure angle- and energy-distributions of secondary neutrons in one run for a broad range of primary-neutron energies. Pulse-shape discrimination is applied to distinguish detected neutrons from γ rays. As shown in Fig. 27. the anode signals are split: one branch is connected directly to a pulse-shape discriminator; the other branch is first attenuated before it enters a second pulse-shape discriminator, and the neutron outputs of the two are

mixed. In this way the pulse-shape discrimination works properly over a dynamic range of more than a factor of 300.

The secondary-neutron energy distributions above a bias of 500 keV are obtained by unfolding the pulse-height spectra observed in the NE 213 detectors. The relative response functions of the detectors were measured in the energy range from 0.3 to 16 MeV in steps of 0.1 MeV using the neutrons from the Linac target. These measurements were repeated for some energies in the range from 0.4 to 7.5 MeV and 13 to 16 MeV using monoenergetic neutrons produced by the reactions $T(p,n)^3He$, $D(d,n)^3He$ and $T(d,n)^4He$ at the 7 MeV Van de Graaff. A relative efficiency curve was established by relying on the differential cross-section data of the neutron producing reactions. At the same time also the absolute detection efficiency has been determined by measuring the incident neutron flux with a proton recoil telescope at five different energies. The experimentally determined absolute response functions have been compared with Monte-Carlo calculations using the code NRESP4 developed at PTB, Braunschweig.

The shape of the incident neutron flux is measured with a ^{235}U fission chamber placed in the neutron beam at 100 m from the Linac target. Absolute cross sections will be obtained by normalization to the differential-elastic scattering cross section of ^{12}C below 2 MeV.

As first isotope to be investigated with this set-up, ^7Li was chosen because of its importance as a blanket material for fusion reactors. The code FORIST has been used for the unfolding.

Figure 28 shows an example of two secondary neutron spectra. The incident neutron energy was from 5.6 MeV to 6.5 MeV and the average emission angles 24° and 60°. The statistical uncertainties are from 1 % in the elastic peak to 10 % for the small continuum neutron emission cross sections. At present, the systematic uncertainties are estimated between 5 % and 10 %. They are due to the normalization of the data, the relative efficiencies of the NE 213 scintillators, the background and the multiple scattering effects in the sample. Continuum neutron emission through the $^7Li(n,n'\alpha)T$ reaction is seen as well as discrete peaks due to elastic scattering and inelastic scattering to the 4.6 MeV state. Also shown on this figure are

the results of Lisowski et al. for the double-differential continuum cross sections at the emission angle of 60°. The differential elastic plus inelastic cross sections to the 478 keV level agree within 5 % with the results of Shibata obtained with a 5.96 MeV incident monoenergetic neutron beam from a pulsed Van de Graaff. The inelastic peak due to the 4.63 MeV state falls in the threshold region for this energy.

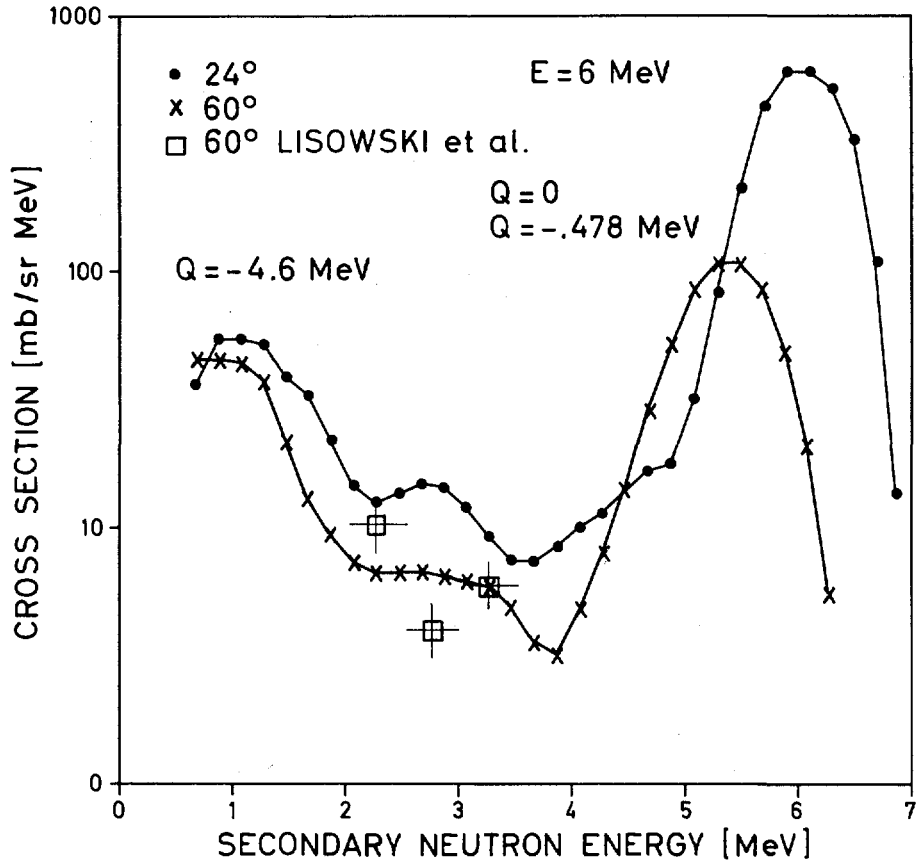

Fig. 28. Examples of secondary neutron spectra

The analysis of a first series of measurements has been completed up to 8.5 MeV. Above that energy, the statistical accuracy is not sufficient for applying the involved unfolding procedure on the pulse-height spectra. Meanwhile a second series of measurements has been completed but again the statistical accuracy of the data above 10 MeV is insufficient. Therefore, we are planning a third series of measurements using a new neutron-producing target at GELINA which should yield a harder neutron spectrum.

In addition the necessary work has been done to extend the spectrometer from six to eight neutron detectors.
A Monte-Carlo code has been written to correct for the multiple interaction of the elastically scattered neutrons in the sample and for the attenuation of the emitted neutrons in the sample and the surrounding wall of the vacuum chamber.

Be(n,t) Cross Sections

H. Liskien, R. Widera, S. Qaim*, R. Wölfle*

In view of the importance of beryllium as a potential neutron multiplier material and its relatively large (n,t) cross sections we have irradiated 11 samples (20 mm ø, 5 mm thick) with monoenergetic neutrons of 13 to 19 MeV. The neutron fluence in the order of $5 \cdot 10^{11}$ cm^{-2}, has been determined by sandwiching the samples between aluminium sheets and determining the induced ^{24}Na activity due to $^{27}Al(n,\alpha)$, thus relying on this well-known standard cross section. The samples have been transported to KFA Jülich for quantitative tritium extraction.

Measurements of Double-Differential (n,α) Cross Sections

E. Wattecamps, F. Arnotte
(WRENDA request N$^{os.}$ 801147, 781062, 781064)

The combined effect of displacement damage and the presence of helium in alloys is known to have a strong influence on mechanical properties such as tensile strength, fatigue, creep and crack growth. To design the first wall and the blanket of fusion reactors, and to estimate the radiation effect on structural materials of the magnets, it is important to know the (n,α) cross-section data of the elements involved. Therefore, a program has been started to measure double-differential (n,α) cross sections by direct detection of the α particles with a multi-telescope.
The multi-telescope has five telescopes surrounding the sample. Each telescope consists of two proportional counters, measuring the energy loss ΔE_1 and ΔE_2 in the counter gas, and one surface barrier detector, measuring the energy E of the α-particle. The telescopes are positioned at 14°, 51°, 79°, 109° and 141° relative to the direction of the primary neutron.

---

* KFA, Jülich, Germany.

Each event in a telescope is a triple coincidence between ΔE_1, ΔE_2 and E. The energy loss $\Delta E = \Delta E_1 + \Delta E_2$, and the energy E for each telescope, are analyzed and stored in a ND 6600 analyzer as five separate two-dimensional spectra. The time resolution of the triple coincidence (50 ns) and the difference in specific energy loss of protons and alphas in the counter gas allow a very specific particle discrimination. The X(n,α)-sample can be replaced by samples of ^{241}Am, polyethylene or Ta. The ^{241}Am source is used for energy and relative efficiency calibration. The polyethylene sample is used to measure relative to the H(n,p) elastic scattering cross section and the Ta-sample is used for background determination.

Recently measurements on natural Cu were made. Because of the small values of the cross sections to be determined, the source-sample distance was fixed to 8.7 cm and no collimator used. The single count rates of the proportional counters are very high under these conditions, especially in normalization runs with the polyethylene sample: proton-recoil detection needs ten times higher gain than α-particle detection with accordingly large dead-time losses. Therefore is was preferred to measure the cross-section ratio of ^{nat}Cu(n,α)/^{nat}Ni(n,α). The measured ratio of cross sections of ^{nat}Cu(n,α) to ^{nat}Ni(n,α) is systematically larger, by almost two standard deviations, than the same ratio calculated from the best available information.

To clear up this discrepancy, the reliability of our measuring device was improved by setting up a more complex acquisition system that also provides the exact dead-time effect correction factor. This allows now also measurements relative to the H(n,p) reaction. Such measurements for Ni(n,α) were made at 5, 6.5, 7, 7.5, 8.0 and 9.5 MeV. The angle and alpha-energy integrated (n,α) cross section of Ni is shown in Fig. 29 together with various measurements. The data of Kovacs et al.[1] obtained via activation are the largest. The multi telescope data of A. Paulsen et al.[2] obtained earlier in this laboratory are 10 to 15 % larger than our present data, whereas the data of S.L. Graham et al.[3] are consistent with our results. Since our data are systematically the lowest, runs at 6.5 MeV and 8.0 MeV were repeated but confirmed the earlier low results. As soon as accelerator time becomes available

---

(1) Kovacs et al., NEANDC(E) - 262"U", Vol.V, p. 24 (1985).

(2) A. Paulsen et al., Nucl. Sci. Eng. 78, 377 (1981).

(3) S.L. Graham et al., Nucl. Sci. Eng., to be published.

additional measurements will be performed to get values at the intermediate energies 5.5, 6.0, 8.5 and 9.0 MeV; thus covering the range from 5 to 9.5 MeV, in steps of 0.5 MeV.

Measurements of ratios of (n,α) rates of Cu to Ni done previously (1984), and also with the improved acquisition system (1985) were used to deduce the Cu(n,α) cross section using our Ni(n,α) cross section data (see above). They are given in Fig. 30 together with additional results of measurements

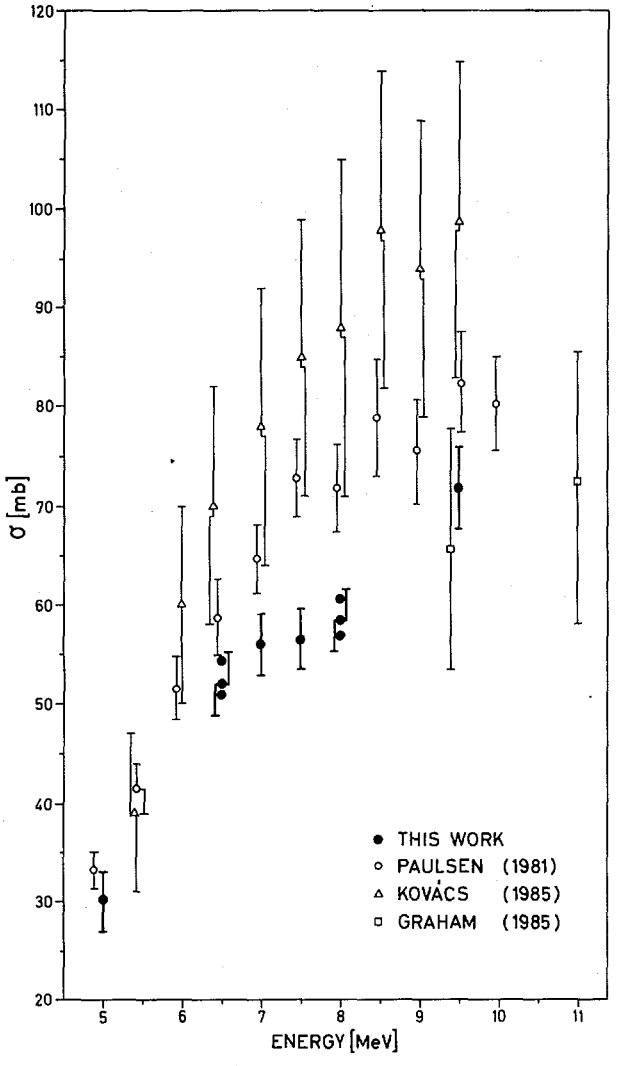

Fig. 29. Cross sections of Ni(n,α)

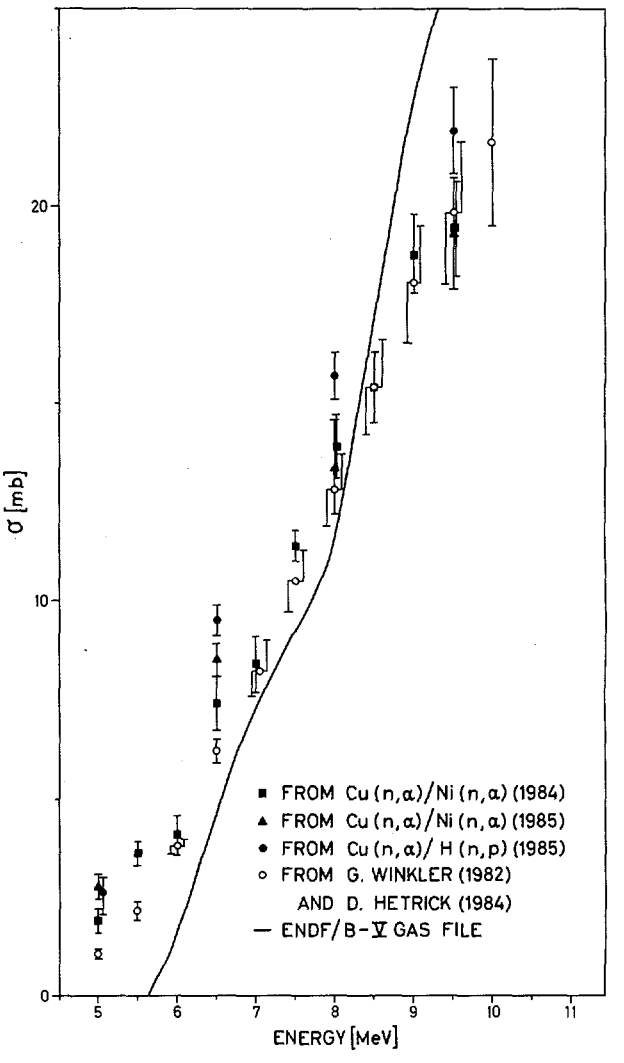

Fig. 30. Cross sections of Cu(n,α)

of Cu(n,α) to H(n,p) done with the improved detection system at 5.0, 6.5, 8.0 and 9.5 MeV. Also given are values obtained for natural copper by combining measurements for ^{63}Cu of G. Winkler et al.[1] with the small contribution of ^{65}Cu deduced from an evaluation of D.M. Hetrick et al.[2]. Three types of measurements were done, namely: Cu to Ni, Ni to H and Cu to H. The measured cross-section data obtained are consistent, the Ni(n,α) data disagree slightly with previous data of this laboratory and the Cu(n,α) data confirm recently published data. A detailed analysis and summary of the available double-differential (n,α) cross-sections versus alpha-particle emission angle and versus alpha-particle energy is in progress.

---

(1) G. Winkler et al., Proc. Europhysics Conf., Smolenice, p. 417 (1982).

(2) D.M. Hetrick et al.,ORNL/TM-9083 (1984).

1.4 SPECIAL STUDIES

Neutron Resonance Spectroscopy of $^{28}Si + n$

P.W. Martin*, L. Mewissen**, F. Poortmans**, J.A. Wartena, H. Weigmann

As part of a systematic study of the basic properties of neutron resonance reactions, the total and partial radiative capture cross sections of ^{28}Si have been measured. This nucleus is known as a test case for intermediate structure phenomena, and it also may be expected to show a relatively large magnetic-dipole strength which recently has received much theoretical interest.

A new set of total cross-section data with a nominal time-of-flight resolution of 3.6 ps/m has been obtained from transmission measurements at a 388 m neutron flight-path station of the Linac pulsed neutron source.

Capture γ-ray measurements were performed with a 130 m flight path. The Si sample was viewed by four BGO detectors placed under different angles with respect to the neutron-beam direction. The neutron flux was monitored by a ^{235}U fission chamber placed in the neutron beam at 30 m from the Linac target. Alternatively to the Si sample, a Fe sample has been placed in the neutron beam and the γ rays from neutron capture in Fe resonances have been recorded. The yield of high energy γ rays from the 1.15 keV Fe resonance is being used for normalization of neutron flux and detector efficiency.

Resonance analysis of the experimental data is in progress. The transmission data are analyzed with the R-matrix code MULTI[1]. Neutron widths are obtained for resonances up to 2.75 MeV neutron energy, and in many cases information on the inelastic width is also extracted from the analysis. Resonance spins are obtained by combining the information from the total cross-section analysis with the γ-ray yield and angular-distribution data. In the capture data resonances are sufficiently well resolved for resonance analysis up to a neutron energy of about 2 MeV. The data are analysed with a modified version of the area analysis code TACASI[2]. The code takes into account resonance self-shielding and

---

* Visiting Scientist from University of British Columbia, Vancouver, Canada.

** SCK/CEN, Mol, Belgium.

(1) G.F. Auchampaugh, LANL Report LA-5473-MS (1974).

(2) F.H. Fröhner, Report GA-6906 (1966).

includes a Monte-Carlo subroutine for multiple-scattering corrections. The analysis yields partial radiative widths of resonances for γ transitions populating the ground and first excited states of ^{29}Si.

Neutron Resonance Spectroscopy of $^{207}Pb + n$

R. Köhler*, L. Mewissen**, F. Poortmans**, S. Raman***, J.A. Wartena, H. Weigmann

Lead is a possible candidate to be used as a neutron multiplier in fusion reactor blankets. Therefore the cross sections of lead isotopes have to be known, and for evaluations on the basis of nuclear model calculations the basic statistical properties of ^{208}Pb (nuclear level densities, neutron and radiative strength functions) are required.

The present measurements which were also partly undertaken to search for the physically interesting magnetic-dipole strength, yield nuclear level densities as well as neutron strength functions and their energy dependent structures. Additionally to a high resolution total cross-section measurement and a measurement of the neutron capture γ rays elastic scattering angular distributions have been measured recently in order to obtain supplementary information on resonance spins and parities.

The 388 m flight path of GELINA was used for these measurements. Neutrons elastically (and inelastically) scattered from the ^{207}Pb sample were recorded with three NE 110 plastic-scintillator detectors placed under different angles with respect to the neutron-beam direction. Additionally, two BGO γ-ray detectors were placed close to the sample to record γ rays from inelastic scattering. Neutron time-of-flight, the detector pulse height, and the number of the detector giving the event recorded, are stored in list mode on a magnetic tape.

As an example, Fig. 31 shows the spectra of elastically scattered neutrons for three scattering angles in the neutron energy range from 450 to 550 keV. The dependence of the scattering yield for different scattering angles on the resonance spin and parity is clearly seen. The obtained data allowed to assign or confirm the spins and parities of 69 resonances up to 700 keV neutron energy.

---

* EC Fellow

** SCK/CEN, Mol, Belgium.

*** ORNL, Oak Ridge, Tenn., USA.

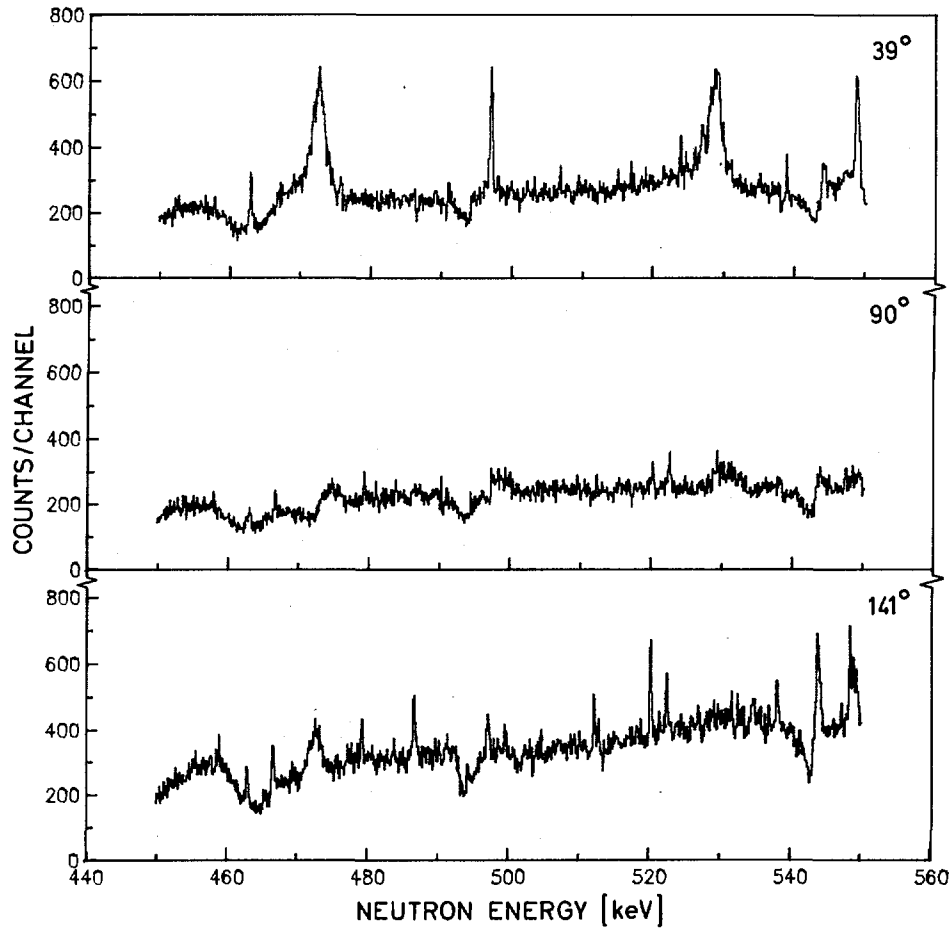

Fig. 31. Yield of neutrons (arbitrary units) elastically scattered under 39°, 90°, and 141°

The capture γ-ray measurements were done at a 130 m flightpath. The sample was viewed by four BGO detectors placed under different angles with respect to the neutron beam direction. The neutron flux was monitored by a ^{235}U fission chamber placed in the neutron beam at 30 m from the linac target. Neutron time-of-flight, γ-ray energy, and the number of the detector giving the event detected, are stored in list mode on a magnetic tape together with the events recorded by the flux monitor. Alternatively to the ^{207}Pb sample, a Fe sample has been placed in the neutron beam and the γ rays from neutron capture in Fe resonances have been recorded. The yield of high energy γ rays from the 1.15 keV Fe resonance is being used for normalization of neutron flux and detector efficiency. The data have

been analysed with a modified version of the resonance area analysis code TACASI[1]. This code takes into account resonance self-shielding and incorporates a Monte-Carlo subroutine for multiple-scattering corrections. The analysis yields values of partial radiative widths of resonances for the γ transitions populating the ground and first excited (3^-) states of ^{208}Pb.

The resonance parameter analysis of all data obtained for ^{207}Pb is completed and includes a total number of 380 resonances. The final interpretation of the data in terms of level densities, strength functions and radiative strengths is in progress.

Nuclear Quadrupole Interaction of Fluorine in Intercalated Carbon Compounds

C. Budtz-Jørgensen, P.W. Martin*

By inserting layers of guest molecules into anisotropic materials such as graphite, compounds can be produced with controlled electronic, magnetic, structural and thermal properties. An interesting example is graphite intercalated with AsF_6. This material can be produced having electrical conductivity as high as Cu but of course with a much lower specific density.

A possible method for characterizing such material is offered by measurements of the hyperfine quadrupole interaction of probes imbedded in the crystalline structure. The quadrupole interactions yield information about the product of the nuclear quadrupole moment Q times the electric field gradient (EFG), which depends strongly on the environment of the nucleus under consideration. In the present case these interactions were studied employing the so-called method of "time-dependent perturbed angular distributions" (TDPAD), whereby the time dependent angular distribution of γ rays emitted from an isomeric level populated by a nuclear reaction is determined.

Bombarding fluorine with protons the 197 keV, $5/2^+$ level of the ^{19}F nucleus is excited by the (p,p')-reaction and decays with a mean life τ = 125 ns by γ-ray emission. The decay of the γ radiation is given by

$$N(\theta,t) = N_o \cdot e^{-t/\tau}\left[1 + a_2 g_2(t) \cdot P_2(\cos\theta)\right] \qquad (1)$$

---

(1) F.H. Fröhner, Report GA-6906 (1966).

* Visiting Scientist from University of British Columbia, Vancouver, Canada

a_2 is the anisitropy of the γ radiation and $g_2(t)$ is the time-dependent attenuation coefficient, which contains the information about the nuclear moment interaction with the surrounding fields. In the case of pure electric-quadrupole interaction, I = 5/2, $g_2(t)$ has the form

$$g_2(t) = a_o + \sum_{i=1}^{3} a_i \cdot \cos \omega_i t \qquad (2)$$

where a_o, a_i and ω_i depend on the nuclear quadrupole moment Q and the EFG at the position of the excited nucleus. Experimentally $g_2(t)$ is determined by measurement of the γ-ray emission under two angles (θ = 0°, 90°) with respect to the proton beam axis and forming the ratio:

$$a_2 g_2(t) = R(t) \equiv \frac{N(0^\circ,t) - N(90^\circ,t)}{\frac{1}{2}(N(0^\circ,t) + N(90^\circ,t))}$$

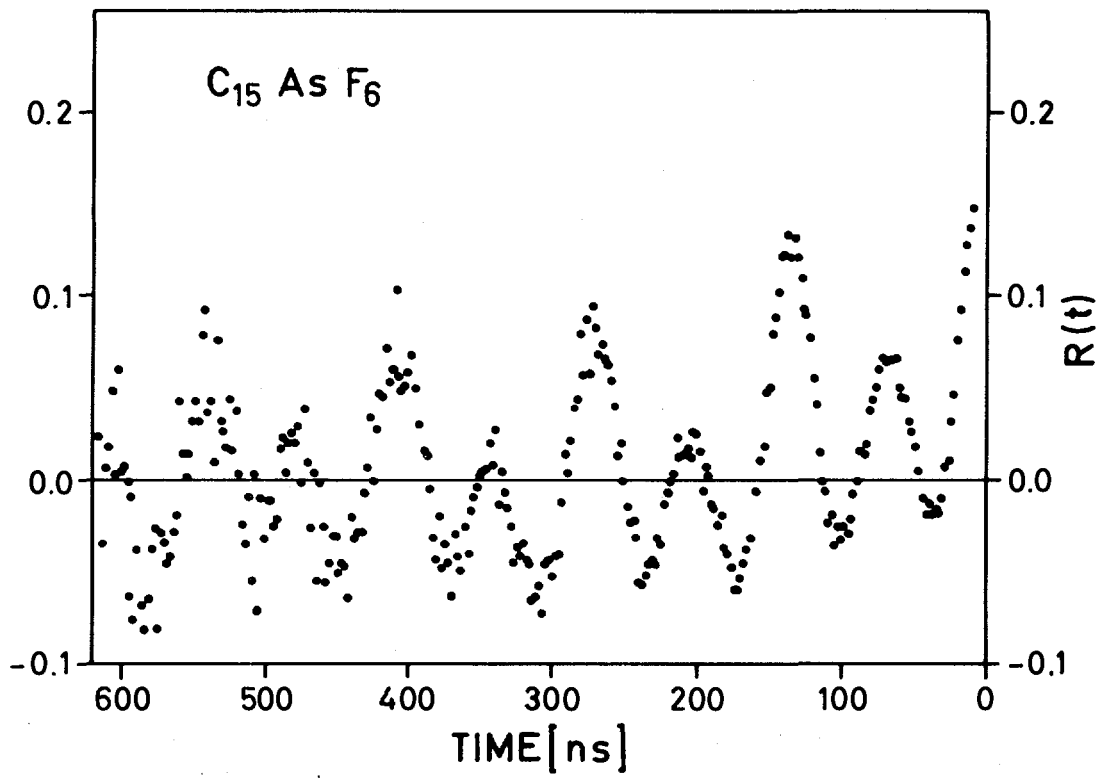

Fig. 32. Time dependent attenuation coefficient R(t) for $C_{15}AsF_6$

The JRC-Geel Van de Graaff was used to produce a 3 MeV pulsed (~ 1 ns) proton beam. Five different targets - $C_{10}AsF_6$, $C_{11.4}AsF_6$, $C_{12}AsF_6$, $C_{15}AsF_6$ and $C_{18}AsF_6$ - were investigated. All samples were manufactured at the University of British Columbia. A 1" x 1½" NaI scintillator was used to detect the γ rays. The excellent performance of the experimental set-up is illustrated in Fig. 32, which shows the measured $R(t)$ spectrum found for the $C_{15}AsF_6$ sample. The spectrum was obtained after ~ 2 ns of beam time and the high signal to background ratio makes it possible to study the attenuation factor for more than 5 lifetimes. Two interactions of the form (2) can be seen. At present the further data evaluation is made at the University of British Columbia, where the necessary computer codes are available.

A Method to determine the pairing energy for excited nuclei

G. Rohr

A paper with this title has been presented at the Fourth International Conference on Neutron Induced Reactions held at Smolenice in June 1985. The method is based on the Bethe level density expression, where the parameters are used with constraints. It is applied to the level density of compound resonances observed at neutron separation energy. The change of the pairing energy compared to the ground state value determined by mass differences has been discussed for different mass regions.

2. NUCLEAR METROLOGY

2.1. RADIONUCLIDE METROLOGY

International Comparison of Activity-Concentration Measurements of a ^{109}Cd Solution

D. Reher, E. Celen, B. Denecke, R. Vaninbroukx, W. Zehner

The nuclide ^{109}Cd is of interest for gold mining and for efficiency calibration of solid state detectors in the energy region between 10 and 100 keV. It decays by electron capture to an excited level at 88 keV which decays with a half life of about 40s by emission of γ rays and conversion electrons.

On behalf of Section II (Mesures des Radionucléides) of the Comité Consultatif pour les Etalons de Mesure des Rayonnements Ionisants (CCEMRI) the Bureau International de Poids et Mesures, Sèvres, launched an international comparison of activity-concentration measurements of a ^{109}Cd solution. Besides CBNM five experienced laboratories (AECL, Canada; BIPM, France; LMRI, France; NPL, United Kingdom; PTB, Federal Republic of Germany) were invited to exercise a trial intercomparison. The ^{109}Cd solution was distributed by OMH, Hungary.

Each participant received one flame-sealed NBS-type ampoule containing about 2 g of solution with a ^{109}Cd activity concentration of about 1.2 MBq g^{-1} in an aqueous solution of HCl (0.1 mol per dm^3). At CBNM three different methods were employed for the standardization.

A 4π-CsI(Tl)-sandwich spectrometer was used to measure the disintegration rate of ten ^{109}Cd sources which were prepared from two dilutions of the original solution. The activity was derived from the area of the full-energy peak in the spectrum containing the conversion electrons and the 88 keV γ rays. The only correction to be applied was an exponential tailing of 0.6 % to 1.2 % of the peak area. Figure 33 shows a typical spectrum. The accuracy obtained by this method is 0.4 %.

The ^{109}Cd solution was also standardized by the 4π-liquid-scintillation method. The scintillator, Aqualuma Plus from Lumac, was preloaded with about 0.5 µg $CdCl_2$ per ml scintillator in order to avoid adsorption on the walls of the scintillator vials. Accurately weighed fractions of the original ^{109}Cd solution and of a 1:10 dilution were dispensed into 12 ml of scintillator. The scintillation vials were put on top of a RCA 8850

photomultiplier and the spectrum of the conversion electrons was measured. A typical spectrum is shown in Fig. 34.

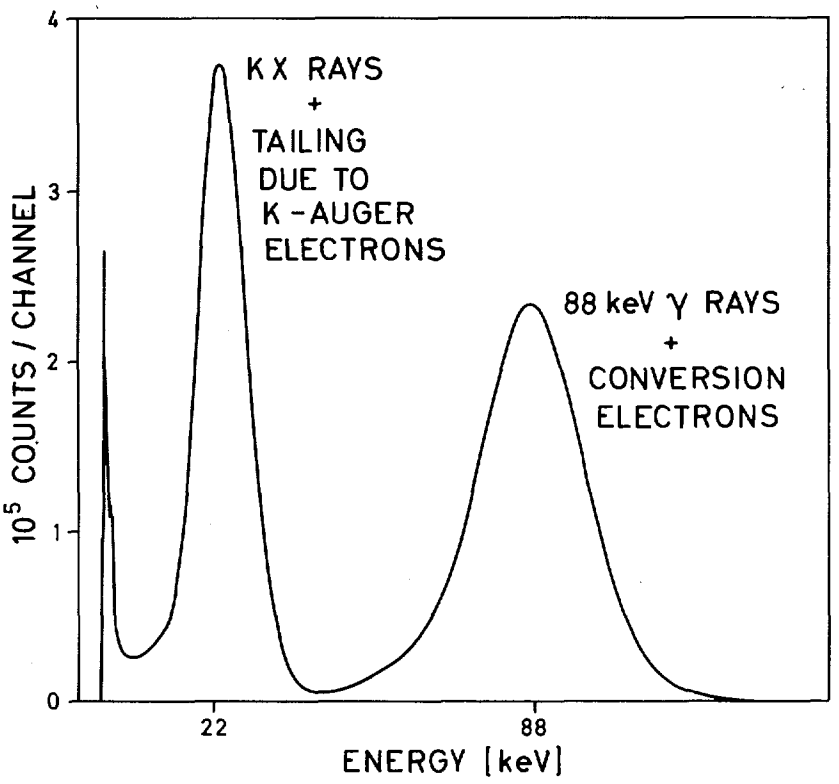

Fig. 33. Pulse-height spectrum of a ^{109}Cd source measured with the 4π-CsI(Tl) sandwich detector

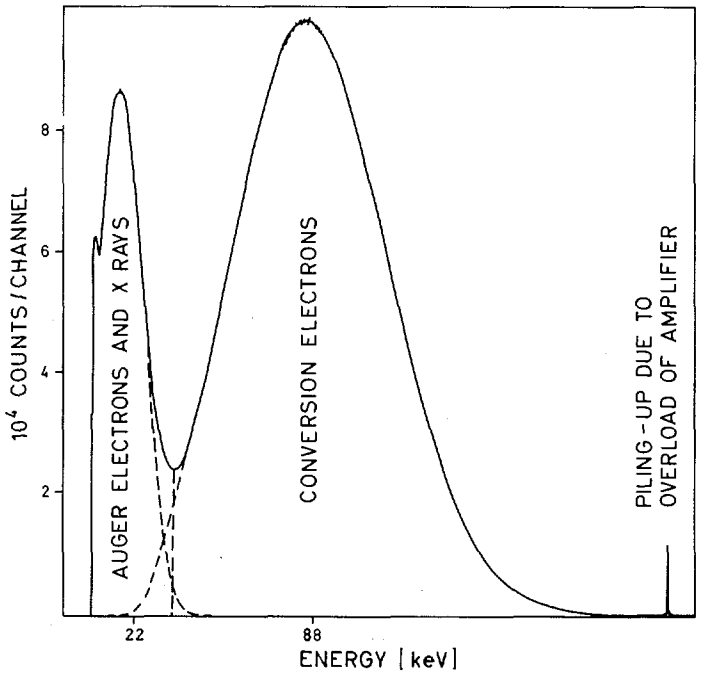

Fig. 34. Pulse-height spectrum of ^{109}Cd measured by liquid scintillation

Nearly all counts above the valley originate from the conversion electrons of the 88 keV transition. The disintegration rate was deduced from the measured events above the valley. Corrections allowed for the loss of conversion electrons below the valley (1.4 %) and the contribution of Auger electrons and X rays above the valley (0.2 %). The reproducibility of the measurements of five sources was 0.1 %. The accuracy was estimated to be 0.3 %.

As a third independent method to standardize the ^{109}Cd solution a 4π proportional counter operated at high pressure was used. Six sources were measured each at three different pressures (0.3 MPa, 0.4 MPa and 0.5 MPa). A typical spectrum is shown in Fig. 35.

The number of conversion electrons was deduced from these spectra allowing for a small tailing correction (0.1 to 0.3 % of the total counts). In addition a correction was applied for the 88-keV γ rays which were not detected. The reproducibility of the measurements was 0.1 %. The accuracy was estimated to be 0.4 %.

In Table 4 the results of the ^{109}Cd measurements are listed. It can be noticed that the agreement is excellent.

Table 4. Results of the ^{109}Cd measurements

Method	Standard deviation (%)	Activity concentration Bq/g
4π CsI(Tl)	0.1	1193.0 ± 5.0
4π Liquid scintillation	0.1	1194.0 ± 3.0
4π Proportional counter	0.1	1189.2 ± 4.8

The results of this trial intercomparison have been sent to the organizer. A discussion took place at the meeting of CCEMRI Sec. II in June 1985. A graphical representation of all the results submitted is shown in Fig. 36.

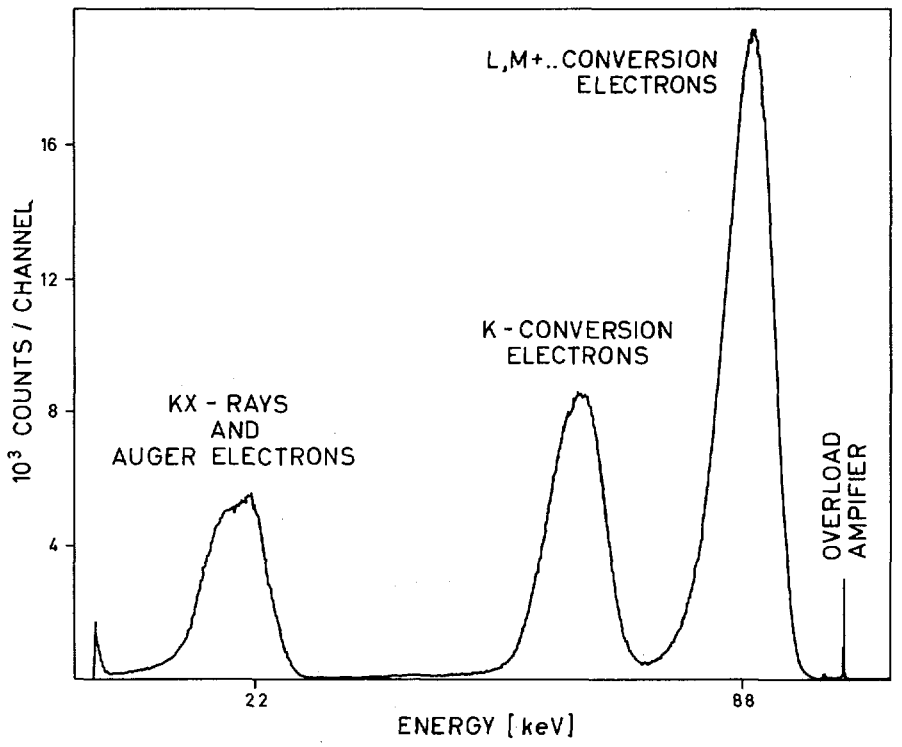

Fig. 35. Pulse-height spectrum of a ^{109}Cd source measured with a 4π proportional counter filled with Ar + CH_4 (9:1) at a pressure of 0.3 MPa

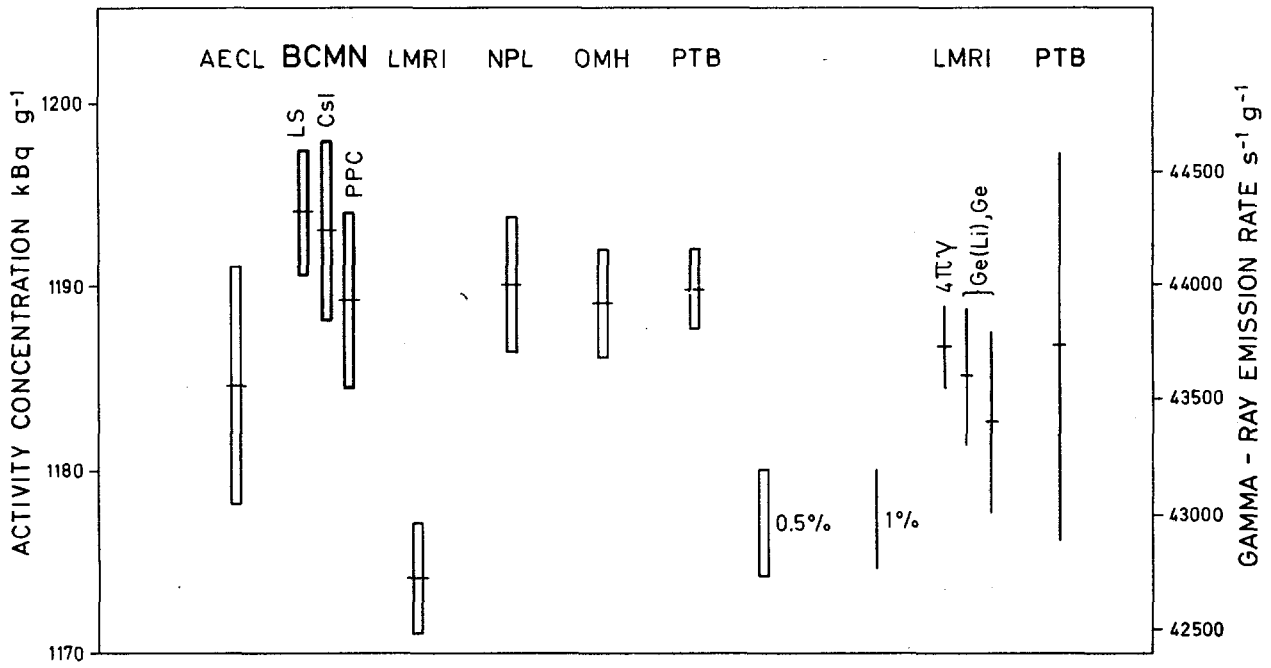

Fig. 36. Graphical representation of the results of the trial comparison of activity concentration measurements of a ^{109}Cd solution

Development of a Tracer Technique for the Standardization of ^{109}Cd

D. Reher, E. Celen, W. Zehner, C. Ballaux*

The effort to standardize ^{109}Cd solutions by the tracer technique using ^{65}Zn as tracer has been continued. The results were better than those obtained in 1984. However, they cannot compete with the results from counting conversion electrons with a proportional counter operated at high pressure. The efficiency parameter for counting Auger electrons and X rays could not be increased above 0.27 with the present equipment. An increase up to 0.6 is expected with a new proportional counter to be constructed as a part of the coincidence equipment. This counter will allow measurements at high counting-gas pressure. It is planned to have this counter operational in 1987.
In addition, the feasibility of using ^{203}Hg as tracer for the standardization of ^{109}Cd has been studied. A solution of ^{203}Hg has been standardized. The sources are very stable and β efficiencies of better than 90 % were obtained. This is very promising for the measurement of ^{109}Cd-^{203}Hg mixed sources which are planned for 1986. The work is carried out in collaboration with SCK/CEN.

Standardization of ^{14}C by $4\pi\beta$-Liquid-Scintillation Efficiency Tracing

B.M. Coursey**, W.B. Mann**, A. Grau Malonda***, E. Garcia-Toraño***, J.M. Los Arcos***, J.A.B. Gibson+, D. Reher

Carbon-14 in the form of ^{14}C-tartaric-acid solution was standardized by means of $4\pi\beta$-liquid-scintillation efficiency tracing using the NBS ^{3}H-water standard. This work was a joint effort with NBS (USA), JEN (Spain) and AERE (UK). A method of computing the detector efficiency for a two-phototube counting system using a ^{3}H standard was developed. The combined uncertainty in the ^{14}C radioactivity concentration, corresponding to one

---

* SCK/CEN, Mol, Belgium.

** NBS, Gaithersburg, USA.

*** JEN, Madrid, Spain.

+ AERE, Harwell, UK.

standard deviation, is 0.2 %. A paper has been published[1].

Low-Energy X-Ray Standards

B. Denecke, G. Grosse

The effort towards the preparation of reference sources emitting X rays of 1.5 keV has been continued.
The control unit, built during the previous reporting period, works satisfactorily. It keeps constant, within tolerable limits, the density of the counting gas in the gas-flow proportional counter and consequently also the peak positions of the detected X rays in the pulseheight spectrum.
The reproducibility of the peak-area determination was found to be 0.3 % for the 5.9 keV manganese K X rays and 0.8 % for the 1.5 keV aluminium K X rays. However, very large pulses originating from the background radiation cause very long dead times which result in a loss of X-ray events. The pulse shaping of the electronic chain has to be improved. A research contract was made with a specialized group to develop the optimal non-overloading charge-sensitive preamplifier for our proportional counter.
The K X-ray emission rates of ten ^{55}Fe sources (nominal activity 185 MBq each) were measured. These sources will be used as excitation sources for the forthcoming measurements.

Automatic NaI(Tl) γ-Ray Counter

A.B. Idzerda, R. Vaninbroukx

The automatic γ-ray counter is in effective use for standardization work since July 1985. The reproducibility of the detection efficiency has been

---

(1) B.M. Coursey, W.B. Mann, A. Grau Malonda, E. Garcia-Toraño, J.M. Los Arcos, J.A.B. Gibson, D. Reher, Int. J. Appl. Radiat. Isot., 37, 403 (1986).

tested at regular intervals with a ^{241}Am source for three different geometrical arrangements. Under these conditions the count rates varied between 1600 s^{-1} and 11000 s^{-1}. The reproducibility for 20 series of measurements was found to be ± 0.04 % for each of the three geometries.
The detector is calibrated for the following nuclides: ^{7}Be, ^{54}Mn, ^{57}Co, ^{60}Co, ^{65}Zn, ^{109}Cd, ^{133}Ba, ^{137}Cs, and ^{241}Am.

4π CsI(Tl) Sandwich-Detector Spectometer

B. Denecke

The 4π-CsI(Tl) sandwich-detector system, constructed for measurements of photons between 10 and 200 keV, was improved resulting from the experiences gained during a ^{109}Cd intercomparison.
For spectrometry with high accuracy the count rates must be kept low to reduce pile-up effects as much as possible. As a consequence also the background must be kept as low as possible. To reduce the background a special shield has been constructed.
A second problem concerns the signal processing in the photomultipliers and amplifiers. Background pulses release a very high amount of energy in the CsI(Tl) crystals resulting in a high-overload pulse at the anodes of the photomultipliers. This effect causes paralysis of the pulse amplifiers for milliseconds and an incorrect dead-time processing. To overcome this difficulty the amplitude of the anode pulses was limited to 0.5 V. Schottky-barrier diodes were selected for high reverse resistance and fast response and were wired into the dynode chains of the photomultipliers. The emitter-followers were replaced by home-made, integrated fast buffer amplifiers.
In addition, a 3 μs amplitude-to-digital converter was incorporated into the system and adapted for remote control by the data-acquisition system RNDAS.
The spectrometer was used for the standardization of ^{109}Cd. The emission rate which is the sum of the 88 keV γ rays and of the 85 keV and 63 keV conversion electrons could be measured with an accuracy of 0.4 %. Measurements of the photon-emission rates in the ^{241}Am decay have been started.

A report describing the detector system has been submitted for publication [1].

Determination of Particulate Matter Concentration in Air by a Light Reflection Technique

B. Denecke, P. Clayton*

A detailed report has been prepared[2] together with Warren Spring Laboratory, UK, describing the new method of automatically measuring the darkness index of dust stains on filter membranes. The technique is compared with the standard OECD Black-Smoke Method and, in addition, with both an electron absorption and a gravimetric analysis method.
The field investigations, carried out several years ago as part of a CEC intercomparison programme for air pollution parameters showed a wide range of relationships between gravimetrically determined particulate matter concentrations and various black smoke indices.

---

* Warren Spring Laboratory, Stevenage, UK.

(1) B. Denecke, EUR Report, submitted for publication.

(2) B. Denecke, P. Clayton, EUR Report, submitted for publication.

2.2 METROLOGY FOR NEUTRON FLUX AND DOSE

International Neutron Fluence Intercomparison

H. Liskien, A. Paulsen, R. Widera, S. Bao*

At CBNM's 7 MV Van de Graaff accelerator the intercomparison of neutron fluence determinations was started with two multi-plate ionization chambers as transfer instruments containing ^{235}U and ^{238}U layers (provided by AERE Harwell). These instruments will be calibrated in quasi-monoenergetic neutron fields at 0.565, 2.5, 5.0 and 14.8 MeV neutron energy in terms of fission counts per neutron/cm^2 by means of proton-recoil counting techniques (proportional and telescope counters). Experimental results are not yet available.

Neutron Dosimetry via Calorimetry

A. Paulsen, R. Widera, H. Nerb

The graphite calorimeter which was constructed as an intermediate step to a tissue-equivalent calorimeter is operational. A cross-sectional view of the calorimeter and its housing is shown in Fig. 37. Under normal circumstances the calorimeter is operated in an additional graphite phantom with variable thickness of the front plate in order to perform the absorbed-dose measurements at selectable graphite depths. The components of the graphite phantom are covered on their inside and outside surfaces with an aluminized Mylar foil to minimize energy exchange by thermal radiation.

The calorimeter is mounted onto a turbo-molecular vacuum pump with 50 l/s pumping speed.

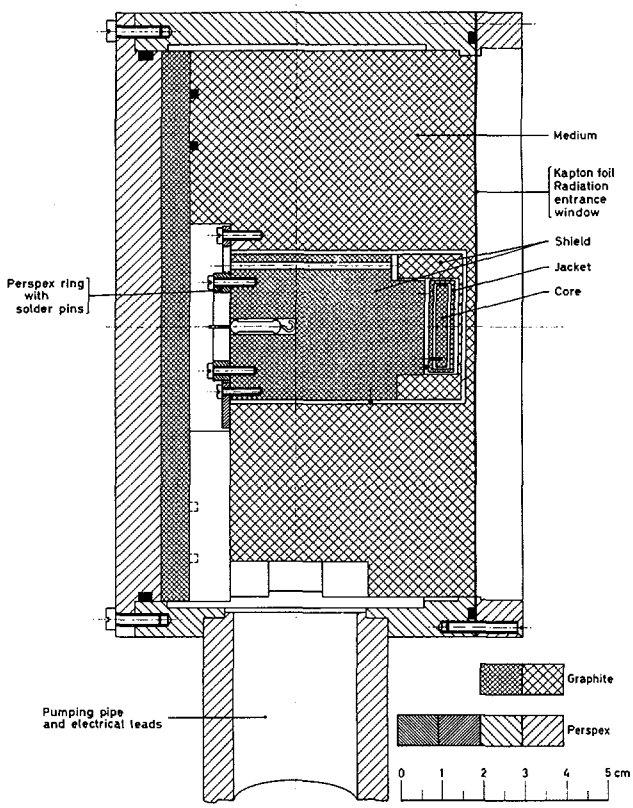

Fig. 37. Cross-sectional view of the graphite calorimeter

---

* Visiting Scientist from University of Beijing, Beijing, PR of China.

The vacuum achieved in the 40 mm inner diameter exhaustion tube after 10 h of pumping is $2 \cdot 10^{-3}$ Pa. Electrical connection of the built-in thermistors to the electronic registration circuitry shown in Fig. 38 is also made via the mentioned exhaustion tube and special vacuum-tight connector sockets.

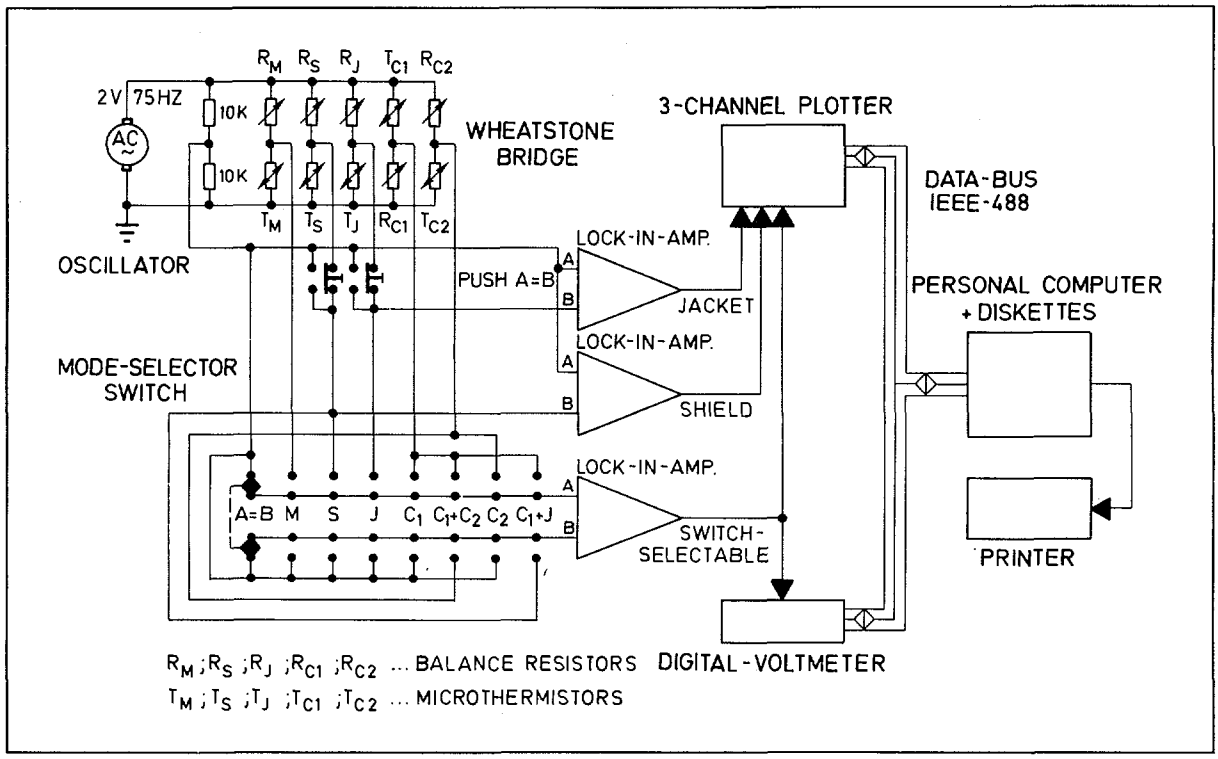

Fig. 38. Schematic circuitry for operating the Wheatstone bridge

The a.c. Wheatstone bridge is driven by a 75 Hz oscillator with high amplitude stability ($\Delta V/V = 2 \cdot 10^{-4}/°C$). Three lock-in amplifiers are available for simultaneous registration of the resistances of three thermistors. Two of these amplifiers have fixed connections to observe jacket and shield temperatures. For the third amplifier the thermistor (or thermistor combination in opposite arms of the bridge) to be measured is switch-selectable. The simultaneous registration in three channels is used for the determination of the temperature drifts of core, jacket and shield in order to extinct these drifts via the means of the connected personal computer and off-line (in future on-line) temperature adjustments

(raising only) of these three bodies. The electronic system for heating core, jacket and shield by well-defined electrical powers (calibrator) is not shown for simplicity in Fig. 38. Also not shown in Fig. 38 is the electronic temperature controller of the medium which maintains the medium temperature at 27°C within one m°C for at least 24 hours.

The switch-selectable amplifier is used (mainly in C1+J or C1+C2 mode) for the calorimeter calibration and absorbed-dose measurements by means of a digital voltmeter with high resolution and stability connected again to the personal computer. The calibration and measurement data are stored on diskettes. Measurements of the calorimeter parameters (heat transfer coefficients and the quasi-adiabatic calibration factor) have been started but are not yet finished.

The tissue-equivalent plastic calorimeter for neutron dosimetry is under construction according to the design shown in Fig. 39. This calorimeter is constructed in such a way that it can be operated with the same electronic system as the graphite calorimeter. This is not only true for the system shown in Fig. 38 but also for the calibrator and temperature controller. However, due to a somewhat different concept of the plastic calorimeter the shield measuring chain is cancelled since the plastic shield is thermally controlled like the graphite medium and the plastic medium forms a freely drifting temperature buffer.

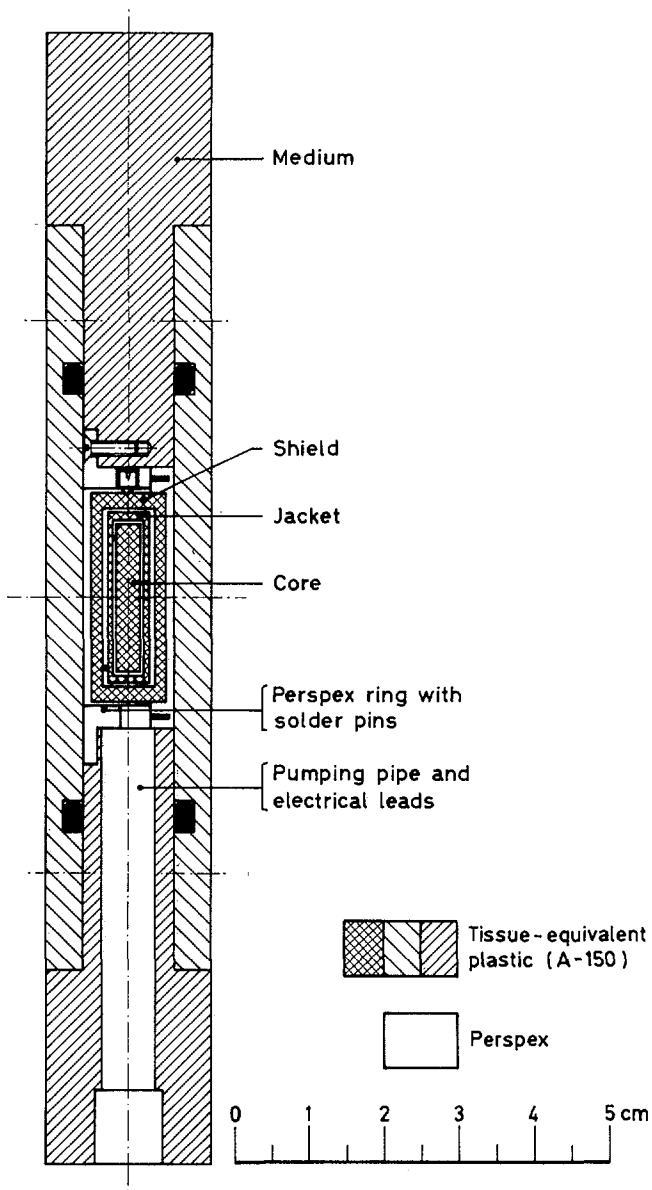

Fig. 39 Cross-sectional view of the tissue-equivalent calorimeter

Study of a Graphite Calorimeter

A. Paulsen, A. Janssens*, E. Cottens**, A. Poffijn*, R. Widera, H. Nérb, L. van Rhee

(Research contract between the European Atomic Energy Community, and the University of Ghent (RUG)).

The cooperation between RUG and CBNM in terms of this contract aimed in the first place at the transfer of the know-how on absorbed dose calorimetry gained at the RUG, and to allow the CBNM staff to acquire experience with the operation of the calorimeter and of the associated electronics. In the course of the period not only numerous tests and exercises were performed but also theoretical work was done and the principles of absorbed dose calorimetry were thoroughly discussed. The results of this work have been written down in detail in five reports, which are now available. The contents of these reports are summarized in the following paragraphs.

The first report entitled : "The RUG graphite absorbed dose calorimeter: set-up and procedures" describes the apparatus installed at CBNM, in particular the data acquisition with a microcomputer, which was essential for the new developments described later. Also a number of tests are described and conclusions for the improved design of new electronics. Furthermore the results of numerous calibration experiments are discussed. These were performed for dissipation time periods ranging from 50 to 1600 s, and for electrical powers of 1 mW down to 10 µW. The latter could be regarded as a test for the performance of the calorimeter at low dose rates.

An important point in the design of the bridge system is the permitted self-dissipation in the thermistors. A proper design assures that its effect is minimal, and correspondingly a significant gain in sensitivity could be achieved. The question is discussed in detail in the report : "Study of the effect of self-dissipation in the thermistors".

In view of the future application of the calorimeter at low dose rates, far more stringent conditions for the initial equilibrium of the calorimeter bodies should be met. This was achieved through the development of an original method of computer controlled equilibration. This method and the underlying theory are described in the report: "Equilibration of the absorbed dose calorimeter".

---

* University of Ghent (RUG), Ghent, Belgium.

** Ministry of Public Health, Brussels, Belgium.

The equilibration method proved to be very powerful for the experimental determination of the heat transfer coefficients between the bodies. Very reproducible values were obtained, giving evidence for a direct heat transfer from core to shield (report: "Measurement of heat transfer coefficients in the absorbed dose calorimeter").
The transfer coefficients are directly related to the heat loss corrections on the temperature rise of the calorimeter. The theoretical basis for this correction and the comparison between the experimental and theoretical data are discussed in the report: "Heat loss correction on the temperature rise of the calorimeter".
It may be concluded that in the course of the contract work not only the existing know-how has been transferred, but also important original work was done and a firm basis for future developments was established.

Neutron Dosimetry via Ionometry

A. Paulsen, R. Widera, H. Nerb

Neutron partial irradiations of rats have been carried out at CBNM for the Radiobiology Department of the SCK/CEN, Mol.
For the study of late effects in the brain of adult rats of low dose irradiations carried out during embryonic life in total 22 pregnant rats were partially irradiated with 2.5 MeV neutrons at doses of 5, 10 and 15 rads. These irradiations must be considered as a first test concerning the effect of neutrons. Irradiations of this type will go on in 1986, probably with somewhat increased doses.
The neutron collimator used for these irradiations is shown in Fig. 40 by a vertical cut in a plane containing the neutron-beam axis. The relative neutron-dose distributions on a horizontal and vertical line crossing the neutron beam 2.75 cm behind the collimator are also displayed. The FWHM of these distributions is 8 and 7 cm, respectively. The collimator duct is of rectangular shape. A 3 mg/cm^2 TiT target is used with the T(p,n) reaction at 3.28 MeV proton energy. Up to 35 µA of proton beam is applied with water cooling of the target. At the collimator exit the neutron beam passes a flat 30 cm^3 air ion chamber. Calibration of this monitor chamber was carried out by means of a T2/MG2 ion chamber pair (EXRADIN) in a dead rat at reference position in the specimen holder. Free in air behind the collimator a 5 % contribution of γ rays was determined whereas this contribution was only 1 % inside the rat fixed in the specimen holder.

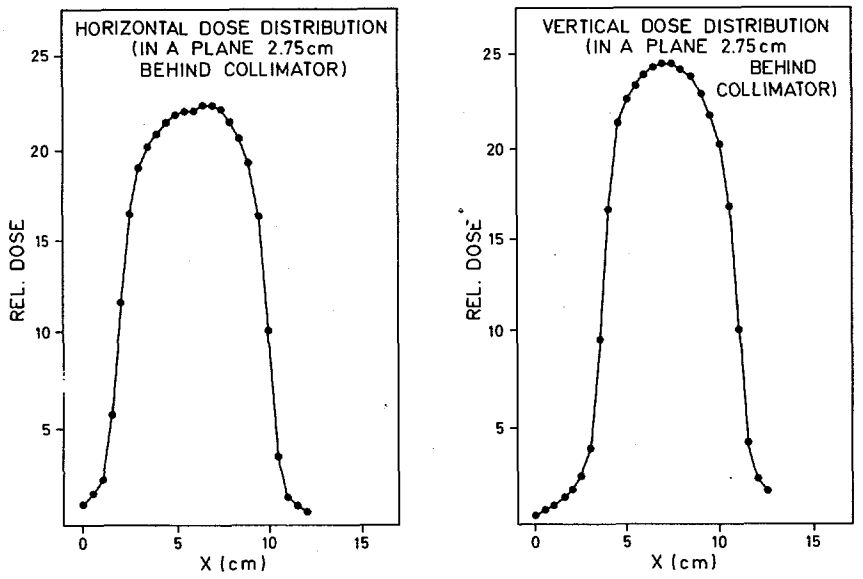

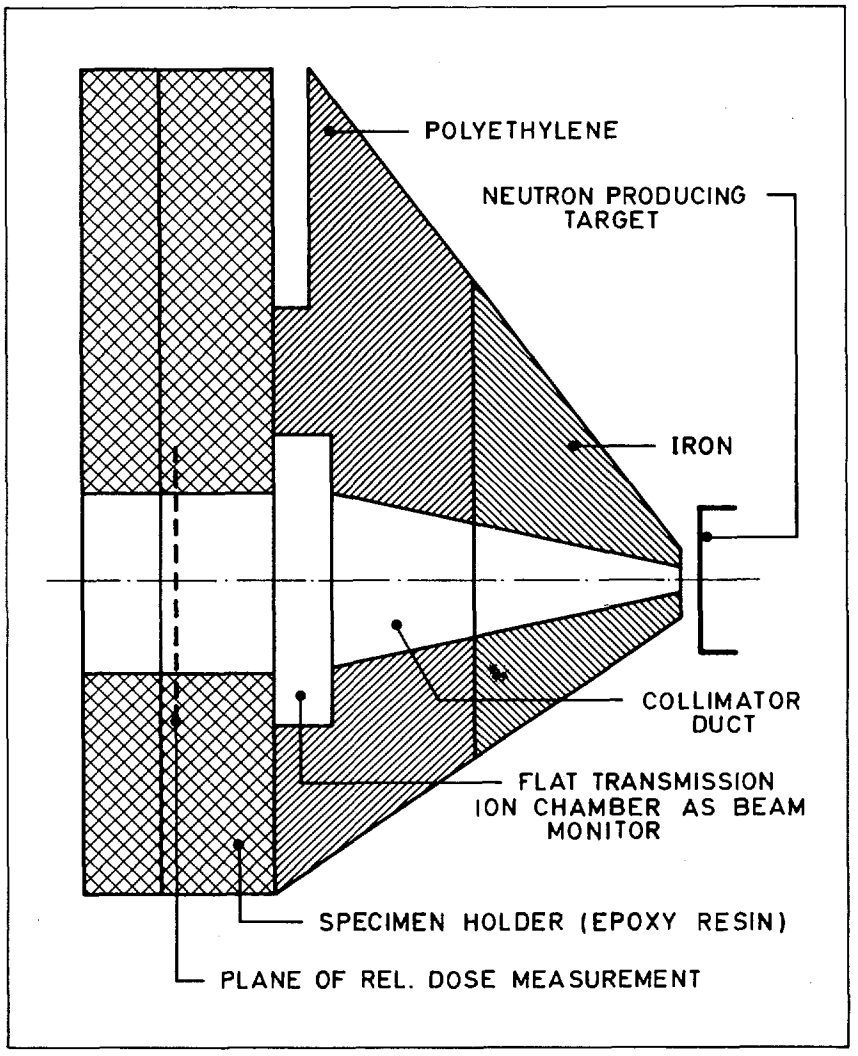

Fig. 40. Vertical cut of neutron irradiation facility and relative horizontal and vertical dose distributions in a plane 2.75 cm behind collimator (free in air)

Relative dose measurements are accurate within ± 2 %, absolute dose to ICRU soft muscle at present cannot be more accurate than ± 10 %.

Another series of neutron irradiations was carried out for the Radiobiology Department of the SCK/CEN, Mol. For analysis of chromosomic aberrations induced in human lymphocytes by low doses of high-LET radiation in total 28 human blood samples were irradiated with 2.5 MeV neutrons at doses of 0.5, 1, 2, 5, 10, 20 and 50 rads. The cells are cultured in appropriate conditions and chromosome analysis is performed on metaphase preparations at the first cell division after irradiation. Also further radiations of this type will be performed in 1986, especially also with neutrons of 0.5 MeV energy.

A third neutron irradiation project is at present prepared in collaboration with the Radiobiology Department of the SCK/CEN Mol. This study deals with the kinetics of diethylnitrosamine hepatocarcinogenesis in high-LET irradiated mice. A special neutron collimator is under construction for the partial and simultaneous irradiation of 8 mice at 2.5 MeV neutron energy.

TECHNICAL APPENDIX

Electron Linear Accelerator (GELINA)
Liquid Methane Moderator

R. Cools, F. Menu, J.M. Salomé

To supply neutrons with very low energies (~ 1 meV) a cryo-moderator filled with liquid methane has been installed at the Linac target. It is composed of a vacuum-isolated double box connected through special pipes to a liquid methane "factory" situated outside the target room. A new remote controlled mechanism has been realized to facilitate the change from one moderator configuration to another one. Few minutes are necessary to remove the Be-canned water moderator and to put the cryo-moderator in the right position. Filling this up with liquid methane takes about two hours.

Description of the moderator

Liquid methane was selected as the most suitable neutron moderator for our purpose as the melting point is 90.7 K and the boiling point 111.7 K which is well adapted to the use of liquid nitrogen as a coolant (77.3 K). This temperature of the moderator was considered as sufficiently low for achieving the projected cold neutron measurements. The number of H atoms per volume is relatively high: $6.9 \cdot 10^{22}$ H atoms/cm^3. Radiation damage should not be very important because the average fast neutron flux in the vicinity of the target at 2 kW electron beam power is about 10^{11}n/s·cm^2. (1)(2)(3)(4).

Dimensions of the moderator were extensively discussed as well as the wall material and its thickness. Assisted by computer calculations it was concluded that, in the available space, boxes of 130 x 85 x 75 mm with two

---

(1) W. Van Dingenen, S. Hautecler, R. 1895, Dept. Physique du Neutron, WVD-SH/jvt, C.E.N. Rue Belliard 31, Bruxelles.

(2) W. Van Dingenen, S. Hautecler, Bulletin de la Société Belge de Physique, Sér. II, N° 3, 1960.

(3) D.F.R. Mildner and B.C. Boland, R.N. Sinclair, C.G. Windsor and L.J. Bunce, J.H. Clarke, Nucl. Instr. & Methods 152 (1978) 437-446.

(4) D.F.R. Mildner, R.N. Sinclair, "Annals of Nuclear Energy, Vol. 6, pp. 225 to 237, Pergamon Press Ltd.', 1979.

walls 1.5 mm thick in stainless steel could be a tolerable compromise. It was also accepted that the rotary target is used as this has a more suited shape than the cylindrical one (Fig. 1).

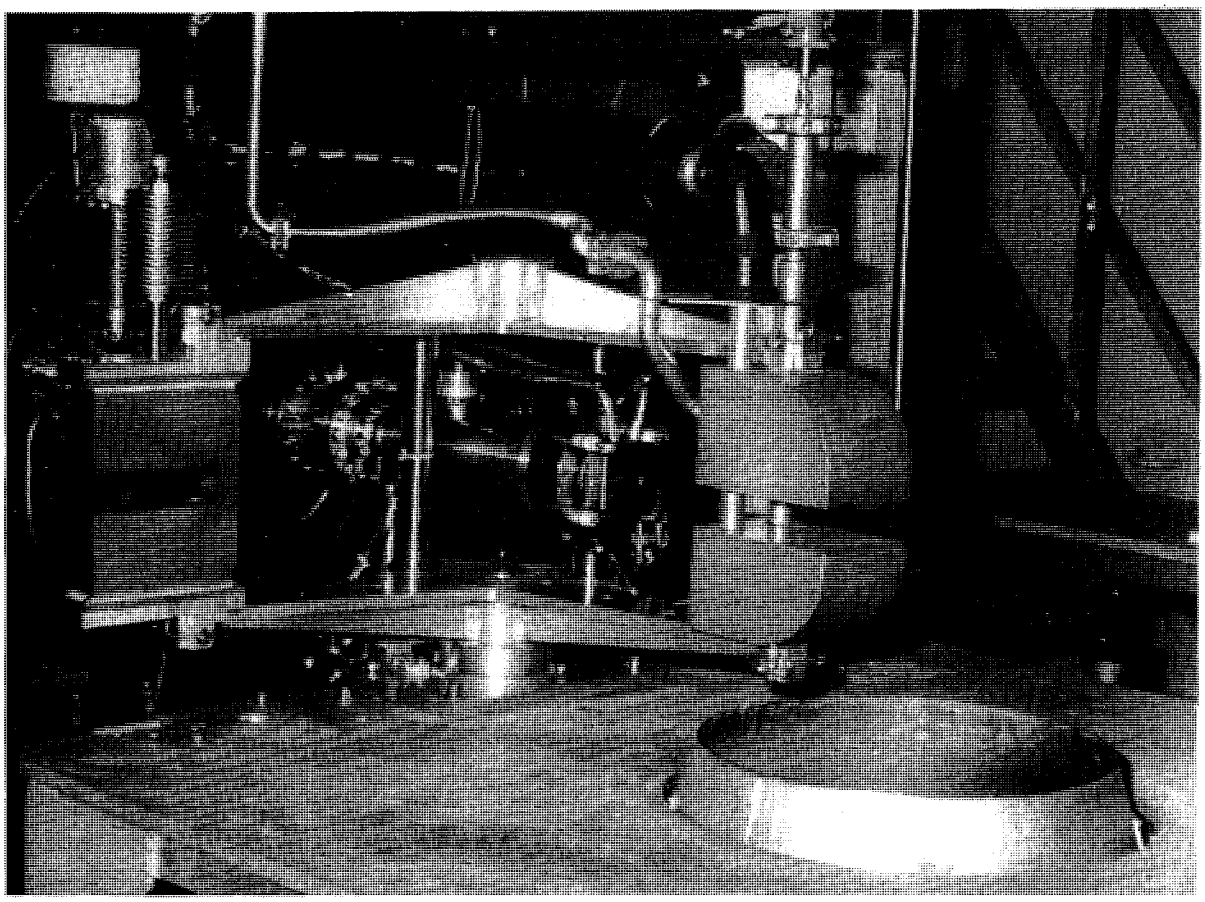

Fig. 1. The neutron moderators of the Linac. In working position, the cryo-moderator, liquid methane filled and on the left side, the beryllium canned water moderator

In order to design the cooling system, calorimetric measurements have been performed to evaluate the power dissipated by γ-heating in the moderator. A thermically isolated box of appropriate dimensions, methanol filled, was placed close to the Linac target. This organic liquid was chosen as its chemical composition and density are not too far from those of the liquid methane. Methanol is also easy to handle. Two thermocouples were placed in the box and the temperatures registered while the Linac was operated at 1.9 kW average beam power (100 MeV, 19 μA). The power registered in the methanol was respectively 1.5 % and 2.75 % of the beam power depending on

the place of the measuring thermocouple. This rather big difference could be explained by the position of the thermocouples in the double box, the inhomogeneite of the radiation field and the heat gradient in the liquid. The power which has to be removed from the moderator with 2 kW Linac beam power was estimated to 60 W. For security reasons a value of 80 W has been chosen for the design of the cryogenic system.

Cooling installation

The parameters mentioned above were transmitted to the firm Air Products and its subcontractor Leybold-Heraeus, Woerden, NL. After agreement on the position of the LN2 source and the exchangers, the super-isolated piping was defined, the losses calculated and the whole installation designed. Total losses are 110 W (pipings and moderator) which correspond to 9500 kJ/day or 26 Nm^3/day of methane to be pumped (the latent heat of vaporisation is 510 kJ/kg). The required amount of LN2 is then 68 l/day. Two temperature sensors PT 100 are placed in the moderator. Their indications are used for injection of liquid methane to compensate its vaporization. A third PT 100 adjusts the right consumption of LN2. Methane gas is compressed by a two stage vacuum pump with a capacity of 100 N l/min at $0.6 \cdot 10^5$ Pa, Fig. 2. These devices are mounted in a small cabin outside the target room (close to the detector station FP 1, 10 m). The control panels with indicators, switches and meters are located in the control room.
Besides the classical measures normally applied for safety on such an installation, a methane detector with three measuring heads was placed. One head is in the cabin, another one above the moderator and a third on the target room ventilation duct. Moreover, the methane loop will be automatically rinsed with dry nitrogen in case of a sudden loss of methane.

Removing the moderator

A new mechanism was designed by the CBNM drawing office and realized by the main workshop. From the control room, it is now easy to operate the accelerator either with the Be canned water moderator or with the cryo-moderator. This operation takes some minutes. Nevertheless, it is

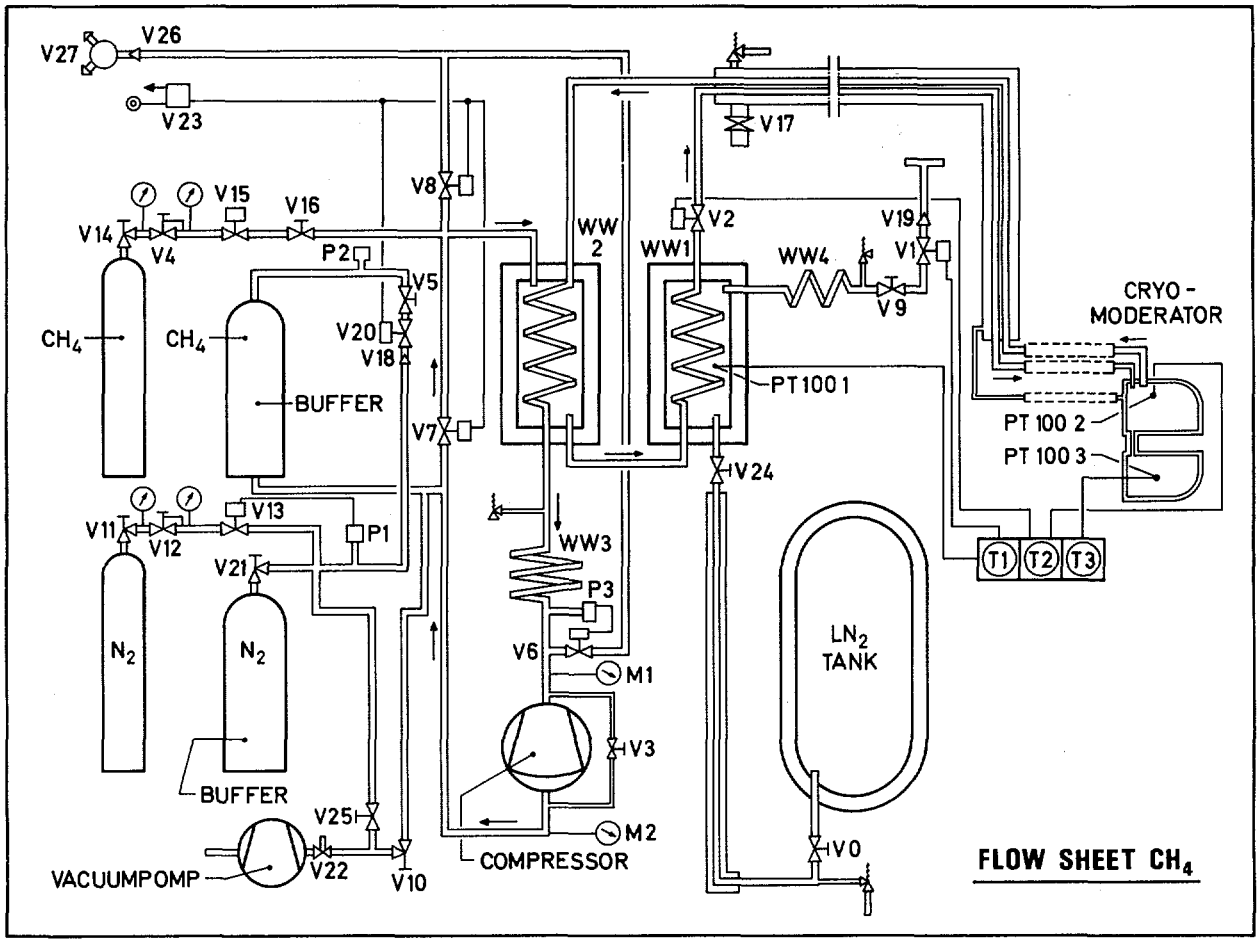

Fig. 2. Schematic drawing of liquid methane moderator

advisable to warm up the system before moving out the cryo-moderator. This liquid methane moderator has been used as a low energy neutron source during about 500 h without problems.

Van de Graaff Accelerators

New Target Installation

A. Crametz, P. Falque, J. Leonard, W. Schubert

At the CN-7MV accelerator a new target and its accessories were installed at level 0 (Fig. 3) in order to realize a high intensity neutron source using the $^{9}Be(d,n)^{10}B$ reaction.

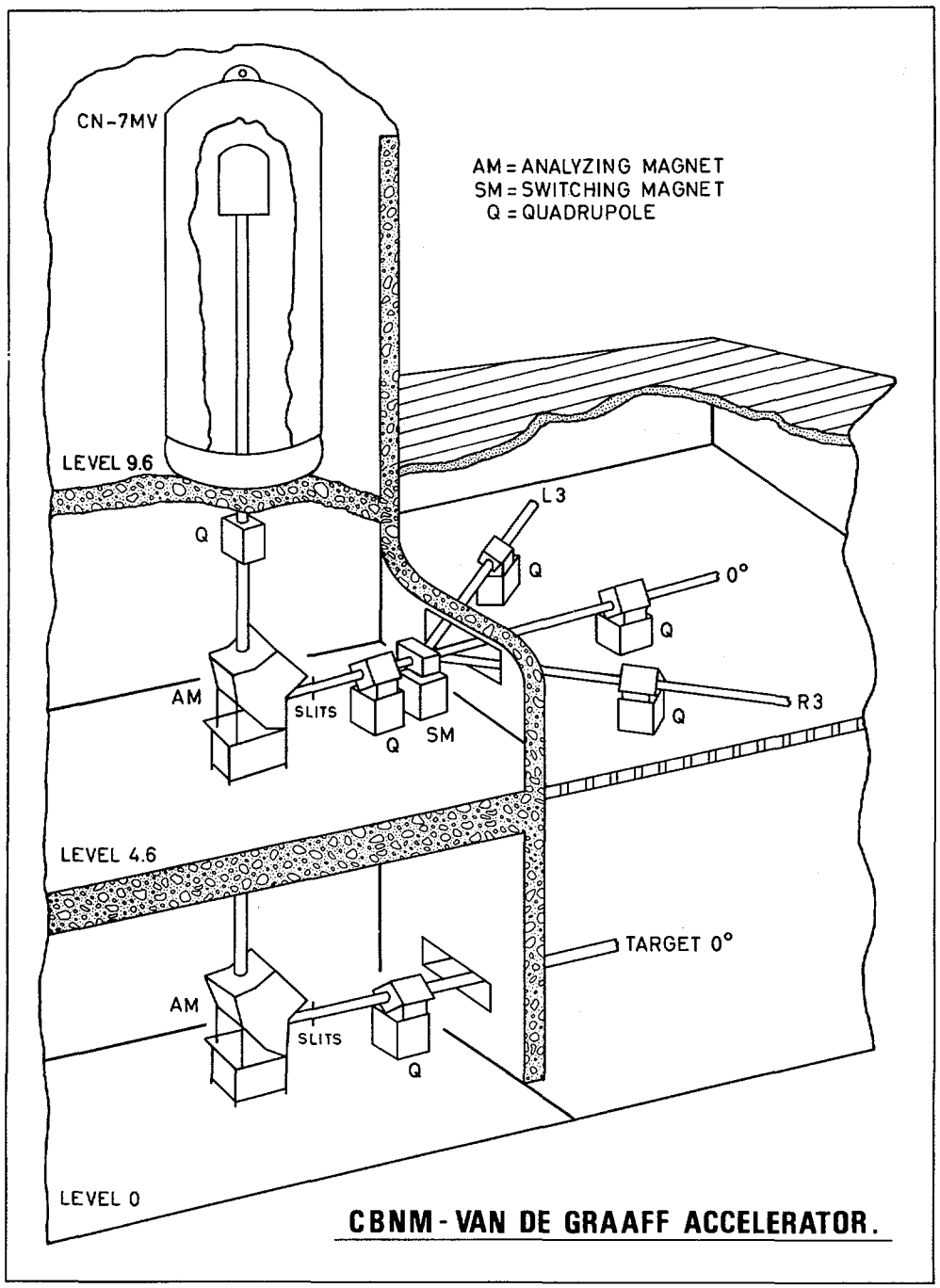

Fig. 3. Installation of a new target at level 0

Improved Exploitation

T. Babeliowsky, A. Crametz, W. Schubert

To increase the number of exploitation hours of the CN-7MV VG, and to reduce the presence of the VG-machine team outside the normal working hours, an automatic control of the accelerator parameters based on an APPLE II plus personal computer is nearby completion and will be operational when the present series of neutron experiments will be ended.
Signals read into the PC are of two kinds :

- signals corresponding to the readings of 16 meters
- signals corresponding to the positions of 12 stepping motors (number of turns of the potentiometer).

All parameters of the accelerator are scanned at regular time intervals and printed.
If one parameter is modified, the target current will cross one of the two preselected limits (lower or upper). After five minutes, if the target current value is not back within its normal range of variation, the time and the data will be printed and an automatic shut-down procedure will be started.
The program for these two phases : data logging and automatic shut-down, has been written in Applesoft BASIC with some ASSEMBLER subroutines.

LIST OF PUBLICATIONS

TOPICAL REPORTS

Multiannual Programme of the Joint Research Centre 1984-1987 - Annual Status Report 1984: Nuclear measurements and reference materials - EUR 9806 EN

DENECKE, B. -
Properties of a 4π-Cs(Tl)-sandwich spectrometer for the measurements of photons with an energy between 10 and 200 keV - Submitted for publication as EUR Report

DENECKE, B., CLAYTON, P. -
A comparison of methods for the measurement of particulate matter concentrations in the ambient atmosphere - Submitted for publication as EUR Report

LORENZ, A., VANINBROUKX, R. -
Status of actinide half lives - INDC/NEANDC Standard File, in press - ART 26586

CONTRIBUTIONS TO CONFERENCES

AXTON, E.J. -
Evaluation of the thermal neutron constants of ^{233}U, ^{235}U, ^{239}Pu and ^{241}Pu and the fission neutron yield of ^{252}Cf - IAEA Advisory Group Meeting on Nuclear Standard Reference Data, Proc. IAEA-TECDOC-335 (1985) p. 214.

BAMBYNEK, W. -
Emission probabilities of selected X rays for radionuclides used as detector-calibration standards - ibidem - p. 412

BASTIAN, C., RIEMENSCHNEIDER, H. -
Measurement of the $^{6}Li(n,\alpha)/^{10}B(n,\alpha)$ ratio with a xenon gas scintillator - ibidem - p. 118

BÖCKHOFF, K.H., POORTMANS, F., SALOME, J.M. -
The production and measurement of ultra-short intense electron and neutron bursts at GELINA - Int. Conf. Basic Appl. Sci., Santa Fe, USA (1985)

BRUSEGAN, A., BUYL, R., CORVI, F., MEWISSEN, L., POORTMANS, F., ROHR, G., SHELLEY, R., van der VEEN, T., VAN MARKE, I. -
High resolution neutron capture and total cross section measurements of ^{50}Cr, ^{52}Cr and ^{53}Cr - Ibidem

BUDTZ-JØRGENSEN, C., KNITTER, H.-H. -
Correlation between neutron emission fragment angle, mass and energy in the spontaneous fission of ^{252}Cf - Ibidem

BUDTZ-JØRGENSEN, C., KNITTER, H.-H. -
Simultaneous investigation of fission fragments and neutrons in $^{252}Cf(SF)$ - Proc. of 15th Intern. Symp. on Nuclear Physics, Nuclear Fission, Technical University Dresden, Gaußig, German Democratic Republic, 11-15 Nov. 1985 (to be published)

BUDTZ-JØRGENSEN, C., KNITTER, H.-H. -
Assaying of ^{235}U fission layers for nuclear measurements with a gridded ionization chamber - IAEA Advisory Group Meeting on Nuclear Standard Reference Data, Proc. IAEA-TECDOC-335 (1985) p. 476

BUDTZ-JØRGENSEN, C., KNITTER, H.-H., VOGT, R. -
Neutron emission from the spontaneous fission of ^{252}Cf - Ibidem - p. 315

CORVI, F., RIEMENSCHNEIDER, H., van der VEEN, T. -
Flux detector intercomparisons: High-efficiency detectors -Ibidem - p. 371

DEKEMPENEER, E., LISKIEN, H., MEWISSEN, L., POORTMANS, F. -
Double-differential neutron emission cross section for the $^{7}Li(n,Xn)$ reaction between 1.6-15 MeV - Int. Conf. Basic Appl. Sci., Santa Fe, USA (1985)

DERUYTTER, A.J. -
Summary report IAEA Advisory Group Meeting on Nuclear Standard Reference Data - IAEA Advisory Group Meeting on Nuclear Standard Reference Data, Proc. IAEA-TECDOC-335 (1985) p. 65

DERUYTTER, A.J. -
Requirements for nuclear standard reference data from the users - Ibidem - p. 48

DERUYTTER, A.J., BÖCKHOFF, K.H., LISKIEN, H. -
Facilities for nuclear data determination in Europe - KTG/ENS Seminar on Nuclear Data, Bonn, September 30 - October 2, 1985

KNITTER, H.-H., BUDTZ-JØRGENSEN, C. -
Neutron induced fission cross section of ^{243}Am from 1 to 4 MeV - Int. Conf. Basic Appl. Sci., Santa Fe, USA (1985)

KNITTER, H.-H., BUDTZ-JØRGENSEN, C., BAX, H. -
Investigation for a precise and efficient neutron fluence detector based on the n-p scattering process - IAEA Advisory Group Meeting on Nuclear Standard Reference Data, Proc. IAEA-TECDOC-335 (1985) p. 470

KÖHLER, R., MEWISSEN, L., POORTMANS, F., RAMAN, S., WARTENA, H., WEIGMANN, H. -
Doorways in the reaction $^{207}Pb+n$ - Int. Conf. Basic Appl. Sci., Santa Fe, USA (1985)

KÖHLER, R., MEWISSEN, L., POORTMANS, F., THEOBALD, J.P., WEIGMANN, H. -
Hochauflösende Neutronen Resonanz Spektroskopie - Frühjahrstagung der DPG, München, Germany (1985)

LISKIEN, H. -
Angular distribution for $^{7}Li(n,n')^{7}Li^{*}(478)$ by analyzing Doppler-broadened gamma lines - Int. Conf. Basic Appl. Sci., Santa Fe, USA (1985)

LISKIEN, H., LEWIS, V.E. -
International fluence rate intercomparison for 2.5, 5.0 and 14 MeV neutrons - IAEA Advisory Group Meeting on Nuclear Standard Reference Data, Proc. IAEA-TECDOC-335 (1985) p. 324

REICH, C.W., VANINBROUKX, R. -
Current status of nuclear decay data and report on the IAEA coordinated research programme on the measurement and evaluation of transactinium isotope nuclear decay data - IAEA Third Advisory Group Meeting on Transactinium Isotope Nuclear Data, Proc. IAEA-TECDOC-336 (1985) p. 275

ROHR, G. -
Eine Methode zur Bestimmung der Restwechselwirkung in Atomkernen - Frühjahrstagung der DPG, München, Germany (1985)

ROHR, G. -
A method to determine the pairing energy for excited nuclei - 4th International Conference on Neutron Induced Reactions, Smolenice, Czechoslovakia, 17-21 June 1985

SCHILLEBEECKX, P., WAGEMANS, C., DERUYTTER, A.J., BARTHELEMY, R. -
Shell effects in the spontaneous and thermal neutron induced fission of the plutonium isotopes - Ibidem

STRAEDE, Ch., BUDTZ-JØRGENSEN, C., KNITTER, H.-H. -
$^{235}U(n,f)$ fragment mass, kinetic energy and angular distribution - Ibidem

STRAEDE Ch., BUDTZ-JØRGENSEN, C., KNITTER, H.-H. -
Data for $^{235}U(n,f)$, $E_n \leq 6$ MeV, on fragment mass, kinetic energy and angular distribution - results and interpretation - Frühjahrstagung der DPG, München, Germany (1985)

STRAEDE, Ch., BUDTZ-JØRGENSEN, C., KNITTER, H.-H. -
Fission fragment mass, kinetic energy and angular distribution for $^{235}U(n,f)$ in the neutron energy range from thermal to 6 MeV - IAEA Advisory Group Meeting on Nuclear Standard Reference Data, Proc. IAEA-TECDOC-335 (1985) p. 181

STRAEDE, Ch., BUDTZ-JØRGENSEN, C., KNITTER, H.-H. -
$^{235}U(n,f)$ fragment mass, kinetic energy and angular distribution at energies below 6 MeV - results and interpretation - 4th International Conference on Neutron Induced Reactions, Smolenice, Czechoslovakia, 17-21 June 1985

VANINBROUKX, R. -
Emission probabilities of selected gamma rays for radionuclides used as detector-calibration standards - IAEA Advisory Group Meeting on Nuclear Standard Reference Data, Proc. IAEA-TECDOC-335 (1985) p. 403

VANPRAET, G., CORNELIS, E., RAMAN, S., ROHR, G. -
Neutron capture measurements on ^{241}Am - Int. Conf. Basic Appl. Sci., Santa Fe, USA (1985)

WAGEMANS, C., DERUYTTER, A.J. -
New results on the $^{235}U(n,f)$ fission integrals - IAEA Advisory Group Meeting on Nuclear Standard Reference Data, Proc. IAEA-TECDOC-335 (1985) p. 156

WAGEMANS, C., DERUYTTER, A.J. -
Sub-thermal fission cross-section measurements - Int. Conf. Basic Appl. Sci., Santa Fe, USA (1985)

WAGEMANS, C., SCHILLEBEECKX, P., DERUYTTER, A.J., BARTHELEMY, R. -
Fission fragment mass and energy distributions for spontaneous and thermal neutron induced fission of several plutonium isotopes - Conference paper Algemene Wetensch. Vergadering van de Belgische Natuurk. Vereniging, Antwerpen, 6-7 June 1985

WARTENA, J.A., KNITTER, H.-H., BUDTZ-JØRGENSEN, C., BAX, H., BÜRKHOLZ, Cl.-D., PIJPSTRA, R., VOGT, R. -
A neutron detector comparison in the GELINA spectrum - IAEA Advisory Group Meeting on Nuclear Standard Reference Data, Proc. IAEA-TECDOC-335 (1985) p. 360

WEIGMANN, H. -
Recent advances and future trends in neutron resonance spectroscopy - Int. Conf. Basic Appl. Sci., Santa Fe, USA (1985)

SCIENTIFIC OR TECHNICAL ARTICLES

BAMBYNEK, W.
International Committtee for Radionuclide Metrology - Int. J. Appl. Radiat. Isot. 36 (1985) 171

BUDTZ-JØRGENSEN, C., KNITTER, H.-H., BORTELS, G. -
Assaying of targets for nuclear measurements with a gridded ionization chamber - Nucl. Instrum. Methods Phys. Res. A236 (1985) 630

COURSEY, B.M., MANN, W.B., GRAU MALONDA, A., GARCIA-TORAÑO, E., LOS ARCOS, J.M., GIBSON, J.A.B., REHER, D. - Standardization of carbon-14 by $4\pi\beta$ liquid scintillation efficiency tracing with hydrogen-3 - Int. J. Appl. Radiat. Isot. 37 (1986) 403

CRAMETZ, A., de JONGE, S., LISKIEN, H., JAESCHLE, E., INGWERSEN, H. - Post acceleration bunching system for a CN-type Van de Graaff accelerator - Nucl. Instrum. Methods Phys. Res. A242 (1986) 179

EYKENS, R., PAUWELS, J., VAN AUDENHOVE, J. - The hydrofluorination of uranium and plutonium - Nucl. Instrum. Methods Phys. Res. A236 (1985) 497

GEERTS, K., VAN GESTEL, J., PAUWELS, J. - Thin ^{33}S layers for $^{33}S(n,\alpha)$ cross section measurements - Nucl. Instrum. Methods Phys. Res. A236 (1985) 527

HANSEN, H.-H. - Compilation of experimental values of internal conversion coefficients and ratios for nuclei with Z > 60 - Physik Daten-Physics Data 17-2 (1985)

HANSEN, H.-H. - Evaluation of K-shell and total internal conversion coefficients for some selected nuclear transitions - Eur. Appl. Res. Rep. - Nucl. Sci. Technol. Sect. 6 (1985) 777

PAUWELS, J. - The development of a method for the preparation of large amounts of ^{234}Th-purified ^{238}U-oxide - Nucl. Instrum. Methods Phys. Res. A236 (1985) 495

PAUWELS, J., VAN GESTEL, J., VANDECASTEELE, C., STRIJCKMANS, K. - Irradiation tests of thin substrate materials for nuclear targets - Nucl. Instrum. Methods Phys. Res. A236 (1985) 651

PAVLIK, A., WINKLER, G., UHL, M., PAULSEN, A., LISKIEN, H. -
Neutron-induced reactions on ^{58}Ni - Nucl. Sci. Eng. 90 (1985) 186

REHER, D., HANSEN, H.H., VANINBROUKX, R., WOODS, M.J., GRANT, C.E., LUCAS, S.E.M., BOUCHARD, J., MOREL, J., VATIN, R. -
The decay of ^{47}Sc - Submitted for publication in Int. J. Appl. Radiat. Isot.

SPIRLET, J.C., MÜLLER, W., VAN AUDENHOVE, J. -
Direct reduction of actinide oxide and carbide to metal: application to the preparation of Pu metal - Nucl. Instrum. Methods Phys. Res. A236 (1985) 500

SPIRLET, J.C., MÜLLER, W., VAN AUDENHOVE, J. -
Single crystal growth of actinide compounds - Nucl. Instrum. Methods Phys. Res. A236 (1985) 489

VAN AUDENHOVE, J., PAUWELS, J., FUDGE, A.J. -
A european community source of reference materials for neutron metrology requirements - Nucl. Instrum. Methods Phys. Res. A236 (1985) 600

VANDENBERG, M., PAULSEN, A., BERTHELOT, Ch., BABELIOWSKY, T. -
The feasibility of electromagnetic actinide isotope separation in the European Community - Nucl. Instrum. Methods Phys. Res. A236 (1985) 463

VANINBROUKX, R., BAMBYNEK, W. -
Evaluation of selected decay data for some actinides. Decay Data of the Transactinium Nuclides. - Technical Report Series No. ... (International Atomic Energy Agency, Vienna, 1985) - in press

WEIGMANN, H., WARTENA, J.A., BÜRKHOLZ, Cl.-D. -
Neutron-induced fission cross section of ^{242}Pu - Nucl. Phys. A438 (1985) 333

TECHNICAL NOTES

BALLAUX, C. -

4π(PC)-γ efficiency-tracing and extrapolation of ^{109}Cd with ^{65}Zn: Interpretation of the first results - GE/R/RN/09/85

BAMBYNEK, W. -

Evaluation of the γ-ray emission probabilities of selected transitions in the decay of ^{241}Am - GE/R/RN/1/85

BAO SHANGLIAN -

Comparison of different source-sample geometries - GE/R/VG/47/85

BAO SHANGLIAN -

Corrections for $^{7}Li(n,n'\gamma)$(478 keV) due to the anisotropy of the γ-ray angular distribution in the laboratory system - GE/R/VG/48/85

COTTENS, E., JANSSENS, A., NERB, H., PAULSEN, A., VAN RHEE, L., WIDERA, R.

The RUG graphite absorbed dose calorimeter: set-up and procedures - GE/R/VG/46/85

IDZERDA, A.B. -

An automatic gamma-ray spectrometer - GE/R/RN/4/85

REHER, D., DENECKE, B., VANINBROUKX, R. -

Standardization of a ^{109}Cd solution - GE/R/RN/7/85

VAN AUDENHOVE, J. TRIFFAUX, J. -

Fabrication report Ti (12 ppm H) - GE/NI/SP/17/85

VAN AUDENHOVE, J., TRIFFAUX, J. -

Fabrication report Cu (P and S) - GE/NI/SP/21/85

VANINBROUKX, R. -

KX-ray-emission-rate measurements of 5 millicurie ^{55}Fe sources - GE/R/RN/12/85

VANINBROUKX, R., BAMBYNEK, W. -
Evaluation of selected decay data for some actinides (Revised) - GE/R/RN/3/85

VANINBROUKX, R., ZEHNER, W. -
Measurement of the relative activity concentration of $^{238}UO_2$ spheres to be used for neutron dosimetry - GE/R/RN/2/85

WATTECAMPS, E., ARNOTTE, F. -
$^{nat}Cu(n,\alpha)$ and $^{nat}Ni(n,\alpha)$ cross sections in the 5 to 10 MeV neutron energy range - GE/R/VG/49/85

COMMUNICATIONS

DEBUS, G.H. (Ed.) -
Programme Progress Report January-June 1985 - COM 4258

DEBUS, G.H. (Ed.) -
Programme Progress Report July-December 1985 - COM 4272

CINDA ENTRIES LIST

ELEMENT		QUANTITY	TYPE	ENERGY		DOCUMENTATION		LAB	COMMENTS
S	A			MIN	MAX	REF VOL PAGE	DATE		
LI	006	N, ALPHA	EXPT-PROG	10+0	40+5	INDC(EUR)20 3	986	GEL	BASTIAN + REL TO $^{10}B(N,A)$
LI	007	INELASTIC G	EXPT-PROG	40+6	85+6	INDC(EUR)20 38	986	GEL	LISKIEN + NEUTR ANG DISTR
LI	007	NEM	EXPT-PROG	16+6	16+7	INDC(EUR)20 42	986	GEL	DEKEMPENEER + DOUBLE DIFF XSECT
BE	009	N, TRITON	EXPT-PROG	13+7	19+7	INDC(EUR)20 46	986	GEL	LISKIEN + TRITIUM DETERM
B	010	N, ALPHA	EXPT-PROG	10+0	40+5	INDC(EUR)20 3	986	GEL	BASTIAN + REL TO $^{6}LI(N,A)$
SI	028	TOT	EXPT-PROG	10+3	28+6	INDC(EUR)20 50	986	GEL	MARTIN + LINAC TOF
SI	028	NG	EXPT-PROG	10+3	28+6	INDC(EUR)20 50	986	GEL	MARTIN + LINAC TOF
SI	028	RESON PARAMS	EXPT-PROG	10+3	28+6	INDC(EUR)20 50	986	GEL	MARTIN + NEUTR + GAMMA WIDTHS
CR	050	RESON PARAMS	EXPT-PROG	10+3	10+6	INDC(EUR)20 36	986	GEL	BRUSEGAN + NEUTR + GAMMA WIDTHS
CR	052	RESON PARAMS	EXPT-PROG	10+3	10+6	INDC(EUR)20 36	986	GEL	BRUSEGAN + NEUTR + GAMMA WIDTHS
CR	053	RESON PARAMS	EXPT-PROG	10+3	20+5	INDC(EUR)20 36	986	GEL	BRUSEGAN + NEUTR + GAMMA WIDTHS
FE	054	RESON PARAMS	EXPT-PROG	50+4	80+5	INDC(EUR)20 34	986	GEL	CORNELIS + NEUTRON WIDTHS
FE	056	RESON PARAMS	EXPT-PROG	12+3		INDC(EUR)20 35	986	GEL	BRUSEGAN + NEUTR + GAMMA WIDTHS
NI		N, ALPHA	EXPT-PROG	50+6	10+7	INDC(EUR)20 46	986	GEL	WATTECAMPS + DOUBLE DIFF XSECT
CU		N, ALPHA	EXPT-PROG	50+6	10+7	INDC(EUR)20 46	986	GEL	WATTECAMPS + DOUBLE DIFF XSECT
PB	207	RESON PARAMS	EXPT-PROG	10+3	70+5	INDC(EUR)20 51	986	GEL	KOEHLER + NEUTR + GAMMA WIDTHS
U	235	N, FISSION	EVAL-PROG	25−2		INDC(EUR)20 7	986	GEL	AXTON
U	235	N, FISSION	EXPT-PROG	75−4	10−1	INDC(EUR)20 24	986	GEL	WAGEMANS + LINAC TOF
U	235	ETA	EVAL-PROG	25−2		INDC(EUR)20 7	986	GEL	AXTON
U	235	ETA	EXPT-PROG	10−3	50−1	INDC(EUR)20 25	986	GEL	WAGEMANS + LINAC TOF
U	235	FRAG SPECTRA	EXPT-PROG	25−2	10+6	INDC(EUR)20 6	986	GEL	HAMBSCH + ANG AND ENERGY DISTR
U	235	FISS YIELD	EXPT-PROG	25−2	10+6	INDC(EUR)20 6	986	GEL	HAMBSCH + PROMPT MASS SPECTRUM
U	238	NG	EXPT-PROG	20−3	10−1	INDC(EUR)20 28	986	GEL	CORVI + LINAC TOF, C_6D_6 SCINT
PU	238	FISS YIELD	EXPT-PROG	SPON		INDC(EUR)20 30	986	GEL	WAGEMANS +
PU	238	FRAG SPECTRA	EXPT-PROG	SPON		INDC(EUR)20 30	986	GEL	WAGEMANS +
PU	240	FISS YIELD	EXPT-PROG	SPON		INDC(EUR)20 30	986	GEL	WAGEMANS +
PU	240	FRAG SPECTRA	EXPT-PROG	SPON		INDC(EUR)20 30	986	GEL	WAGEMANS +
PU	242	FISS YIELD	EXPT-PROG	SPON		INDC(EUR)20 30	986	GEL	WAGEMANS +
PU	242	FRAG SPECTRA	EXPT-PROG	SPON		INDC(EUR)20 30	986	GEL	WAGEMANS +
AM	243	N, FISSION	EXPT-PROG	10+2	14+6	INDC(EUR)20 30	986	GEL	KNITTER + REL TO $^{235}U(N,F)$ + $^{6}LI(N,A)$
AM	243	N, FISSION	EXPT-PROG	40+6	94+6	INDC(EUR)20 30	986	GEL	KNITTER + REL TO $^{235}U(N,F)$ + $^{6}LI(N,A)$
CF	252	SPECT FISS N	EXPT-PROG	SPON		INDC(EUR)20 9	986	GEL	BUDTZ-JØRGENSEN + TOF
CF	252	FISS YIELD	EXPT-PROG	SPON		INDC(EUR)20 9	986	GEL	BUDTZ-JØRGENSEN + GRIDDED TWIN ION CH
CF	252	FRAG SPECTRA	EXPT-PROG	SPON		INDC(EUR)20 9	986	GEL	BUDTZ-JØRGENSEN + GRIDDED TWIN ION CH

Edited by G.H. DEBUS and H.H. HANSEN